1-1-2015

# Between Slit and Repulsion: Cell and Molecular Mechanisms Underlying Robo-Mediated Midline Guidance

Rebecca K. Chance
*University of Pennsylvania*, rebeccachance@alumni.brown.edu

# Between Slit and Repulsion: Cell and Molecular Mechanisms Underlying Robo-Mediated Midline Guidance

**Abstract**
Understanding how axon guidance receptors are activated by their extracellular ligands to regulate growth cone motility is critical to learning how proper wiring is established during development. Roundabout (Robo) is one such guidance receptor that mediates repulsion from its ligand Slit in both invertebrates and vertebrates. Here we show that endocytic trafficking of the Robo receptor in response to Slit-binding is necessary for its repulsive signaling output. Dose-dependent genetic interactions and in vitro Robo activation assays support a role for Clathrin-dependent endocytosis, and entry into both the early and late endosomes as positive regulators of Slit-Robo signaling. We identify two conserved motifs in Robo's cytoplasmic domain that are required for its Clathrin-dependent endocytosis and activation in vitro, and gain of function and genetic rescue experiments provide strong evidence that these trafficking events are required for Robo repulsive guidance activity in vivo. Our data support a model in which Robo's ligand-dependent internalization from the cell surface to the late endosome is essential for receptor activation and proper repulsive guidance at the midline by allowing recruitment of the downstream effector Son of Sevenless in a spatially constrained endocytic trafficking compartment. We then go on to provide evidence for the placement of Robo endocytosis after the previously reported kuzbanian-mediated juxtamembrane activating cleavage and before a newly reported inactivating presenilin-mediated transmembrane cleavage that serves to curtail the timecourse of signaling from activated Robo.

**Degree Type**
Dissertation

**Degree Name**
Doctor of Philosophy (PhD)

**Graduate Group**
Neuroscience

**First Advisor**
Greg J. Bashaw

**Keywords**
Axon Guidance, Endocytosis, Rab GTPase, Roundabout, Slit, Son of Sevenless

**Subject Categories**
Developmental Biology | Genetics | Neuroscience and Neurobiology

# BETWEEN SLIT AND REPULSION:

# CELL AND MOLECULAR MECHANISMS UNDERLYING

# ROBO-MEDIATED MIDLINE GUIDANCE

Rebecca Kent Chance

A DISSERTATION

in

Neuroscience

Presented to the Faculties of the University of Pennsylvania

in

Partial Fulfillment of the Requirements for the

Degree of Doctor of Philosophy

2015

Supervisor of Dissertation

_____

Gregory J. Bashaw

Professor of Neuroscience

Graduate Group Chairperson

_____

Joshua I. Gold, Professor of Neuroscience

Dissertation Committee

Jonathan A. Raper, Professor of Neuroscience

Michael Granato, Professor of Cell and Developmental Biology

Matthew Dalva, Associate Professor, Department of Neuroscience, Thomas Jefferson University

Mark A. Lemmon, George W. Raiziss Professor of Biochemistry and Biophysics

Chair, Department of Biochemistry and Biophysics

BETWEEN SLIT AND REPULSION:

CELL AND MOLECULAR MECHANISMS UNDERLYING

ROBO-MEDIATED MIDLINE GUIDANCE

*Dedication page*

*I dedicate this page to those who encouraged me to ask questions when I was a child, and those who continue to inspire curiosity in me now:*

*PEC, JME, BC, CMC, WJK, MCK.*

## ACKNOWLEDGMENTS

I would like to thank Greg for both his unwavering support and his ability to provide the perfect balance between space for creativity and critical feedback and guidance-- all of which have proved ideal for fostering the mentality necessary for independent research.

I would like to thank members of the Bashaw lab for their thoughtful comments during the development of this work. I thank Avital Rodal for providing the WT GFP-Rab5&11 plasmids, Valérie CASTELLANI for a pHluorin plasmid, Marcos González-Gaitán for *ada*[3], Anne Schmidt for *endoA*[10], and Peter Robin Hiesinger for the gift of *rab7*$^{\text{knock-out}}$ flies. This work was supported by National Institutes of Health Grants R01NS-046333 and R01NS-054739 to G.J.B and F31-NS071800 to R.K.C.

# ABSTRACT


## SLIT-DEPENDENT ENDOCYTIC TRAFFICKING OF THE ROBO RECEPTOR IS REQUIRED FOR SON OF SEVENLESS RECRUITMENT AND MIDLINE AXON REPULSION

Rebecca Kent Chance

Greg J. Bashaw

Understanding how axon guidance receptors are activated by their extracellular ligands to regulate growth cone motility is critical to learning how proper wiring is established during development. Roundabout (Robo) is one such guidance receptor that mediates repulsion from its ligand Slit in both invertebrates and vertebrates. Here we show that endocytic trafficking of the Robo receptor in response to Slit-binding is necessary for its repulsive signaling output. Dose-dependent genetic interactions and *in vitro* Robo activation assays support a role for Clathrin-dependent endocytosis, and entry into both the early and late endosomes as positive regulators of Slit-Robo signaling. We identify two conserved motifs in Robo's cytoplasmic domain that are required for its Clathrin-dependent endocytosis and activation *in vitro*, and gain of function and genetic rescue experiments provide strong evidence that these trafficking events are required for Robo repulsive guidance activity *in vivo*. Our data support a model in which Robo's ligand-dependent internalization from the cell surface to the late endosome is essential for receptor activation and proper repulsive guidance at the midline by allowing recruitment of the downstream effector Son of Sevenless in a spatially constrained endocytic trafficking compartment. We then go on to provide evidence for the placement of Robo endocytosis after the previously reported *kuzbanian*-mediated juxtamembrane activating cleavage and before a newly reported inactivating *presenilin*-mediated transmembrane cleavage that serves to curtail the timecourse of signaling from activated Robo.

TABLE OF CONTENTS

## LIST OF TABLES

## LIST OF ILLUSTRATIONS

## PREFACE

This dissertation is an original intellectual product of the author, R. Chance. All experiments were performed by the author except those at the beginning of Chapter 3 performed by Hope Coleman and Greg Bashaw (Coleman Labrador Chance & Bashaw 2010) clearly demarcated in the figure legend that are included to introduce the rationale behind the experiments performed in the rest of the Chapter 3.

# CHAPTER 1: Introduction

The complex wiring patterns of the adult central nervous system are established by the stepwise navigation of growth cones and migrating cells through a series of choice points during development. At each choice point, the complement of guidance receptors expressed on the growth cone's plasma membrane determines which of the cues in the extracellular environment will inform the cell's guidance decision as it navigates toward its eventual synaptic partner (Yu and Bargmann 2001; Dickson 2002; Huber et al. 2003; Garbe and Bashaw 2004). Understanding how an individual growth cone deploys its guidance receptors to make specific guidance decisions is critical to learning how proper wiring is established in development.

Researchers have discovered several phylogenetically conserved families of guidance cues and receptors, including (*a*) semaphorins (semas) and their plexin (Plex) and neuropilin receptors (Pasterkamp and Kolodkin 2003) , (*b*) netrins and their deleted in colorectal carcinoma (DCC) and UNC5 receptors (Kennedy 2000), and (*c*) ephrins and their Eph receptors (Kullander and Klein 2002) (Figure 1.1). More recently, additional protein families previously recognized for other developmental functions have been implicated in growth cone guidance including sonic hedgehog (Shh) (Charron et al. 2003), bone morphogenetic proteins (BMPs) (Butler and Dodd 2003), and Wingless-type (Wnt) proteins (Lyuksyutova et al. 2003; Yoshikawa et al. 2003).

Roundabout (Robo) receptors comprise another family of highly conserved axon guidance receptors that mediate repulsion in response to their Slit ligands during neuronal development (Kidd et al. 1998a; Brose et al. 1999a; Kidd et al. 1999a; Wang et al. 1999b). Robo receptors have also been implicated in genome-wide association studies with the pathogenesis of several human diseases including autism and

schizophrenia (Anitha et al. 2008; Potkin et al. 2009c), and they are thought to be causatively linked to dyslexia and periventricular nodular heterotopia (Hannula-Jouppi et al. 2005; Chang et al. 2007; Bates et al. 2011), suggesting roles in guidance of more diverse axonal projections in the human cortex that are yet to be characterized.

In both invertebrates and vertebrates, Slits serve as repulsive cues to their Robo receptors by demarcating regions into which axons cannot maintain their exploratory projections. In the case of the Drosophila embryonic ventral nerve cord (VNC), Slit is expressed by midline glia, which creates a barrier for axonal projection for any growth cones expressing Robo at their surface (Kidd et al. 1998a; Kidd et al. 1999b). In *robo* mutants normally ipsilaterally-projecting (ipsilateral or post-crossing commissural) axons ignore the presence of this repulsive cue and project into the midline and even circle there in namesake roundabouts (Seeger et al. 1993). Repulsive guidance can also instruct axonal projections by corralling fascicles into relative valleys of Slit expression- mouse callosal axons project between the indusium griseum and the glial wedge structures (Shu and Richards 2001; Lopez-Bendito et al. 2007)- or by directing a 90° turn in bifurcating branches of sensory axons into the dorsal funiculus (Ma and Tessier-Lavigne 2007). Analogously, there exists a relative valley in Slit expression in medio-lateral axis of the *Drosophila* VNC through which a sizeable set of longitudinal fascicles project (Johnson et al. 2004).

The mechanism by which Slit triggers repulsion at the cellular level is not completely understood, but must involve an initial mis-projection into Slit-expressing regions in order to sense and then respond to the presence of the repulsive cue. One growth cone phenotype resulting from loss of Robo is defective filopodial retraction from the Slit-containing embryonic midline in *Drosophila*, resulting in stabilization of

contralateral filopodial projections (Murray and Whitington 1999). Similarly, loss of *robo2 (astray)* in zebrafish leads to abnormal stabilization of mis-projecting growth cones in the ventral forebrain, 'errors' that are normally corrected in wild-type (Hutson and Chien 2002). The error-correction implicit in repulsive guidance from an initially adhesive protein-protein interaction requires some sort of physical severing which has been ascribed to juxtamembrane cleavage, endocytosis, or both (Hattori et al. 2000; Marston et al. 2003; Zimmer et al. 2003; Cowan et al. 2005; Janes et al. 2005; Lin et al. 2008a).

**Regulated Endocytosis and Axon Guidance Receptor Function**

Regulating the delivery of guidance receptors to the growth cone plasma membrane can have profound influences on axon growth and guidance; therefore, it is not surprising that the regulation of receptor expression at the cellular level is not confined strictly to surface expression, as reviewed in (O'Donnell Chance and Bashaw 2009), but also includes regulated removal by endocytosis. In several cases, receptor endocytosis appears to be an obligate step in receptor activation that is evoked by ligand binding, whereas other examples point to the modulation of guidance responses by receptor endocytosis that is triggered by an independent pathway. Here I will briefly consider a few examples of endocytosis as a prerequisite for receptor signaling; in particular, I discuss the role of the Rac specific GEF Vav2 in the regulation of Eph receptor endocytosis. In addition, I will highlight the role of protein kinase C (PKC) activation in the regulation of responses to netrin through the specific endocytosis of the UNC5 receptor (Figure 1.2).

Ephrin ligands and Eph receptors contribute to the guidance of retinal ganglion cell (RGC) axons in the visual system; specifically, EphB receptor mutations in mice

result in a reduction in the ipsilateral projection to the dorsal lateral geniculate nucleus. Disruption of *vav-2* and *vav-3*, members of the Vav family of RacGEFs, leads to similar defects in the targeting of ipsilateral RGC axons in mice (Cowan et al. 2005). Unlike *wild-type* RGCs, growth cones of RGCs cultured from *vav*-deficient mice do not collapse in response to ephrin. Surface labeling of Ephrin in *vav*-deficient RGC growth cones reveals a selective deficit in Ephrin ligand endocytosis in response to pre-clustered ephrin- A1 treatment, suggesting that endocytosis of activated Eph receptors at the growth cone is necessary to allow for proper forward signaling, leading to growth cone retraction (Cowan et al. 2005) (Figure 1.2B). A similar dependency on endocytosis to trigger axon retraction is observed in neurons responding to sema 3A, where the L1 IgCAM, a component of the sema receptor complex, mediates endocytosis of the sema 3A holoreceptor in response to ligand binding (Castellani et al. 2004).

In addition to contributing to receptor signaling, endocytosis can also modulate axon responses by regulating which receptors are expressed at the surface of the growth cone. This type of mechanism is best exemplified by regulated endocytosis of the repulsive netrin receptor UNC5 in vertebrate neurons. Here, activation of protein kinase C (PKC) triggers the formation of a protein complex including the cytoplasmic domain of UNC5H1, protein interacting with C-kinase 1 (Pick1), and PKC and leads to the specific removal of UNC5H1 (but not DCC) from the growth cone surface; reducing surface levels of UNC5H1 correlates with the inhibition of the netrin-dependent collapse of cultured hippocampal growth cones (Williams et al. 2003). Furthermore, PKC activation leads to colocalization of UNC5A with early endosomal markers, supporting the idea that the observed inhibition of growth cone collapse is due to UNC5A endocytosis (Bartoe et al. 2006). Thus, PKC-mediated removal of surface UNC5 provides a means to switch Netrin responses from repulsion, mediated by either UNC5 alone or an UNC5-DCC

complex, to attraction mediated by DCC. How then is this switch activated, or which signals lead to the activation of PKC? Interestingly, recent evidence supports the model that the G protein-coupled Adenosine 2B (A2b) receptor is a likely mediator of PKC activation because activation of A2b leads to the PKC-dependent endocytosis of UNC5 (McKenna et al. 2008). A2b is a Netrin receptor that, together with DCC, appears to be required to mediate axon attraction (Corset et al. 2000), although this proposal has been quite controversial, and other evidence indicates either that A2b plays no role in Netrin signaling (Bouchard et al. 2004, Stein et al. 2001) or that its role in Netrin signaling is to modulate Netrin responses (Shewan et al. 2002). In the context of UNC5 regulation, A2b acts independently of Netrin, and its ability to regulate UNC5 surface levels supports its role as a potent modulator of Netrin responses (Figure 1.2A).

Another piece of evidence pointing to the importance of control over the surface of guidance receptors comes from the regulation over Robo surface levels provided by the fly-specific protein Commisureless, and the analogous vertebrate protein Rig-1/Robo3. Several lines of evidence, including subcellular localization experiments and transgenic expression of mutant forms of *comm*, indicate that Comm can recruit Robo receptors directly to endosomes for degradation before they ever reach the cell surface and that this sorting function is important for regulating midline repulsion (Keleman et al. 2002) (Figure 1.2*C*). The endosomal sorting model has been extended to show that Comm can prevent Robo delivery to the growth cone surface in living embryos (Keleman et al. 2005). Expression of green fluorescent protein (GFP) tagged Robo in sensory axons provides investigators with live visualization of the anterograde axonal transport of Robo positive vesicles. When Comm is genetically introduced into these Robo-GFP-positive neurons, the transport of Robo positive vesicles is almost completely abolished, providing strong evidence for the *in vivo* significance of Comm-directed endosomal

targeting of Robo (Keleman et al. 2005).

Are there vertebrate Comm homologs that serve similar functions during commissural axon guidance in the spinal cord, or instead do other molecules play this role? So far, no vertebrate Comm proteins have been found; however, compelling genetic evidence indicates that another molecule may have an analogous function in the spinal cord. Rig-1/Robo3, a divergent vertebrate-specific Robo family member, is required in pre-crossing commissural neurons to down-regulate the sensitivity to midline Slit proteins, although this function is achieved by a distinct mechanism (Sabatier et al. 2004).

Based on these findings suggesting a role for endocytosis in modulating axon guidance receptor activity and signaling, we could envision at least two plausible models for how Robo receptor endocytosis might regulate axon repulsion (Figure 1.3). If endocytosis' dominant contribution to the Slit/Robo pathway is to modulate the amount of Robo receptor on the surface of the growth cone, as reported previously by diversion of Robo from the biosynthetic pathway (Keleman et al. 2002; Keleman et al. 2005), a reduction in receptor endocytosis would be predicted to lead to increased levels of surface receptor and more robust repulsive signaling. Alternatively, if Robo receptor endocytosis is an obligate step in receptor activation, as has been observed in the case of Wingless signaling (Seto and Bellen 2006), preventing or reducing Robo endocytosis would result in impaired Slit-Robo signaling.

In Chapter 2 we identify a novel mechanism that is required for Robo receptor activation and Robo-dependent axon repulsion *in vivo.* Using a combination of molecular genetic and cell biological approaches, we define a role for Slit-dependent trafficking of Robo from the plasma membrane to the early and late endosomes in contributing to

Robo activation and signaling. In previous work, endocytic trafficking has been shown to modulate axon guidance responses by altering available surface pools of axon guidance receptors. Our observations indicate that rather than acting to modulate responses by regulating surface levels, endocytosis of the Robo receptor itself is a key component of receptor activation and precedes the recruitment of the Ras/Rho GEF Son of Sevenless, a key downstream signaling effector, to the receptor cytoplasmic domain.

**Regulated Proteolytic Processing and Axon Guidance**

Another mode of regulation contributing to axon guidance is that provided by proteolytic processing to both guidance ligands and receptors, which can have profound impacts on path finding. A role for proteolysis in axon guidance was supported by a number of early studies demonstrating that growth cones secrete proteases, and investigators proposed that cleavage of extracellular matrix components is required to advance through the extracellular environment (Krystosek & Seeds 1981, Schlosshauer et al. 1990). Later, genetic screens for defects in axonal navigation at the midline in Drosophila, and subsequent cloning and characterization of mutated genes, implicated the Kuzbanian ADAM family transmembrane metalloprotease in the regulation of axon extension and guidance at the midline (Fambrough et al. 1996). Several additional studies have implicated ADAM metalloproteases as well as matrix metalloproteases in contributing to axon guidance *in vivo* in both invertebrate and vertebrate nervous systems (Chen et al. 2007, Hehr et al. 2005). Here, I focus our discussion on emerging links between these proteases, in particular Kuzbanian/ADAM10, and the regulated proteolysis of axon guidance receptors and their ligands.

Several studies have implicated Kuzbanian/ ADAM10 activity in the signaling

pathways of guidance receptors. For example, in *Drosophila*, mutations in *kuzbanian* (*kuz*) exhibit dose- dependent genetic interactions with Slit, the midline repulsive ligand for Robo receptors. Specifically, ectopic midline crossing of ipsilateral interneurons, a hallmark of defective midline repulsion, is observed in *kuz* zygotic mutant embryos and in embryos where both *slit* and *kuz* activity are partially reduced. This dose-dependent interaction supports the idea that Kuz may be a positive regulator of Slit-Robo signaling (Schimmelpfeng et al. 2001). Antibody staining for Robo1 in *kuz* mutants reveals that the midline phenotype is accompanied by a failure to exclude Robo1 protein expression from the midline-crossing portions of axons, which suggests that *kuz* activity may be necessary for exclusion from, but more likely clearance of Robo from, axons (Coleman Labrador Chance & Bashaw 2010). Galko & Tessier-Lavigne (2000) observed a similar effect on receptor expression in the context of metalloprotease-dependent ectodomain shedding of DCC. Specifically, blocking the function of metalloprotease activity results in enhanced DCC receptor expression at the membrane, suggesting that proteolytic cleavage regulates clearance of receptors from the plasma membrane. The outcome of preventing metalloprotease function in these two examples is opposite: Elevated levels of DCC potentiate DCC's ability to mediate Netrin-induced axon outgrowth, whereas Robo expression in axon commissures evidently reflects impaired receptor function. Together, the alteration in Robo receptor expression and the reduction in midline repulsion in *kuz* mutants led to the intriguing conclusion that Kuz likely regulates guidance by regulating the cleavage of Robo (Figure 1.3, Coleman et al 2010, Chapter 3).

Investigators have detailed more direct links between Kuz/ADAM10 and guidance molecule cleavage of Eph receptors and ephrin-A2 ligands. Eph receptors and their ephrin ligands are both capable of transmitting signals in the cell in which they are

expressed: Eph receptor signaling is termed forward signaling, and ephrin ligand signaling is termed reverse signaling (reviewed in (Egea and Klein 2007)). ADAM10 forms a stable complex with ephrin-A2, and upon EphR interaction with ephrin-A2, the resulting ligand-receptor complex is clipped by selective ADAM10-dependent cleavage of ephrin-A2 (Hattori et al. 2000) (Figure 1.4). This model has been extended through the study of additional EphR/ephrin receptor/ligand pairs, and Janes et al. (2005) have beautifully elucidated the molecular and structural basis for how cleavage events are restricted to only those ephrin ligands that are engaged by receptors. Ligand/receptor binding and formation of an active complex expose a new recognition sequence for ADAM10, resulting in the optimal positioning of the protease domain with respect to the substrate (Janes et al. 2005). The ligand-dependence of the cleavage event provides an elegant explanation for how an initially adhesive interaction can be converted to repulsion and offers an efficient strategy for axon detachment and attenuation of signaling. Emerging evidence indicates that the matrix metalloprotease family can play a similar role in converting ephrinB/EphB adhesion into axon retraction by specific cleavage of the EphB2 receptor (Lin et al. 2008b) and the EphA4 receptor (Gatto et al. 2014). Thus, both ephrin ligands and Eph receptors can be substrates for regulated proteolysis, and these proteolytic events appear to be critical in mediating axon retraction.

**Processive Proteolysis: *Gamma*-Secretase and Guidance Receptors**

Kuzbanian (Kuz) was originally identified in Drosophila for its role in regulating Notch signaling during neurogenesis (Rooke et al. 1996; Pan and Rubin 1997a). Kuz-directed cleavage of Notch releases the extracellular domain and triggers the subsequent cleavage and release of the Notch intracellular domain (ICD) by the *gamma*-secretase

complex. This second cleavage event releases Notch ICD from the membrane, allowing it to translocate to the nucleus where it acts as a transcriptional regulator (Mumm et al. 2000). This well-characterized model of processive proteolytic cleavage of Notch is becoming increasingly relevant to an expanding list of type I transmembrane receptors, including axon guidance molecules (Beel and Sanders 2008). More specifically, evidence is mounting for a common regulatory mechanism for DCC and a number of ephrin ligands in which metalloprotease- mediated ectodomain shedding is followed by intra-membrane gamma-Secretase cleavage (Figure 1.4). These sequential cleavage events produce an ectodomain fragment which is shed into the extracellular space and a C- terminal fragment (CTF) that is subsequently cleaved within the membrane to release the ICD (Selkoe and Wolfe 2007).

In the case of DCC, metalloprotease- dependent proteolytic fragments are detected in endogenous tissue and explant cultures (Galko and Tessier-Lavigne 2000; Bai et al. 2011). Furthermore, detection of DCC fragments in mouse brain lysates that correspond in size to fragments engineered to estimate the size of presumptive DCC CTF is enhanced in Presenilin-1 (PS1) knockout mice (Taniguchi et al. 2003; Parent et al. 2005). Accordingly, in primary neural cultures from PS1 mutant mice, accumulation of surface DCC is enhanced. The functional significance of these processing events is underscored by the fact that accumulation of transmembrane forms of DCC in neuronal cells transfected with both full-length DCC and DCC-CTF is correlated with enhanced neurite outgrowth in the presence of a gamma-Secretase inhibitor. This observation suggests a role for Presenilin-mediated cleavage of DCC- CTF in attenuating the intracellular signaling process that drives neurite outgrowth (Parent et al. 2005). Inhibiting gamma-Secretase activity by either PS1/*columbus* mutants or by direct application of a gamma-secretase inhibitor to mouse motor neuron explant cultures is

sufficient to confer Netrin-dependent outgrowth (Bai et al. 2011). This effect is likely mediated by the DCC-CTF fragment as membrane-tethering an ICD construct with a myristoylation sequence, distinguishing it from soluble ICD, confers responsiveness to midline Netrin, as assayed by midline crossing in electroporated chick embryonic neural tube. That membrane-tethering is required for this effect suggests that the mechanism of Netrin-attraction depends on local signaling at the plasma membrane. DCC CTF's mechanism of action was further attributed to Robo silencing by the authors but may in fact simply reflect an enhancement of DCC signaling by addition of the simulated product of an activating cleavage, as the authors also show that Netrin treatment induces the formation of CTF. Further experiments would be required to elucidate whether Presenilin activity in fact regulates DCC which directly regulates Robo as opposed to only modulating the Netrin/DCC pathway signal strength. In addition to DCC, several ephrin ligands and Eph receptors appear to undergo a similar ADAM10/gamma-secretase sequential proteolysis (Georgakopoulos et al. 2006; Tomita et al. 2006; Litterst et al. 2007). As in the case of DCC, *in vitro* evidence supports the idea that these cleavage events lead to functional consequences for ephrin-EphR- dependent process extension (Figure 1.4C,D).

What is the *in vivo* significance of these processing events, and what is the fate of the released extracellular and ICD domains? Although *in vivo* evidence supporting physiological roles for these gamma-Secretase-directed cleavage events has yet to emerge, several observations from *in vitro* studies hint at potentially important regulatory activities of released receptor ICDs. In the case of Notch and APP, the ICD generated by *gamma*-Secretase cleavage is translocated to the nucleus to control gene transcription (Selkoe & Wolfe 2007). A chimeric version of DCC with a Gal4 DNA- binding domain inserted in its intracellular domain can initiate transcription in a *gamma*-secretase-

dependent manner, suggesting that like Notch ICD, DCC-ICD could be acting as a transcriptional regulator in mammalian cells (Taniguchi et al. 2003). In the case of Ephrin's ICD, *in vitro* evidence supports an additional model in which the released ICD can bind to and activate Src family kinases, thereby contributing to ephrin-dependent cytoskeletal rearrangement (Georgakopoulos et al. 2006) (Figure 1.4D). An alternative possibility is that these cleavage events represent a mechanism to limit the duration of receptor signaling because once the ICD is released from the full-length receptor, the spatial regulation of signaling conferred by directional detection of ligand would presumably be rapidly lost. If and how these processing events contribute to *in vivo* receptor function will be an important area of future research.

In Chapter 3 we provide genetic interactions and *in vitro* activation assay evidence in support of a model in which a second transmembrane cleavage by *gamma*-Secretase is required for the termination of signaling from activated Robo. Like the proteolytic cascades described here, the second cleavage likely depends on the first juxtamembrane, activating cleavage of Robo by the ADAM10 Kuzbanian (Coleman et al. 2010), which I briefly review for the purpose of highlighting my contributions and the motivation for having pursued evidence for a second cleavage of Robo. Finally I provide preliminary evidence for an inactivating, transmembrane cleavage by *gamma*-Secretase that serves to curtail the signaling from activated and likely internalized Robo receptor.

**Figure 1.1: A diverse array of axon guidance signaling molecules competent to be expressed on the growth cone plasma membrane**

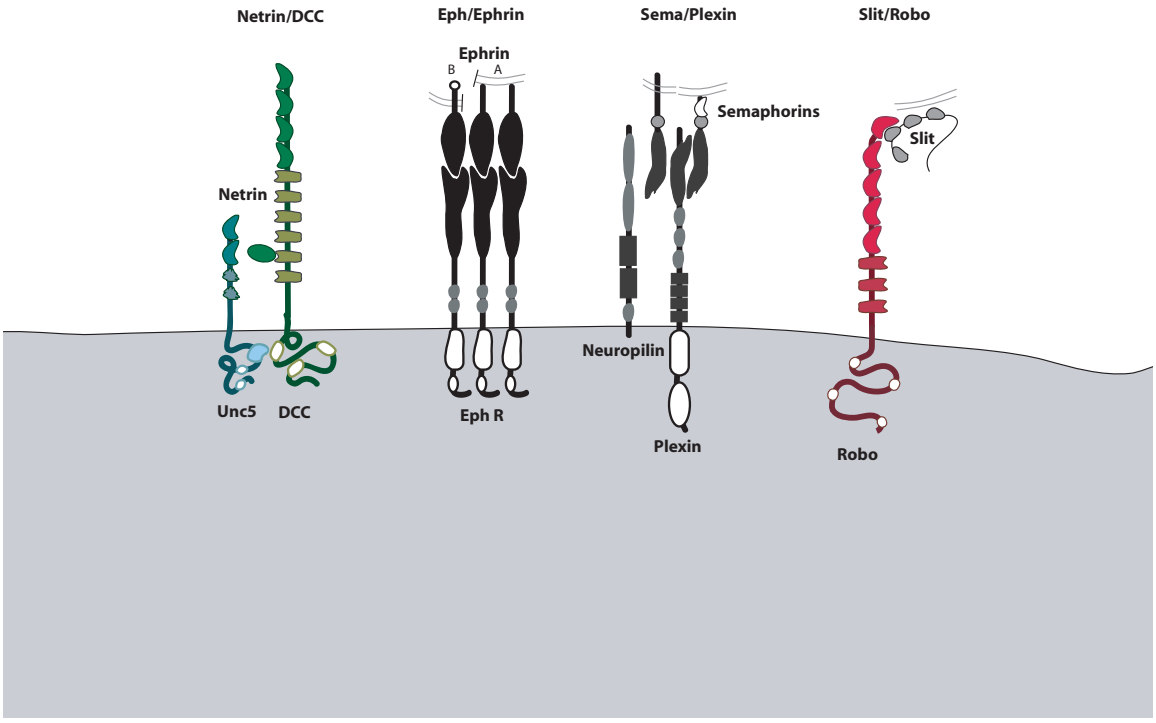

**Figure 1.1: A diverse array of axon guidance signaling molecules competent to be expressed on the growth cone plasma membrane**

While navigating through each choice point on the path to its eventual synaptic partner, the complement of guidance receptors expressed on the growth cone's plasma membrane determines which of the cues in the extracellular environment will inform the cell's guidance decision. Here I'm showing you four conserved families of guidance receptors and their ligands – Netrin Unc5 and DCC, Ephrin and Eph, Semaphorin Plexin and Neuropilin and the pair I'll be focusing on in this document- the repulsive guidance receptor Roundabout (Robo) that mediates repulsion from its ligand Slit in both invertebrates and vertebrates. Control over the combinatorial array of the illustrated guidance molecules, and others, is by definition an important biological process, and therefore likely to be subject to regulation.

**Figure 1.2: Endocytic trafficking modulates growth cone surface receptor availability**

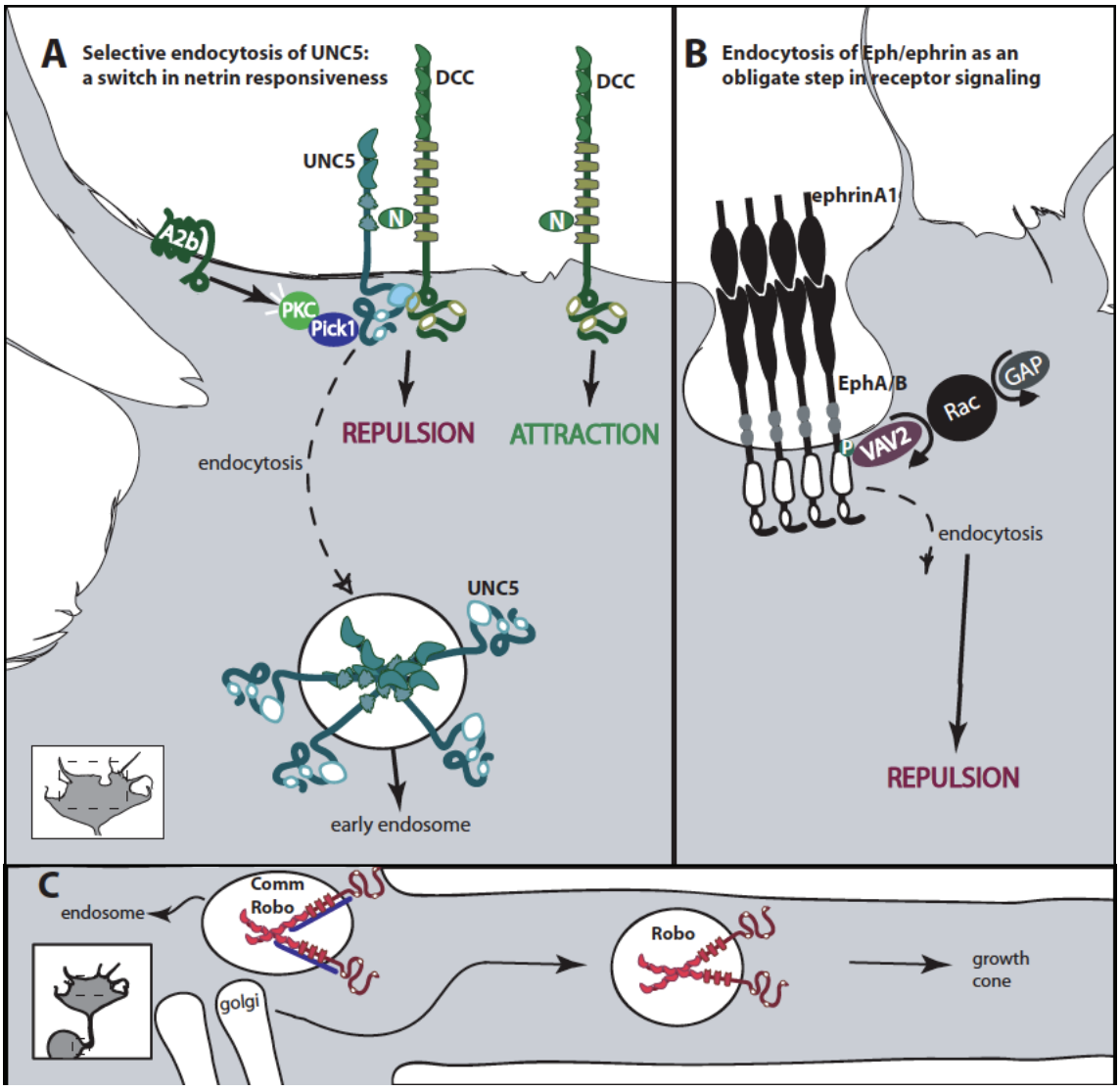

**Figure 1.2: Endocytic trafficking modulates growth cone surface receptor availability**

A: Adenosine2b receptor (A2b) activity leads to PKC-dependent endocytosis of UNC5, which requires a physical interaction between PKC, Pick1, and the cytoplasmic domain of UNC5. This change in receptor composition at the plasma membrane leads to a switch in responsiveness to netrin from repulsion mediated by UNC5 alone, or by an UNC5/DCC complex, to attraction mediated by DCC. N, netrin. B: The Vav family of Rac GEFs is required for endocytosis of ephrin ligand (and presumedly Eph receptor in complex) in retinal ganglion cell growth cones. Vav2 is recruited to the ephrin-stimulated juxta-membrane phosphorylated tyrosine of EphA and EphB receptors and then stimulates endocytosis. This endocytotic event is an obligate step in the forward signaling leading to growth cone retraction or repulsion. C: Diversion of Robo from growth cone delivery to endosomal compartments following biosynthesis in the Trans-Golgi Network is controlled by Commissureless, which negatively regulates the amount of Robo competent to respond to Slit on the growth cone surface.

**Figure 1.3: A dichotomous model for how endocytic trafficking might modulate Robo signaling in the growth cone**

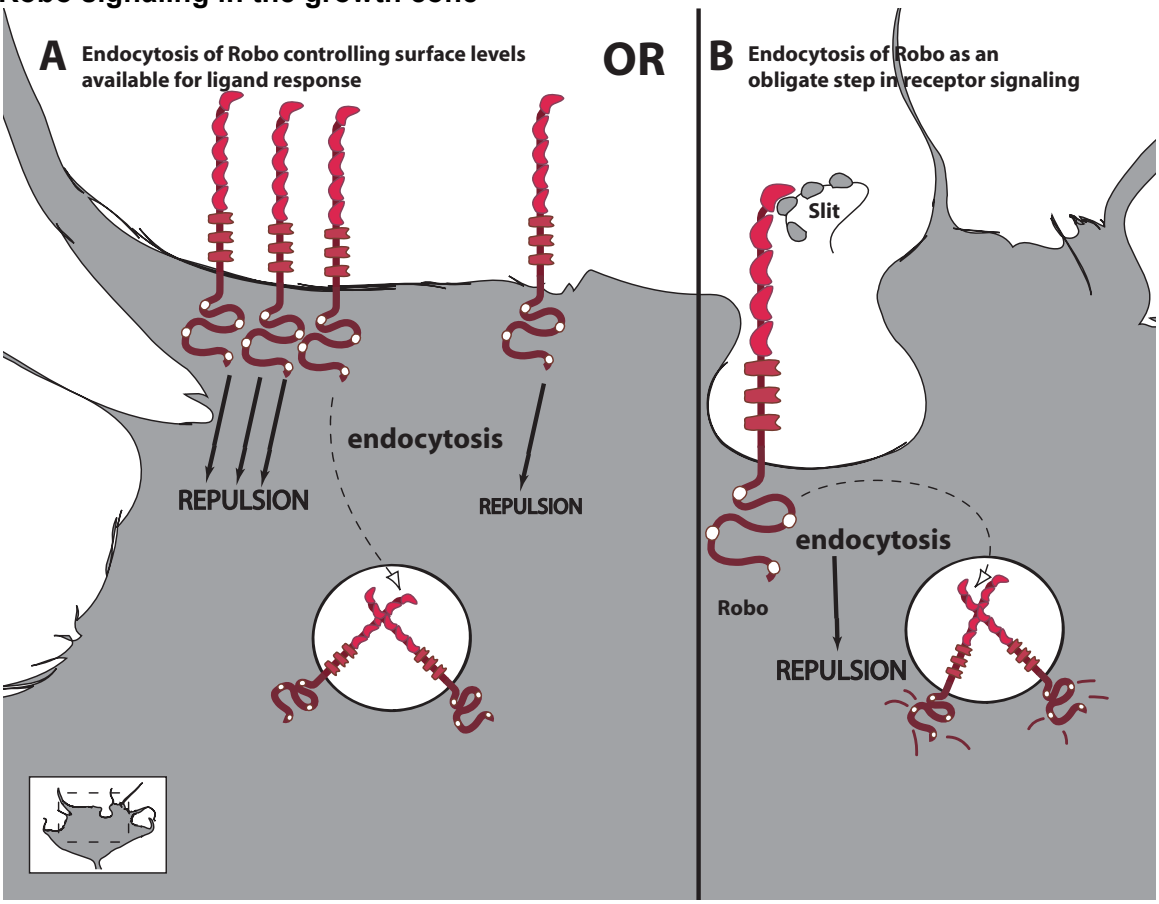

**Figure 1.3: A dichotomous model for how endocytic trafficking might modulates Robo signaling in the growth cone**

If endocytosis regulates our ligand-receptor pair of interest Slit-Robo, we envisioned that this could occur either by contributing to surface occupancy levels before ligand-binding (A), or be an active step in signaling (B). In the first case, endocytosis would remove a portion of the total pool of Robo on the growth cone surface, which would in turn reduce the magnitude of repulsion upon Slit binding, thereby negatively regulating repulsive signaling. Endocytosis that occurs as part of Robo's signaling mechanism would instead positively regulate repulsive guidance.

**Figure 1.4: Regulated proteolysis contributes to guidance molecule function**

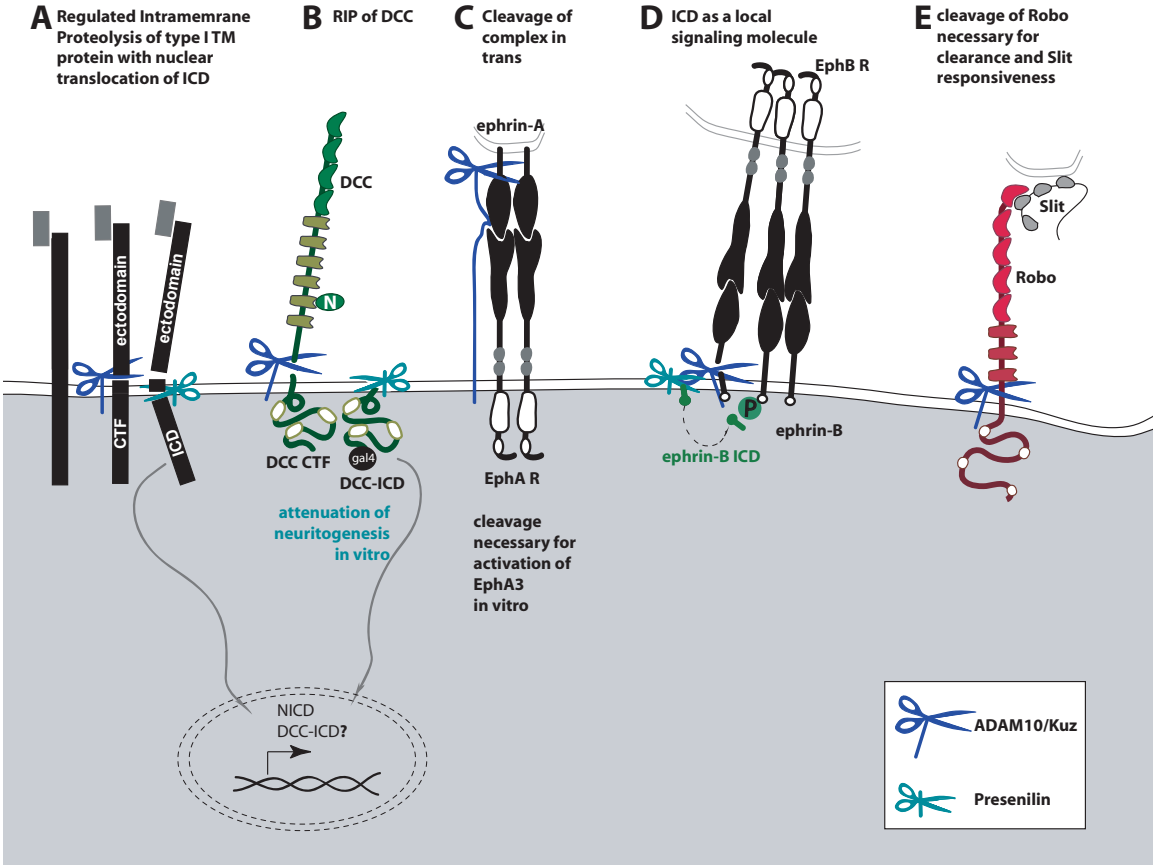

**Figure 1.4: Regulated proteolysis contributes to guidance molecule function**

A: Processive proteolysis of a prototypical type I transmembrane (TM) protein, such as Notch or APP. Upon ligand-binding, cleavage by an ADAM10 in the juxta-membrane region causes release of an N-terminal fragment into the extracellular space (ectodomain) and generates a C-terminal fragment (CTF) with a small extracellular stub. A second, constitutive cleavage by the gamma-Secretase complex within the plane of the plasma membrane releases the intracellular domain (ICD). In the case of Notch, the ICD translocates to the nucleus, where it regulates transcription. B: Regulated proteolysis of DCC occurs by ADAM10-mediated creation of a CTF, followed by gamma-secretase-mediated intramembraneous cleavage releasing DCC ICD. This ICD is competent to translocate to the nucleus when fused to Gal4. The cleavage event by ADAM10 leads to attenuation of neuritogenesis in vitro. C: Following ligand-receptor complex formation, ADAM10 cleaves the ephrin-A5 ligand. This regulated proteolytic event leads to release from the initial cell-cell adhesion, allowing for growth cone retraction, and is necessary for the transduction of the EphA3 forward signal. D: Processive cleavage in the ephrinB/ephB system indicates that the released ephrinB ICD may activate SRC-family kinases to contribute to reverse signaling. On the other hand, cleavage of the EphB2 receptor, in this case by matrix metalloproteases, is required for activation in vitro. E: Kuzbanian acts positively in the Slit-Robo signaling pathway. On the basis of genetic observations and the abnormal presence of Robo protein on the commissural portions of axons in *kuz* mutants, we postulate that Kuz cleaves Robo to regulate receptor activity.

## BIBLIOGRAPHY


Anitha, A., Nakamura, K., Yamada, K., Suda, S., Thanseem, I., Tsujii, M., Iwayama, Y., Hattori, E., Toyota, T., Miyachi, T. et al. 2008. Genetic analyses of roundabout (ROBO) axon guidance receptors in autism. American journal of medical genetics Part B, Neuropsychiatric genetics : the official publication of the International Society of Psychiatric Genetics 147B(7): 1019-1027.

Bai, G., Chivatakarn, O., Bonanomi, D., Lettieri, K., Franco, L., Xia, C., Stein, E., Ma, L., Lewcock, J.W., and Pfaff, S.L. 2011. Presenilin-dependent receptor processing is required for axon guidance. Cell 144(1): 106-118.

Bartoe, J.L., McKenna, W.L., Quan, T.K., Stafford, B.K., Moore, J.A., Xia, J., Takamiya, K., Huganir, R.L., and Hinck, L. 2006. Protein interacting with C-kinase 1/protein kinase Calpha-mediated endocytosis converts netrin-1-mediated repulsion to attraction. J Neurosci 26(12): 3192-3205.

Bashaw, G.J. and Goodman, C.S. 1999. Chimeric axon guidance receptors: the cytoplasmic domains of slit and netrin receptors specify attraction versus repulsion. Cell 97(7): 917-926.

Bashaw, G.J., Kidd, T., Murray, D., Pawson, T., and Goodman, C.S. 2000. Repulsive axon guidance: Abelson and Enabled play opposing roles downstream of the roundabout receptor. Cell 101(7): 703-715.

Beel, A.J. and Sanders, C.R. 2008. Substrate specificity of gamma-secretase and other intramembrane proteases. Cell Mol Life Sci 65(9): 1311-1334.

Brose, K., Bland, K.S., Wang, K.H., Arnott, D., Henzel, W., Goodman, C.S., Tessier-Lavigne, M., and Kidd, T. 1999a. Slit proteins bind Robo receptors and have an evolutionarily conserved role in repulsive axon guidance. Cell 96(6): 795-806.

Butler, S.J. and Dodd, J. 2003. A role for BMP heterodimers in roof plate-mediated repulsion of commissural axons. Neuron 38(3): 389-401.

Campbell, D.S. and Holt, C.E. 2001. Chemotropic responses of retinal growth cones mediated by rapid local protein synthesis and degradation. Neuron 32(6): 1013-1026.

Chang, B.S., Katzir, T., Liu, T., Corriveau, K., Barzillai, M., Apse, K.A., Bodell, A., Hackney, D., Alsop, D., Wong, S.T. et al. 2007. A structural basis for reading fluency: white matter defects in a genetic brain malformation. Neurology 69(23): 2146-2154.

Charron, F., Stein, E., Jeong, J., McMahon, A.P., and Tessier-Lavigne, M. 2003. The morphogen sonic hedgehog is an axonal chemoattractant that collaborates with netrin-1 in midline axon guidance. Cell 113(1): 11-23.

Christoforidis, S., Miaczynska, M., Ashman, K., Wilm, M., Zhao, L., Yip, S.C., Waterfield, M.D., Backer, J.M., and Zerial, M. 1999. Phosphatidylinositol-3-OH kinases are Rab5 effectors. Nature cell biology 1(4): 249-252.

Coleman, H.A., Labrador, J.P., Chance, R.K., and Bashaw, G.J. 2010. The Adam family metalloprotease Kuzbanian regulates the cleavage of the roundabout receptor to control axon repulsion at the midline. Development 137(14): 2417-2426.

Cowan, C.W., Shao, Y.R., Sahin, M., Shamah, S.M., Lin, M.Z., Greer, P.L., Gao, S., Griffith, E.C., Brugge, J.S., and Greenberg, M.E. 2005. Vav family GEFs link activated Ephs to endocytosis and axon guidance. Neuron 46(2): 205-217.

Das, B., Shu, X., Day, G.J., Han, J., Krishna, U.M., Falck, J.R., and Broek, D. 2000. Control of intramolecular interactions between the pleckstrin homology and Dbl homology domains of Vav and Sos1 regulates Rac binding. J Biol Chem 275(20): 15074-15081.

Dickson, B.J. 2002. Molecular mechanisms of axon guidance. Science 298(5600): 1959-1964.

Diefenbach, T.J., Guthrie, P.B., Stier, H., Billups, B., and Kater, S.B. 1999. Membrane recycling in the neuronal growth cone revealed by FM1-43 labeling. J Neurosci 19(21): 9436-9444.

Egea, J. and Klein, R. 2007. Bidirectional Eph-ephrin signaling during axon guidance. Trends Cell Biol 17(5): 230-238.

Falk, J., Konopacki, F.A., Zivraj, K.H., and Holt, C.E. 2014. Rab5 and Rab4 regulate axon elongation in the Xenopus visual system. J Neurosci 34(2): 373-391.

Fan, X., Labrador, J.P., Hing, H., and Bashaw, G.J. 2003. Slit stimulation recruits Dock and Pak to the roundabout receptor and increases Rac activity to regulate axon repulsion at the CNS midline. Neuron 40(1): 113-127.

Fukuhara, N., Howitt, J.A., Hussain, S.A., and Hohenester, E. 2008. Structural and functional analysis of slit and heparin binding to immunoglobulin-like domains 1 and 2 of Drosophila Robo. J Biol Chem 283(23): 16226-16234.

Galko, M.J. and Tessier-Lavigne, M. 2000. Function of an axonal chemoattractant modulated by metalloprotease activity. Science 289(5483): 1365-1367.

Galperin, E. and Sorkin, A. 2003. Visualization of Rab5 activity in living cells by FRET microscopy and influence of plasma-membrane-targeted Rab5 on clathrin-dependent endocytosis. Journal of cell science 116(Pt 23): 4799-4810.

Garbe, D.S. and Bashaw, G.J. 2004. Axon guidance at the midline: from mutants to mechanisms. Crit Rev Biochem Mol Biol 39(5-6): 319-341.

Gatto, G., Morales, D., Kania, A., and Klein, R. 2014. EphA4 receptor shedding regulates spinal motor axon guidance. Curr Biol 24(20): 2355-2365.

Georgakopoulos, A., Litterst, C., Ghersi, E., Baki, L., Xu, C., Serban, G., and Robakis, N.K. 2006. Metalloproteinase/Presenilin1 processing of ephrinB regulates EphB-induced Src phosphorylation and signaling. EMBO J 25(6): 1242-1252.

Gilestro, G.F. 2008. Redundant mechanisms for regulation of midline crossing in Drosophila. PLoS One 3(11): e3798.

Gonzalez-Gaitan, M. and Jackle, H. 1997. Role of Drosophila alpha-adaptin in presynaptic vesicle recycling. Cell 88(6): 767-776.

Guichet, A., Wucherpfennig, T., Dudu, V., Etter, S., Wilsch-Brauniger, M., Hellwig, A., Gonzalez-Gaitan, M., Huttner, W.B., and Schmidt, A.A. 2002. Essential role of endophilin A in synaptic vesicle budding at the Drosophila neuromuscular junction. The EMBO journal 21(7): 1661-1672.

Gupta, G.D., Swetha, M.G., Kumari, S., Lakshminarayan, R., Dey, G., and Mayor, S. 2009. Analysis of endocytic pathways in Drosophila cells reveals a conserved role for GBF1 in internalization via GEECs. PloS one 4(8): e6768.

Hattori, M., Osterfield, M., and Flanagan, J.G. 2000. Regulated cleavage of a contact-mediated axon repellent. Science 289(5483): 1360-1365.

Hines, J.H., Abu-Rub, M., and Henley, J.R. 2010. Asymmetric endocytosis and remodeling of beta1-integrin adhesions during growth cone chemorepulsion by MAG. Nat Neurosci 13(7): 829-837.

Hiramoto, M. and Hiromi, Y. 2006. ROBO directs axon crossing of segmental boundaries by suppressing responsiveness to relocalized Netrin. Nat Neurosci 9(1): 58-66.

Howitt, J.A., Clout, N.J., and Hohenester, E. 2004. Binding site for Robo receptors revealed by dissection of the leucine-rich repeat region of Slit. The EMBO journal 23(22): 4406-4412.

Hsouna, A., Kim, Y.S., and VanBerkum, M.F. 2003. Abelson tyrosine kinase is required to transduce midline repulsive cues. J Neurobiol 57(1): 15-30.

Hu, H., Li, M., Labrador, J.P., McEwen, J., Lai, E.C., Goodman, C.S., and Bashaw, G.J. 2005. Cross GTPase-activating protein (CrossGAP)/Vilse links the Roundabout receptor to Rac to regulate midline repulsion. Proc Natl Acad Sci U S A 102(12): 4613-4618.

Huber, A.B., Kolodkin, A.L., Ginty, D.D., and Cloutier, J.F. 2003. Signaling at the growth cone: ligand-receptor complexes and the control of axon growth and guidance. Annu Rev Neurosci 26: 509-563.

Hutson, L.D. and Chien, C.B. 2002. Pathfinding and error correction by retinal axons: the role of astray/robo2. Neuron 33(2): 205-217.

Itofusa, R. and Kamiguchi, H. 2011. Polarizing membrane dynamics and adhesion for growth cone navigation. Molecular and cellular neurosciences 48(4): 332-338.

Janes, P.W., Saha, N., Barton, W.A., Kolev, M.V., Wimmer-Kleikamp, S.H., Nievergall, E., Blobel, C.P., Himanen, J.P., Lackmann, M., and Nikolov, D.B. 2005. Adam meets Eph: an ADAM substrate recognition module acts as a molecular switch for ephrin cleavage in trans. Cell 123(2): 291-304.

Jekely, G., Sung, H.H., Luque, C.M., and Rorth, P. 2005. Regulators of endocytosis maintain localized receptor tyrosine kinase signaling in guided migration. Dev Cell 9(2): 197-207.

Jen, J.C., Chan, W.M., Bosley, T.M., Wan, J., Carr, J.R., Rub, U., Shattuck, D., Salamon, G., Kudo, L.C., Ou, J. et al. 2004. Mutations in a human ROBO gene disrupt hindbrain axon pathway crossing and morphogenesis. Science 304(5676): 1509-1513.

Johnson, K.G., Ghose, A., Epstein, E., Lincecum, J., O'Connor, M.B., and Van Vactor, D. 2004. Axonal heparan sulfate proteoglycans regulate the distribution and efficiency of the repellent slit during midline axon guidance. Curr Biol 14(6): 499-504.

Jurney, W.M., Gallo, G., Letourneau, P.C., and McLoon, S.C. 2002. Rac1-mediated endocytosis during ephrin-A2- and semaphorin 3A-induced growth cone collapse. J Neurosci 22(14): 6019-6028.

Kamiguchi, H. and Lemmon, V. 2000. Recycling of the cell adhesion molecule L1 in axonal growth cones. J Neurosci 20(10): 3676-3686.

Kapfhammer, J.P. and Raper, J.A. 1987. Collapse of growth cone structure on contact with specific neurites in culture. J Neurosci 7(1): 201-212.

Keleman, K., Rajagopalan, S., Cleppien, D., Teis, D., Paiha, K., Huber, L.A., Technau, G.M., and Dickson, B.J. 2002. Comm sorts robo to control axon guidance at the Drosophila midline. Cell 110(4): 415-427.

Keleman, K., Ribeiro, C., and Dickson, B.J. 2005. Comm function in commissural axon guidance: cell-autonomous sorting of Robo in vivo. Nat Neurosci 8(2): 156-163.

Kennedy, T.E. 2000. Cellular mechanisms of netrin function: long-range and short-range actions. Biochem Cell Biol 78(5): 569-575.

Kidd, T., Bland, K.S., and Goodman, C.S. 1999. Slit is the midline repellent for the robo receptor in Drosophila. Cell 96(6): 785-794.

Kidd, T., Brose, K., Mitchell, K.J., Fetter, R.D., Tessier-Lavigne, M., Goodman, C.S., and Tear, G. 1998a. Roundabout controls axon crossing of the CNS midline and defines a novel subfamily of evolutionarily conserved guidance receptors. Cell 92(2): 205-215.

Kidd, T., Russell, C., Goodman, C.S., and Tear, G. 1998b. Dosage-sensitive and complementary functions of roundabout and commissureless control axon crossing of the CNS midline. Neuron 20(1): 25-33.

Kullander, K. and Klein, R. 2002. Mechanisms and functions of Eph and ephrin signalling. Nat Rev Mol Cell Biol 3(7): 475-486.

Lanahan, A.A., Hermans, K., Claes, F., Kerley-Hamilton, J.S., Zhuang, Z.W., Giordano, F.J., Carmeliet, P., and Simons, M. 2010. VEGF receptor 2 endocytic trafficking regulates arterial morphogenesis. Dev Cell 18(5): 713-724.

Lanier, L.M., Gates, M.A., Witke, W., Menzies, A.S., Wehman, A.M., Macklis, J.D., Kwiatkowski, D., Soriano, P., and Gertler, F.B. 1999. Mena is required for neurulation and commissure formation. Neuron 22(2): 313-325.

Li, G., D'Souza-Schorey, C., Barbieri, M.A., Roberts, R.L., Klippel, A., Williams, L.T., and Stahl, P.D. 1995. Evidence for phosphatidylinositol 3-kinase as a regulator of endocytosis via activation of Rab5. Proc Natl Acad Sci U S A 92(22): 10207-10211.

Lin, K.T., Sloniowski, S., Ethell, D.W., and Ethell, I.M. 2008a. Ephrin-B2 induced cleavage of EphB2 receptor is mediated by matrix metalloproteinases to trigger cell repulsion. J Biol Chem.

Litterst, C., Georgakopoulos, A., Shioi, J., Ghersi, E., Wisniewski, T., Wang, R., Ludwig, A., and Robakis, N.K. 2007. Ligand binding and calcium influx induce distinct ectodomain/gamma-secretase-processing pathways of EphB2 receptor. J Biol Chem 282(22): 16155-16163.

Liu, Z., Patel, K., Schmidt, H., Andrews, W., Pini, A., and Sundaresan, V. 2004. Extracellular Ig domains 1 and 2 of Robo are important for ligand (Slit) binding. Molecular and cellular neurosciences 26(2): 232-240.

Lyuksyutova, A.I., Lu, C.C., Milanesio, N., King, L.A., Guo, N., Wang, Y., Nathans, J., Tessier-Lavigne, M., and Zou, Y. 2003. Anterior-posterior guidance of commissural axons by Wnt-frizzled signaling. Science 302(5652): 1984-1988.

Ma, L. and Tessier-Lavigne, M. 2007. Dual branch-promoting and branch-repelling actions of Slit/Robo signaling on peripheral and central branches of developing sensory axons. J Neurosci 27(25): 6843-6851.

Macia, E., Ehrlich, M., Massol, R., Boucrot, E., Brunner, C., and Kirchhausen, T. 2006. Dynasore, a cell-permeable inhibitor of dynamin. Dev Cell 10(6): 839-850.

Marston, D.J., Dickinson, S., and Nobes, C.D. 2003. Rac-dependent trans-endocytosis of ephrinBs regulates Eph-ephrin contact repulsion. Nat Cell Biol 5(10): 879-888.

Matusek, T., Gombos, R., Szecsenyi, A., Sanchez-Soriano, N., Czibula, A., Pataki, C., Gedai, A., Prokop, A., Rasko, I., and Mihaly, J. 2008. Formin proteins of the DAAM subfamily play a role during axon growth. J Neurosci 28(49): 13310-13319.

Moline, M.M., Southern, C., and Bejsovec, A. 1999. Directionality of wingless protein transport influences epidermal patterning in the Drosophila embryo. Development 126(19): 4375-4384.

Mumm, J.S. and Kopan, R. 2000. Notch signaling: from the outside in. Dev Biol 228(2): 151-165.

Mumm, J.S., Schroeter, E.H., Saxena, M.T., Griesemer, A., Tian, X., Pan, D.J., Ray, W.J., and Kopan, R. 2000. A ligand-induced extracellular cleavage regulates gamma-secretase-like proteolytic activation of Notch1. Mol Cell 5(2): 197-206.

Murray, M.J. and Whitington, P.M. 1999. Effects of roundabout on growth cone dynamics, filopodial length, and growth cone morphology at the midline and throughout the neuropile. J Neurosci 19(18): 7901-7912.

O'Donnell, M., Chance, R.K., and Bashaw, G.J. 2009. Axon growth and guidance: receptor regulation and signal transduction. Annu Rev Neurosci 32: 383-412.

Ohno, H., Stewart, J., Fournier, M.C., Bosshart, H., Rhee, I., Miyatake, S., Saito, T., Gallusser, A., Kirchhausen, T., and Bonifacino, J.S. 1995. Interaction of tyrosine-based sorting signals with clathrin-associated proteins. Science 269(5232): 1872-1875.

Onishi, K., Shafer, B., Lo, C., Tissir, F., Goffinet, A.M., and Zou, Y. 2013. Antagonistic functions of Dishevelleds regulate Frizzled3 endocytosis via filopodia tips in Wnt-mediated growth cone guidance. J Neurosci 33(49): 19071-19085.

Ozdinler, P.H. and Erzurumlu, R.S. 2002. Slit2, a branching-arborization factor for sensory axons in the Mammalian CNS. J Neurosci 22(11): 4540-4549.

Palamidessi, A., Frittoli, E., Garré, M., Faretta, M., Mione, M., Testa, I., Diaspro, A., Lanzetti, L., Scita, G., and Di Fiore, P.P. 2008. Endocytic trafficking of Rac is required for the spatial restriction of signaling in cell migration. Cell 134(1): 135-147.

Pan, D. and Rubin, G.M. 1997a. Kuzbanian controls proteolytic processing of Notch and mediates lateral inhibition during Drosophila and vertebrate neurogenesis. Cell 90(2): 271-280.

Parent, A.T., Barnes, N.Y., Taniguchi, Y., Thinakaran, G., and Sisodia, S.S. 2005. Presenilin attenuates receptor-mediated signaling and synaptic function. J Neurosci 25(6): 1540-1549.

Pasterkamp, R.J. and Kolodkin, A.L. 2003. Semaphorin junction: making tracks toward neural connectivity. Curr Opin Neurobiol 13(1): 79-89.

Piper, M., Anderson, R., Dwivedy, A., Weinl, C., van Horck, F., Leung, K.M., Cogill, E., and Holt, C. 2006. Signaling mechanisms underlying Slit2-induced collapse of Xenopus retinal growth cones. Neuron 49(2): 215-228.

Piper, M., Salih, S., Weinl, C., Holt, C.E., and Harris, W.A. 2005. Endocytosis-dependent desensitization and protein synthesis-dependent resensitization in retinal growth cone adaptation. Nat Neurosci 8(2): 179-186.

Potkin, S.G., Turner, J.A., Guffanti, G., Lakatos, A., Fallon, J.H., Nguyen, D.D., Mathalon, D., Ford, J., Lauriello, J., Macciardi, F. et al. 2009. A genome-wide association study of schizophrenia using brain activation as a quantitative phenotype. Schizophrenia bulletin 35(1): 96-108.

Rooke, J., Pan, D., Xu, T., and Rubin, G.M. 1996. KUZ, a conserved metalloprotease-disintegrin protein with two roles in Drosophila neurogenesis. Science 273(5279): 1227-1231.

Schimmelpfeng, K., Gogel, S., and Klambt, C. 2001. The function of leak and kuzbanian during growth cone and cell migration. Mech Dev 106(1-2): 25-36.

Seeger, M., Tear, G., Ferres-Marco, D., and Goodman, C.S. 1993. Mutations affecting growth cone guidance in Drosophila: genes necessary for guidance toward or away from the midline. Neuron 10(3): 409-426.

Selkoe, D.J. and Wolfe, M.S. 2007. Presenilin: running with scissors in the membrane. Cell 131(2): 215-221.

Seto, E.S. and Bellen, H.J. 2006. Internalization is required for proper Wingless signaling in Drosophila melanogaster. J Cell Biol 173(1): 95-106.

Shu, T. and Richards, L.J. 2001. Cortical axon guidance by the glial wedge during the development of the corpus callosum. J Neurosci 21(8): 2749-2758.

Slessareva, J.E., Routt, S.M., Temple, B., Bankaitis, V.A., and Dohlman, H.G. 2006. Activation of the phosphatidylinositol 3-kinase Vps34 by a G protein alpha subunit at the endosome. Cell 126(1): 191-203.

Slovakova, J., Speicher, S., Sanchez-Soriano, N., Prokop, A., and Carmena, A. 2012. The actin-binding protein Canoe/AF-6 forms a complex with Robo and is required for Slit-Robo signaling during axon pathfinding at the CNS midline. J Neurosci 32(29): 10035-10044.

Sorkin, A., Mazzotti, M., Sorkina, T., Scotto, L., and Beguinot, L. 1996. Epidermal growth factor receptor interaction with clathrin adaptors is mediated by the Tyr974-containing internalization motif. J Biol Chem 271(23): 13377-13384.

Sorkin, A. and von Zastrow, M. 2009. Endocytosis and signalling: intertwining molecular networks. Nature reviews Molecular cell biology 10(9): 609-622.

Taniguchi, Y., Kim, S.H., and Sisodia, S.S. 2003. Presenilin-dependent "gamma-secretase" processing of deleted in colorectal cancer (DCC). J Biol Chem 278(33): 30425-30428.

Teis, D., Taub, N., Kurzbauer, R., Hilber, D., de Araujo, M.E., Erlacher, M., Offterdinger, M., Villunger, A., Geley, S., Bohn, G. et al. 2006. p14-MP1-MEK1 signaling regulates endosomal traffic and cellular proliferation during tissue homeostasis. J Cell Biol 175(6): 861-868.

Tojima, T., Itofusa, R., and Kamiguchi, H. 2010. Asymmetric clathrin-mediated endocytosis drives repulsive growth cone guidance. Neuron 66(3): 370-377.

Tomita, T., Tanaka, S., Morohashi, Y., and Iwatsubo, T. 2006. Presenilin-dependent intramembrane cleavage of ephrin-B1. Mol Neurodegener 1: 2.

Vaccari, T., Lu, H., Kanwar, R., Fortini, M.E., and Bilder, D. 2008. Endosomal entry regulates Notch receptor activation in Drosophila melanogaster. J Cell Biol 180(4): 755-762.

van Bergeijk, P., Adrian, M., Hoogenraad, C.C., and Kapitein, L.C. 2015. Optogenetic control of organelle transport and positioning. Nature 518(7537): 111-114.

van der Bliek, A.M., Redelmeier, T.E., Damke, H., Tisdale, E.J., Meyerowitz, E.M., and Schmid, S.L. 1993. Mutations in human dynamin block an intermediate stage in coated vesicle formation. J Cell Biol 122(3): 553-563.

Wang, K.H., Brose, K., Arnott, D., Kidd, T., Goodman, C.S., Henzel, W., and Tessier-Lavigne, M. 1999. Biochemical purification of a mammalian slit protein as a positive regulator of sensory axon elongation and branching. Cell 96(6): 771-784.

Whitford, K.L., Marillat, V., Stein, E., Goodman, C.S., Tessier-Lavigne, M., Chedotal, A., and Ghosh, A. 2002. Regulation of cortical dendrite development by Slit-Robo interactions. Neuron 33(1): 47-61.

Williams, M.E., Wu, S.C., McKenna, W.L., and Hinck, L. 2003. Surface expression of the netrin receptor UNC5H1 is regulated through a protein kinase C-interacting protein/protein kinase-dependent mechanism. J Neurosci 23(36): 11279-11288.

Wisco, D., Anderson, E.D., Chang, M.C., Norden, C., Boiko, T., Folsch, H., and Winckler, B. 2003. Uncovering multiple axonal targeting pathways in hippocampal neurons. J Cell Biol 162(7): 1317-1328.

Yang, L. and Bashaw, G.J. 2006. Son of sevenless directly links the Robo receptor to rac activation to control axon repulsion at the midline. Neuron 52(4): 595-607.

Yoo, S., Kim, Y., Noh, H., Lee, H., Park, E., and Park, S. 2011. Endocytosis of EphA receptors is essential for the proper development of the retinocollicular topographic map. The EMBO journal 30(8): 1593-1607.

Yoshikawa, S., McKinnon, R.D., Kokel, M., and Thomas, J.B. 2003. Wnt-mediated axon guidance via the Drosophila Derailed receptor. Nature 422(6932): 583-588.

Yu, T.W. and Bargmann, C.I. 2001. Dynamic regulation of axon guidance. Nat Neurosci 4 Suppl: 1169-1176.

Zimmer, M., Palmer, A., Kohler, J., and Klein, R. 2003. EphB-ephrinB bi-directional endocytosis terminates adhesion allowing contact mediated repulsion. Nature cell biology 5(10): 869-878.

## CHAPTER 2: Slit-dependent endocytic trafficking of the Robo receptor is required for Son of Sevenless recruitment and midline axon repulsion

### Introduction

Endocytosis in the growth cone has been implicated in the plasma membrane dynamics necessary for such responses as collapse (Jurney et al. 2002; Castellani et al. 2004; Cowan et al. 2005; Piper et al. 2006), or, when applied asymmetrically, turning (Hines et al. 2010; Tojima et al. 2010; Onishi et al. 2013). Endocytosis has also been implicated in the control over the complement of guidance receptors expressed on the growth cone surface, thereby fine-tuning sensitivity to extracellular cues (Williams et al. 2003; Bartoe et al. 2006; O'Donnell et al. 2009). Endocytic trafficking of Robo by Commissureless has also been demonstrated to negatively regulate delivery to the growth cone surface (Keleman et al. 2002; Keleman et al. 2005). Endocytic trafficking of guidance receptors might serve not only to control surface receptor levels, but also to gate their activation once inside the cell. Evidence for this idea comes from the correlation between a requirement for the RhoGEFs *vav2* and *vav3* in both Ephrin endocytosis and proper retinogeniculate axon targeting (Cowan et al. 2005), as well as the correlation between Rac activity in EphA receptor endocytosis and retinocollicular targeting (Yoo et al. 2011). Whether receptor endocytosis represents a general mechanism to control activation of repulsive guidance receptor signaling and whether the transit of internalized guidance receptors through distinct endocytic compartments is required for *in vivo* signaling is not known.

In this study, we identify Clathrin-dependent endocytosis of the Robo receptor as an obligate step in receptor activation and repulsive signaling. We present evidence that it is trafficking through endocytic compartments - following ligand-binding on the surface of the cell - that is required for receptor activation. We identify - with subcellular

resolution – the early and late endosomes as compartments from which Robo signals, and identify the sequence motifs in Robo's C-terminus that are required for its Slit-dependent internalization. Finally, we show that Slit-dependent endocytosis is required for both *in vitro* recruitment of the Ras/Rho GEF Son of Sevenless (Sos), a downstream effector of Robo repulsive signaling and for Robo-mediated midline repulsion *in vivo*.

**Endocytic trafficking genes genetically interact with *slit and robo***

Based on previous findings suggesting a role for endocytosis in modulating axon guidance receptor activity and signaling, we could envision at least two plausible models for how Robo receptor endocytosis might regulate axon repulsion. If endocytosis modulates the amount of Robo receptor on the surface of the growth cone, a reduction in receptor endocytosis would be predicted to lead to increased levels of surface receptor and more robust repulsive signaling. Alternatively, if Robo receptor endocytosis is an obligate step in receptor activation, preventing or reducing its endocytosis would result in impaired Slit-Robo signaling. To test which, if either, of these functions endocytosis might contribute to Slit-Robo signaling, we first sought genetic evidence implicating endocytic trafficking in midline axon repulsion. We examined an ipsilateral subset of axons whose projection patterns depend on Robo's repulsive response to Slit. In *robo* mutants the FasII-positive fascicles invariably collapse and circle at the midline. Reducing *slit* and *robo* gene dose by half in heterozygous *slit, robo*/+ embryos results in a partial loss of repulsion, which represents a sensitized background in which we can detect both suppressors and enhancers (Fig. 1). We, and others, have used this sensitized genetic background to uncover additional genes that contribute to midline repulsion (Fan et al. 2003; Hsouna et al. 2003; Hu et al. 2005; Coleman et al. 2010). In addition to offering a sensitive readout for alterations in midline repulsion, this strategy

allows us to detect dominant genetic interactions, which avoids potential complications from removing all endocytic gene function, which would be predicted to have broad and early developmental defects.

We screened mutants in known regulators of endocytosis for genetic interactions with *slit* and *robo*, including mutations in genes involved in (1) Clathrin-dependent endocytosis- alpha-adaptin and endophilinA -, (2) entry into the early endosome –rab5- and (3) entry into the late endosome- rab7. In these experiments, we detect genetic enhancement by endocytic trafficking genes, supporting the model in which endocytosis serves as a positive regulator of *slit-robo* midline repulsion. Removing one copy of *α-adaptin* and *endophilinA*- genes involved in cargo loading and formation of clathrin coated pits (Gonzalez-Gaitan and Jackle 1997; Guichet et al. 2002) – enhances the number of crossing errors compared to *slit, robo/+* heterozygotes (Fig. 1B-D). Removing one copy of either *rab5*, which regulates entry into the early endosome, or *rab7,* which regulates entry into the late endosome also enhances ectopic crossing (Fig. 1E, F). In order to corroborate these findings, we tested for genetic interactions between the mutant alleles of endocytic trafficking genes and *slit* in another, more restricted subset of axons (Fig. 2A). Just like the FasII+ subset of axons, the normally ipsilateral Apterous+ (Ap) axons are sensitive to partial loss of repulsion; a loss of one copy of *slit* alone induces ectopic crossing events in 11% of embryonic segments (Fig. 2B). Inhibiting Clathrin-dependent endocytosis in this sensitized background by removing one allele of *α-adaptin* or *endophilinA* enhances the frequency of ectopic crossing events (Fig. 2F). Removing one copy of *rab5* or *rab7* also enhances ectopic crossing errors. These genetic interactions suggest that trafficking from the plasma membrane, and into the early and late endosome positively regulate repulsive midline guidance. Together these

observations are consistent with endocytosis contributing to receptor activation, as opposed to a modulation of surface levels available to bind Slit.

To determine whether the endocytic trafficking events relevant for midline guidance are occurring in neurons, we mis-expressed Dominant-Negative (DN) transgenes to inhibit components of the endocytosis machinery in the Ap neurons. Ectopic expression of DN forms of *shibire*, *Drosophila* Dynamin, (to block scission of endocytic vesicles (van der Bliek et al. 1993; Moline et al. 1999)), Rab5 and Rab7 (to prevent entry into early and late endosomes, respectively), but not Rab4 and Rab11 (to prevent entry into the recycling endosome), results in enhancement of the ectopic crossing defects that are observed in *slit* heterozygotes (Fig2C-F). These findings are consistent with a model in which endocytic trafficking in neurons is contributing to Slit-Robo mediated repulsion. Further, the ectopic crossing events caused by expressing ShiDN or Rab5DN in the Ap axons in *slit* heterozygotes are fully rescued by increasing signaling of the Robo pathway by co-expression of a wild type Robo transgene (Supplemental Fig. S1A): an observation that is consistent with a specific requirement for endocytic regulation during Slit/Robo repulsion. Taken together, these data are consistent with a model in which endocytic trafficking from the plasma membrane into the early and late, but not the recycling endosome of neurons positively regulates Robo-mediated midline repulsion.

However these interactions alone cannot distinguish between the possibilities of endocytosis positively regulating repulsion from the midline, or negatively regulating attraction to the midline. We directly tested the latter hypothesis by assaying whether reducing the dosage of endocytic trafficking genes could enhance the ectopic crossing errors induced by enhanced midline attraction resulting from ectopic expression of the

attractive guidance receptor Frazzled. We detect no statistically significant difference between the observed crossing frequency and the predicted percentage crossing frequency from an additive interaction (Supplemental Fig. S1B), suggesting that endocytosis is not negatively regulating attractive guidance. These observations further support the interpretation that disrupting endocytosis is specifically affecting midline repulsion.

**Clathrin-dependent endocytosis from the cell surface through the early and late endosome positively regulate Robo signaling in vitro**

Our genetic interaction data are consistent with endocytosis in neurons positively regulating Slit/Robo-mediated repulsive guidance, but they do not provide insight into the cell and molecular mechanism. In order to test whether this positive regulation of repulsive signaling is due to endocytosis of the Robo receptor itself, we assayed whether manipulations to Robo's capacity to undergo endocytosis would affect its signaling. Using sequence alignment with known binding motifs to AP-2, the Clathrin adaptor complex expressed specifically on the surface of cells, we identified two tyrosine-based motifs in Robo's C-terminus that are both conserved in human Robo sequence and predicted to be required for loading of Robo into Clathrin-coated pits - (1) YLQY, of the type YXXΦ (Ohno et al. 1995), and (2) YQAGL, like the tyrosine containing sorting signals in the epidermal growth factor receptor (EGFR) and L1/NgCAM (Sorkin et al. 1996; Wisco et al. 2003) (Supplemental Fig. S2J). If Robo's trafficking through the endocytic pathway is required for its repulsive response to Slit binding, then we would predict that both reducing Shibire function, and disrupting Robo's ability to be loaded into Clathrin-coated pits would disrupt Robo signaling.

To explore these possibilities, we developed an *in vitro* system to determine whether endocytosis of the Robo receptor can occur in response to Slit, and whether this

process contributes to receptor signaling. *Drosophila* embryonic cells transfected with Robo that are bath treated for 10 minutes with Slit-conditioned media exhibit a spreading behavior, forming elaborate branched structures (Fig. 3A). In contrast, cells transfected with Robo and treated with CM from cells expressing empty vector show no such response (Fig. 3 and Supplemental Fig. S2B, S4A, B). We have quantified this spreading behavior in two ways- first, we compute the total area of each cells' processes as a number of pixels, and, average across many cells to get a histogram displaying Average Process Area as a function of transfected Robo and type of CM treatment (Fig. 3D). To characterize the branching of processes in Slit-treated cells, we also performed Sholl analyses to compute the complexity of a cell's process field as a function of its radius starting after the cell cortex. These analyses are graphically displayed as the average Sholl profile of many cells treated with Slit CM (Fig. 3D).

To assay whether the observed process elaboration behavior is indeed a readout of Robo activation in response to Slit we tested the following negative control variants of Robo: 1) deletion of the ectodomain (RoboΔEcto (Supplemental Fig. S2A'), 2) deletion of the first immunoglobulin domain (RoboΔIg1, Fig3B), the minimal region that interacts physically with Slit's D2 domain (Howitt et al. 2004; Liu et al. 2004; Fukuhara et al. 2008), or 3) Robo missing its entire C-terminus (ΔC, Fig3C), which is required for all signaling output (Bashaw and Goodman 1999). Each of these mutated forms of Robo show a loss of process elaboration in response to Slit. Robo that is missing its Conserved Cytoplasmic CC2 and CC3 motifs, required for binding of the downstream effectors Ena, Dock, Pak, SOS and therefore Rac activation (Bashaw et al. 2000; Fan et al. 2003; Yang and Bashaw 2006), also display impaired spreading behavior (Supplemental Fig. S2C). These observations support the idea that Robo signaling in

response to Slit binding is required for the Rac-dependent spreading behavior seen in WT Robo-expressing cells.

Next we wanted to test for a role for Clathrin-dependent endocytosis in Robo's ability to generate branched processes in response to Slit treatment. We find that inhibiting endocytosis directly by co-transfection with DN Shibire (Fig. 3E), or treatment with the Dynamin inhibitor Dynasore (Supplemental Fig. S2D), reduces the complexity of processes generated in response to Slit, as does deleting entirely, or point mutating the tyrosine residues of either of the two putative AP-2 binding motifs in Robo's C-terminus (Fig. 3F, G, Supplemental Fig. S2F-H). Deleting both motifs at the same time also results in a smaller maximum radius of the process field (Fig. 3H,Supplemental Fig. S2E), similar to deleting the entire C-terminus, suggesting that the two AP-2 interacting motifs are each required for, and additively contribute to, Robo signaling. The qualitative and quantitative similarity in the process morphology of Slit-treated cells where Robo endocytosis is prevented, either by global disruption (Dynasore or DN Shibire) or by specific Robo mutations, suggests a contribution of receptor internalization to Robo's activation. In addition, we find that endocytic trafficking, beyond internalization from the surface, through the early and late endosome also positively regulate Slit-dependent process elaboration. Inhibiting entry to the early or late endosome by co-expression of DN-Rab5 (Fig. 3I), or DN-Rab7 (Fig. 3J), respectively, also reduces branching complexity in Robo expressing Slit CM-treated cells. These data are consistent with a requirement for Clathrin-dependent endocytosis of the Robo receptor and trafficking into the early and late endosome for Slit-dependent process branching and outgrowth.

**Slit-dependent Robo removal from surface depends on C-terminal motifs**

In order to assess whether Robo's C-terminal putative AP-2 interaction motifs indeed disrupt ligand-dependent endocytosis we directly assayed for a change in surface Robo levels in response to Slit in the same *in vitro* system. Using pHluorin, a pH sensitive GFP tag, on Robo's N-terminus to isolate the signal of surface Robo from the Robo signal in the lower pH environment of most cytosolic compartments, we analyzed the Slit-dependent reduction in surface receptor levels in S2R+ cells (Fig. 4A-F). In cells transfected with wild-type pHluorin–tagged Robo, there is a reduction in the fluorescence intensity of pHluorin in Slit-treated, as compared to control treated cells, which we quantified as a percent decrease in average signal intensity across many cells (Fig. 4A, B, G). This Slit-dependent decrease in surface signal is inhibited by deleting Robo's C-terminus (Fig. 4C, D), suggesting a requirement for signaling in the Slit-dependent reduction in Robo surface levels. Evidence that our small deletions disrupt Clathrin-dependent endocytosis comes from the similarity of their effect on surface levels to the effect observed by inhibiting Shibire with the Dynamin inhibitor drug Dynasore (Macia et al. 2006). In both cases the Slit-dependent decrease in surface Robo is prevented (Fig. 4E, F, Supplemental FigS3), consistent with Slit stimulating Clathrin-dependent endocytosis of Robo.

Analyzing trends in the spatial distribution of surface Robo intensity with reference to anatomical structures reveals clues about the mechanism of Robo internalization and branch formation. Tips of S2R+ processes bear peaks in surface Robo signal (closed arrowheads in Fig. 4A, Supplemental Fig. 3A), which is similar to Robo localization on the tips of filopodia in the developing fly embryo (Kidd et al. 1998a) and in primary *Drosophila* neuron cultures (Slovakova et al. 2012). In the cells that have responded to Slit treatment by reducing their Robo surface levels, presumably by

Clathrin-dependent internalization from the surface, process branch-points are marked by reduction in surface Robo levels (open arrowhead in Fig. 4B). When inhibiting endocytosis, Robo signal stays high on both the processes with enlarged diameters and in the branch points that do exist (open arrowhead Fig. 4F), likely due to lack of Slit-dependent internalization. The correlation between lack of receptor internalization, either by globally inhibiting endocytosis with Dynasore (Supplemental Fig.S4A, B), or by deleting or point-mutating AP-2 adaptor motifs in Robo's C-terminus (Fig. 4E-G,Supplemental Fig. S3C-G), and decreased process elaboration (Fig. 3H,Supplemental Fig.3F-H) suggests that Clathrin-dependent endocytosis of Robo is required for its signaling output.

To test whether the link between endocytic trafficking and Robo signaling is also observed *in vivo*, we analyzed Robo distribution and midline guidance in the embryo. The endogenous expression pattern of Robo throughout the embryonic ventral nerve cord is characterized by commissural exclusion and longitudinal enrichment (Kidd et al. 1998a). If endocytic trafficking of Robo is required for repulsive signaling, we would expect to see a correlation between Robo mislocalization and guidance errors in embryos with defective endocytic trafficking. In fact, when we induce guidance errors by manipulating entry into the early endosome by expressing DN-Rab5 (asterisks, Fig. 4H), we see mislocalization of Robo to the ectopically midline projecting segments of normally ipsilateral axons (open arrowheads, Fig. 4I). This correlation between Robo mislocalization and guidance errors is specific to endocytic trafficking manipulations; when we induce ectopic crossing events by overexpressing the Frazzled attractive guidance receptor (asterisk, Fig. 4J), we find no mislocalized Robo on the crossing portions of axons, despite the similar strength of ectopic crossing events (closed

arrowhead, Fig. 4L). Further, Robo missing its AP-2 adaptor motif is also mislocalized to the commissural segments (open arrowheads Fig4M) of ectopically crossing axons (asterisks, Fig4L). Finally, Robo is mislocalized to the collapsed Ap axon fascicles in embryos deficient for Slit, and to the ectopically crossing portions of axons in *slit,robo/+* double heterozygotes expressing Robo missing its Slit-binding domain (Supplemental FigS3H). Taken together these data suggest that Slit stimulates endocytosis of the Robo receptor, and that this decrease in surface signal is required for receptor signaling in the receiving cell as evidenced by the reduction in process elaboration in S2R+ cells and midline guidance errors *in vivo*.

**Slit induces Robo colocalization with the early endosomal marker Rab5**

If our receptor manipulations indeed disrupt endocytosis, then we would expect to observe an effect on the intracellular trafficking of internalized Robo in experiments where we track Robo's C-terminus *in vitro* following Slit treatment. We find that not only do our C-terminal motif deletions inhibit the Slit-dependent removal of Robo from the surface, but they also reduce Slit-dependent colocalization of Robo with endogenous Rab5, a marker of the early endosome. Immunostaining for Slit and Rab5 reveals colocalization between Slit and the early endosome in cell processes (Fig. 5A, B, P). In response to Slit treatment, we also observe an induction of colocalization between Robo and Rab5, specifically in the varicosities and branchpoints of cell processes (Fig. 5C-E), the same structures that showed Slit-dependent Robo turnover (arrowheads in Fig. 4B and Fig. 5B). We have quantified this response as the percentage change in Manders' overlap coefficient between Slit and Control CM treatment (Fig. 5C-E, Q). Expression of DN-Shibire (Fig. 5F,G), or deletion of Robo's AP-2-binding motifs (Fig. 5K, L), prevents

the Slit-dependent recruitment of Rab5 in cell processes, resulting in less colocalization of Slit with Rab5. There is a concomitant reduction in colocalization of Rab5 with the Robo C-terminal tag in the same endocytosis-deficient conditions (Fig. 5H-Q). These data provide evidence that Slit stimulates the translocation of Robo to the early endosome, and that this process requires Clathrin-dependent endocytosis specifically from the surface of cells.

**Robo endocytosis is required for Sos recruitment**

If Robo endocytosis is required for downstream signaling, then we would predict that inhibiting Clathrin-dependent endocytosis of Robo may prevent the recruitment of Son of Sevenless, which has previously been shown to be recruited to Robo in response to Slit-treatment in mammalian cells (Yang and Bashaw 2006). First, we assayed the relative contribution of Sos to the spreading behavior in our *in vitro* activation assay by co-expressing Sos missing its RacGEF domain (Fig. 6B). This dominant-negative construct blocks the Slit-dependent spreading behavior so effectively that the morphology of these cells are indistinguishable from those expressing Robo missing its entire C-terminus (Fig. 6A), indicating that this *in vitro* activation assay depends on the ability of Sos to activate Rac. Having shown that Sos is required for Robo-dependent cell spreading, we sought to examine the capacity of Robo to direct the subcellular localization of endogenous Sos in response to Slit treatment. Extracting the feature of endogenous Sos fluorescence intensity in processes reveals an increase in signal in Slit CM (Fig. 6D) over Control CM-treated Robo-expressing cells (Fig. 6C, I), consistent with recruitment of Sos to processes in response to Slit treatment. Not only is Sos required for process elaboration in response to Slit, and actively recruited into the processes in

cells treated with Slit, but it also it is also localized to regions previously shown to carry hallmarks of endocytic activity (reduction in surface receptor levels (Fig. 4B) and receptor colocalization with an early endosomal marker (Fig. 5E)). Peaks in endogenous Sos signal in Slit CM processes occur at varicosities and branchpoints (arrowheads Fig. 6D, F), the analogous structures to those enriched for markers of endocytic activity. Further evidence that Sos recruitment to processes depends on Slit binding comes from the observation that deleting the Ig1 domain or deleting the CC2 and CC3 domains also block Sos recruitment (Fig. 6E-F'). Finally, inhibiting Clathrin-dependent endocytosis also abrogates the increase in endogenous Sos signal intensity in Slit-CM- treated processes over Control CM-treated processes (Fig 6. G-H'), consistent with a model in which Sos recruitment requires, and therefore occurs following, Clathrin-dependent endocytosis of the Robo receptor in response to Slit-binding.

**Robo endocytosis is required for axon guidance in vivo**

Next, to test whether Robo endocytosis is important for its activation *in vivo*, we assayed these Robo constructs that are defective in Clathrin-dependent endocytosis for their midline guidance activity. First, we overexpressed either wild-type or mutant Robo transgenes in an otherwise wild-type background in two ectopic repulsion assays. All of the transgenes that we used were tagged with an HA epitope, inserted in the same genomic site and were expressed at comparable levels based on immunostaining for their HA epitope tags (Fig. 7I-K). Driving expression of wild-type Robo in all neurons (Fig. 7B) is sufficient to signal repulsion so strongly that we see 76% of embryonic segments lose their commissures (Fig. 7L). In contrast, none of our endocytosis-

defective deletion constructs are able to disrupt midline crossing when similarly expressed (Fig. 7C, D, L, Supplemental Fig. S5E). We see a similar requirement for endocytosis motifs in a commissural subset of axons- the EW's- whose projection pattern is imaged in Fig. 7E with GFP and schematized on the right as a crossed fascicle. Overexpressing wild-type Robo specifically in this subset (Fig. 7F, I) causes ectopic repulsion from the midline (Fig. 7M). In contrast, Robo missing its endocytosis motifs (Fig. 7G-K, M, Supplemental Fig. S5F, G) does not cause ectopic repulsion, consistent with a requirement for endocytosis of the Robo receptor for its repulsive midline guidance activity *in vivo*. If these AP-2 interaction motifs are indeed required for repulsive signaling then one would predict that over-expressing them might compete with endogenous receptors for access to ligand, thereby acting as a dominant-negative for midline repulsion. Accordingly, in embryos with reduced Slit dosage, expressing a Robo transgene missing both its AP-2 motifs, like that missing its entire C-terminus, does inhibit midline repulsion causing ectopic crossing of the medial-most FasII fascicles (Supplemental Fig. S5B-D).

Finally, to further assess the *in vivo* repulsive function of these receptor variants, we compared the ability of wild-type versus endocytosis-deficient Robo transgenes to rescue the loss of repulsion defects in *robo* mutant embryos in two normally ipsilateral subsets of axons. The FasII-positive axons project in three (Fig. 8A), and the Ap axons project in one fascicle (Fig. 8G), on either side of the midline. In *robo* mutants the medial-most pair of FasII, and both Ap, fascicles collapse onto the midline (Fig. 8B, H). Adding back wild-type Robo transgene either in all neurons or specifically in the Ap subset (Fig. 8C, I) is sufficient to rescue the ipsilateral projection pattern of these axons. In contrast, expressing Robo transgenes missing the AP-2-binding motifs, either singly

or together, cannot rescue the midline crossing errors in *robo* mutants when expressed in all neurons (Fig. 8D-F) or specifically in the Ap ipsilateral subset (Fig. 8J-L), consistent with a requirement for Robo endocytosis in its repulsive guidance function *in vivo.*

**Discussion**

In this study, we demonstrate genetic interactions between endocytic pathway components and Slit-Robo signaling consistent with endocytosis positively regulating repulsive midline guidance. Several lines of *in vitro* evidence support the idea that Slit-binding triggers Robo endocytosis and that this event is important for receptor activation and downstream signaling. First, we find that inhibiting Clathrin-dependent endocytosis by manipulating Dynamin, or by deleting putative Clathrin adaptor AP-2 consensus sites on Robo leads to increased surface occupancy of Robo. Second, Slit stimulation of Robo-expressing cells leads to co-localization between Slit, Robo and the early endosome marker Rab5, and manipulations that block endocytosis globally or that specifically block Robo endocytosis, prevent Robo co-localization with Rab5. Third, inhibiting Clathrin-dependent endocytosis, entry into the early and into the late endosome inhibit the ability of Robo to induce changes in cell morphology, as well as its ability to recruit the downstream effector Sos. In addition, we present *in vivo* evidence that Robo proteins that lack AP-2 binding motifs are unable to induce ectopic repulsion when expressed in all neurons or in subsets of commissural neurons. Finally, we show that in contrast to wild-type Robo, Robo variants missing their AP-2 binding motifs are unable to rescue the midline crossing defects in *robo* mutant embryos. Taken together, these data strongly support the model that Clathrin-dependent endocytosis of Robo in response to Slit serves is a critical step in transmitting Robo's repulsive signal across the plasma membrane.

**How does Robo endocytosis contribute to spatially restricted repulsive signaling?**

In contexts other than axon guidance, endocytic trafficking has been demonstrated to contribute to receptor signaling by allowing receptor recruitment to specific subcellular compartments. In the case of Wingless (Seto and Bellen 2006), Notch (Vaccari et al. 2008), EGFR and PVR (Jekely et al. 2005) and VEGFR2 (Lanahan et al. 2010), receptor activation is regulated by entry into the early endosome in response to ligand-binding at the surface. Regulation of receptor activation by entry into endocytic compartments can occur by gating spatial access to downstream effectors encountered in signaling complexes – such as Rac or CDC42 in the early endosome (Slessareva et al. 2006; Palamidessi et al. 2008), and MEK1 in the late endosome (Teis et al. 2006), reviewed in (Sorkin and von Zastrow 2009). These observations lend precedent to a model in which endocytic trafficking gates Robo's spatial access to downstream effectors, such as Sos.

The subcellular localization pattern of Slit, Robo, Rab5 and Sos in our *in vitro* process elaboration assay support this model; Slit and Robo-C terminal tag demarcate- with their peaks in fluorescence intensity- varicosities and nascent branch points along processes at the 2' early time point (arrowheads in Fig. 5B, E, Supplemental Fig. 4B) which at 10' become annexes within branch points (arrowhead in Fig. 3A, Supplemental Fig. 4D). Within these enlargements occur correlated valleys in surface Robo signal (arrowhead, Fig. 4B) and peaks in markers of both early endosome, Rab5 (arrowheads, Fig. 4B, E, Supplemental Fig. 4B-D) and Sos (arrowhead, Fig. 6D). Taking the formation of branchpoints to be the readout of repulsive signaling in the process elaboration assay, we propose that Slit binds to Robo to induce recruitment of both Rab5 and Sos to create what become hubs of endocytosis activity by two minutes, a timepoint previously verified

as required for Clathrin-dependent endocytosis in S2R+ cells and in growth cones (Piper et al. 2005; Gupta et al. 2009). In this model, Slit binding to the cell is instructing the spatial location of Robo internalization to the early endosome and recruitment of its downstream effector Sos. Consistent with this, when Clathrin-dependent endocytosis is inhibited, Slit binding is intact, but fails to instruct recruitment of Rab5 and therefore there is a correlation between loss of both translocation of Robo from the cell surface to the early endosome, and a blunting of Sos recruitment.

Our data are consistent with a model in which endocytic trafficking is mechanistically contributing to Robo's activation by fully or partially gating access to its downstream effector Sos. Evidence from the literature suggests that Sos recruitment might not occur exclusively at the surface of the cell as we had previously reported (Yang and Bashaw 2006; Coleman et al. 2010), but also in closely apposed early or late endosomal compartments (Galperin and Sorkin 2003). Sos encodes a Pleckstrin Homology (PH) Domain just C-terminal to the Dbl Homology (DH) domain that is required for both its RacGEF function in Slit/Robo midline guidance in the fly (Yang and Bashaw 2006), and the process elaboration Robo activation readout reported here (Fig. 6B). PH domains bind phosphoinositols of the plasma membrane, and are invariably found adjacent to DH domains strongly suggesting a functional link between DH and PH activity. In the case of Sos the PH domain has been suggested to act as a mechanical switch to allow initiation of the RacGEF activity of the DH domain upon conversion of a bound PIP2 to PIP3 by PI3K (Das et al. 2000). Phosphoinositides have also been linked to early endosome fusion; Rab5 actively recruits PI3K, which in turn is required for Rab5-mediated conversion of plasma membrane to early endosome (Li et al. 1995; Christoforidis et al. 1999). It will be interesting to determine whether Sos activation

downstream of Robo is gated by PI3K in concert with recruitment to the Rab5-positive early endosome, as this would provide a mechanism by which Robo activation requires Clathrin-mediated endocytosis and Rab5 activity.

**How are *in vitro* process elaboration and branching related to *in vivo* repulsion?**

At first glance, the ability of Robo to induce elaboration and branching of cell processes *in vitro* may seem inconsistent with a repulsive output; however, our rescue and gain of function genetic data make a strong case that the signaling output that we observe *in vitro* is critical for repulsion *in vivo*. In addition, there is ample precedent for Slit/Robo signaling to induce branching in both *in vitro* and *in vivo* contexts. For sensory afferents that bifurcate and send collaterals into iterative segments of the spinal cord, uniform Slit treatment induces branching *in vitro* either by suspension cultures of Rat DRGs in collagen gels or bath application to rodent trigeminal neurons (Wang et al. 1999b; Ozdinler and Erzurumlu 2002). The branched morphology of the peripheral arbor of trigeminal projections to the eye requires Slit2 and Slit3 and Robo1 and Robo2 (Ma and Tessier-Lavigne 2007). Interestingly, bath application of Slit is sufficient to induce Robo1-dependent growth and branching of dendritic fields of mouse cortical neurons (Whitford et al. 2002), similar to our observations of Slit-induced branching and process growth in S2R+ cells.

**A role for Robo endocytosis in filopodial dynamics?**

Since Robo is enriched in growth cone filopodia it is likely that during active migration Robo-containing filopodia would mediate adhesive interactions with Slit in the extracellular matrix (ECM). Subsequent Slit-induced filopodial retraction likely requires

more than the filopodial dynamics provided by Ena- a Robo effector that is known to localize to the distal tips of filopodia (Lanier et al. 1999; Matusek et al. 2008), since Robo missing its CC2 domain is not fully deficient for midline repulsion (Bashaw et al. 2000). A commonality between our *in vitro* activation assay and previous analyses of growth cone collapse in culture may provide a clue to the mechanism at play. Filopodial contact of a sympathetic growth cone to a retinal neurite is sufficient to initiate an increased rate of growth cone movement- a rapid retraction of an actin-rich structure along the existing axon (Kapfhammer and Raper 1987a), all while filopodia stay attached, suggesting the existence of a retrograde cue from the filopodial point of contact to more proximal growth cone structures. Similarly, live imaging of pHluorin-Robo-expressing S2R+ cells in our assay reveals that bath-treatment of Slit CM induces an increase in the rate of motility of engorged plasma membrane along existing processes, leaving branch points behind (data not shown). Given that the process elaboration response we observe requires the RacGEF domain of Sos, it is likely that the increased rate of motility upon Slit treatment is due to alterations in Rac-dependent actin dynamics. Since the process elaboration and branching behavior also requires endocytic trafficking from the cell surface to the late endosome, we can speculate that Robo endocytosis is required to direct the Sos-induced actin motility required for spreading *in vitro*. It is the same receptor manipulations that abrogate Clathrin-dependent endocytosis *in vitro* that lead to impaired repulsive signaling *in vivo*, strongly supporting the idea that Robo endocytosis is required for proper repulsive output in the growth cone, perhaps by allowing the actin-based motility that leads to filopodial retraction and growth cone repulsion.

**What might the relevance of Robo endocytosis be to a migrating growth cone?**

Might Slit-binding trigger a similar endocytic trafficking cascade in a growth cone, thereby mobilizing Robo so that it could serve as the retrograde cue informing growth cone behavior from the tips of filopodia? Evidence from others shows that Clathrin-dependent endocytosis exists in the right time and place to play such a role in guidance behavior. First, markers of endocytic compartments, including the early endosome, have been identified in the growth cone (Falk et al. 2014; van Bergeijk et al. 2015). If endocytosis serves as a general mechanism for expanding the spatial range of an activated receptor after exposure to ligand on filopodial tips, then we would expect to see examples of correlation between guidance cues trafficking retrogradely and guidance behavior. Endocytosis of guidance molecules in the growth cone has been shown to be initiated both from the base of the growth cone central domain and from the tips of filopodia (Itofusa and Kamiguchi 2011; Onishi et al. 2013). Retrograde movement of endoyctic compartments has been reported in the growth cone and in the case of internalized L1CAM movement occurs at the rate of F-actin retrograde flow (Diefenbach et al. 1999; Kamiguchi and Lemmon 2000), providing evidence that endocytic trafficking provides an effective spatial track from which a guidance cue might influence the cytoskeleton to affect growth cone behavior. The timing reported by others of endocytosis in the growth cone also shows correlation with the endocytic trafficking of Robo we characterize here *in vitro*. At the same two minute timepoint we report Slit induces Robo removal from S2R+ cell surface here, Sema-3A has affected both a reduction in Neuropilin-1 levels (Piper et al. 2005)– and growth cone collapse in the Xenopus RGC growth cone, albeit with different ligand concentrations (Campbell and Holt 2001). Finally, Frizzled endocytosis in a migrating growth cone reveals a correlation

between filopodial dynamics and Frizzled endocytosis, allowing for the transduction of the presence of an asymmetrically applied gradient of guidance cue into a turning response (Onishi et al. 2013). It remains to be determined whether retrograde Robo movement from the tips of filopodia is required for repulsion in response to Slit.

Finally, here we have addressed how an endocytic cascade positively contributes to signaling from the Robo receptor, effectively expanding our conception of the spatial range of activated receptor within the growth cone. While allowing exposure to the machinery within the growth cone beyond filopodial tips would be required for behaviors such as growth cone retraction or turning in response to filopodial contact with Slit, allowing a receptor to signal too far from the spatial origin of its cue might ultimately prove confusing to a growth cone. It will be interesting to learn if there is a process that serves to curtail signaling from an endocytosed and activated receptor.

## Materials and Methods

### Genetics

The following Drosophila mutant alleles were used: *robo*$^{GA285}$, *robo*$^{z1772}$, *robo*$^{5}$, *slit*$^{1}$, *slit*$^{2}$, *slit*$^{e158}$, *endoA*$^{EP297}$, *endoA*$^{\Delta 4}$, *endoA*$^{10}$, *ada*$^{1}$, *ada*$^{3}$, *rab5*$^{2}$, P[lacW]Rab5$^{k08232}$, P[EPgy2]Rab7$^{EY10675}$, *rab7*$^{FRT82B/knock\text{-}out}$. The following transgenes were used: P[UAS-Shi.K44A]4-1;UAS[*shi.K44A]3-7*, P[UASp-YFP-Rab5.S43N], P[UASp-YFP-Rab7.T22N]06, P[UASp-YFP-Rab4.S22N]37, P[UASp-YFP-Rab5.S25N]35. The following transgenic flies were generated by BestGene Inc (Chino Hills, CA) using ΦC31-directed site-specific integration into landing sites at cytological position 86F8

(controlling for expression level effects from chromosomal position): P*[5xUAS-3xHA-Robo-6xmyc]86Fb, P[5xUAS-3xHA-Robo$^{\Delta YLQY}$-6xmyc]86Fb, P[5xUAS-3xHA-Robo-1xmCherry]86Fb, P[5xUAS-3xHA-Robo$^{\Delta YQAGL}$-1xmCherry]86Fb, P[5xUAS-3xHA-Robo$^{\Delta YQAGL}$-6xmyc]86Fb, P[5xUAS-3xHA-Robo$^{\Delta YLQY\Delta YQAGL}$ -6xmyc]86Fb, P[10xUAS-3xHA-Robo$^{\Delta Ig1}$]86Fb, P[10xUAS-3xHA-Robo$^{\Delta C}$-6xmyc]86Fb, P[GAL4-elav.L]3 (elav-GAL4), eg$^{MZ360}$ eg-GAL4* (Ito *et al.* 1995), *ap-GAL4* (Calleja *et al.* 1996). All crosses were carried out at 25°C. Embryos were genotyped using balancer chromosomes carrying *lacZ* markers or by the presence of epitope-tagged transgenes.

**Molecular Biology**

<u>*pUAST cloning:*</u> Robo coding sequences were cloned into a pUAST vector (p5UASTAttB) including 5xUAS and an attB site for ΦC31-directed site-specific integration. All p5UASTattB constructs include identical heterologous 5' UTR and signal sequences (derived from the Drosophila wingless gene) and an N-terminal 3×HA tag. Robo domain deletion variants created for this study were generated by PCR and include the following amino acids (numbers refer to Genbank reference sequences AAF46887 [Robo]: Robo$^{\Delta Ig1}$ (153-1395) (Evans et al 2014), Robo$^{\Delta C}$ (56-950) (Evans et al 2014), Robo$^{\Delta YLQY}$ (1090-1093), Robo$^{\Delta YQAGL}$ (1233-1237), Robo$^{\Delta YLQY\,\Delta YQAGL}$ (1090-1093; 1233-1237), Robo$^{Y1090A}$ (1090), Robo$^{Y1233A}$ (1233), Robo$^{Y1090A,Y1233A}$ *(1090;1233).* All Robo constructs used in the *in vitro* S2R+ activation assay were cloned into the 5xUAS-AttB plasmid containing 3xHA(N) and 6xMyc(C) tags, or 3xHA no C-terminal Tag (Barry Dickson, shuttled into p5AttB here), or 3xHA-1xpHluorin: The pHluorin-Robo tag was added with the following primers: TAGCTAGCAGCAAAGGAgAAGAAc, CGATCGAGATCCGGAGCTAGCTA. 1x-mCherry C-terminal tag was obtained by PCR

amplification of mCherry CDS genomic extraction of mCherry::CAAX flies (Kyoto DGRC courtesy of Roger Tsien) using the following primers: at**actagt**atggtgagcaagggc, atatata**gcggccgc**TTActtgtacagctcgtcca to swap out the 6xMyc tag using SpeI/NotI sites; or deletion of the 3xHA tag to include 6xMyc tag only by first deleting the BmtI sites in the backbone using the following primers: AAATGCTTGGATTTCACTGGAACTAGGCTTTCATAACTTCGTATAATGTATGCTATAC GAAGTTATGCTAGCG,CGCTAGCATAACTTCGTATAGCATACATTATACGAAGTTATG AAAGCCTAGTTCCAGTGAAATCCAAGCATT,GGCTTTCATAACTTCGTATAATGTATG CTATACGAAGTTATGCTTTCGGATCCAAGCTGGCCG,CGGCCAGCTTGGATCCGAA AGCATAACTTCGTATAGCATACATTATACGAAGTTATGAAAGCC, (also the template for ΔIg1 in p5AttB) then serial overlap extension PCR with the following primers: tatatata**GAATTC**TATCATACCCCGTGTGTCAGTGTG,GCTCGATGATACGTGGATCTA A**GCTAGC**GCGCGCCCTTCCGGAT,ATCCGGAAGGGCGCGCGCTAGCTTAGATCCA CGTATCATCGAGC, GTTTGATTGGCAGGTCCGATTTGAA. Robo ΔEcto (3xHA/6xMyc) was created by PCR using the following primers: tatataCGCTAGCatg**ACCACTGACTACCTATCTGGACC,** tcgggtggctattgggatgc. RoboΔYLQY was created using the following primers: TTGTCAAATCCAAC**CCGGTTGAACCGATCA,**TGATCGGTTCAACCGG**GTTGGATTT GACAA**; ALQY: GTCAAATCCAAC**gcc**CTTCAGTATCCG, CGGATACTGAAGGGCGTTGGATTTGAC; ΔYQAGL: CAGCCAGCGAG**AATGCAGCG,** CGCTGCATTCTCGCTGGCTG; AQAGL: CAGCCAGCGAG**gcCCAGGCT,** AGCCTGGgcCTCGCTGGCTG;

*pALG cloning:* *WT* Rab5 and *WT* Rab11 were obtained from Dr. Avital Rodal in the Actin5C promoter N-terminal GFP-tag pALG plasmid. The Rab5 Dominant-Negative

(DN) S43N point mutation was created with the following primers:CGAGTCCGCTGTGGGCAAGAACTCACTGGTGCTGCGCTTCG,CGAAGCGCAGCACCAGTGAGTTCTTGCCCACAGCGGACTCG. *WT* Rab7 was obtained from BDGP Gold Collection (clone ID GH03685) and shuttled into pALG using the following primers:**tatataGCGGCCGCCCCCTTCACCATG**ATGTCCGGACGTAAGAAATCCCTACTGAA, **TATATATAcgatcg**TTAGCACTGACAGTTGTCAGGATTGCC. The Rab7 T22N point mutation was created by PCR with the following primers:TGTGGGCAAGAACTC

TCTGATGAAT, GATTCATCAGAGAGTTCTTGCCCACACT. *shibire* cDNA was PCR amplified from pOT2 BDGP Gold Collection clone (LD21622) and shuttled to pALG using the following primers:**ataGCGGCCGCCCCCTTCACCATG**atggatagtttaattacaattgtta

acaagctgcaa,**TATATATAcgatcg**attacttgaatcgcgaactgaaggcat. Shibire K44A (DN) was created using the following primers:gaactttgtgggc**GC**agatttcttgcc,**ggcaagaaatctGCgc**

**ccacaaagttc.**

**Immunofluorescence and Imaging**

<u>*in vitro* Robo activation assay</u>: *Drosophila* S2R+ cells were cultured at 25°C in Schneider's media plus 10% FBS and 1% Penicillin-Streptomycin. To assay for Slit response, cells were plated on acid-etched, poly-L-lysine coated coverslips in duplicate in six-well plates (Robo-expressing cells) at a density of 1-2×$10^6$ cells/mL, and transfected with 0.25ug of p5AttB construct and pMT-GAL4/2mL Schneider's (a one-day lag between CM and Robo cells) using Effectene transfection reagent (Qiagen). GAL4 expression was induced with 0.5 mM $CuSO_4$ for 24 hours, then Slit-Conditioned Media

(CM) was collected and concentrated from cells transfected with empty pUAST vector or Slit. Robo-transfected cells were incubated with CM on an orbital shaker at room temperature for 2 (pHluorin, Rab5 colocalization, Sos recruitment) or 10 minutes (process area/Sholl analysis), then fixed for 10 minutes at RT in 4% PFA. Cells were rinsed with 1XPBS, permeabilized with PBS+0.1% Triton X-100 (PBT) for 2 minutes, then blocked for 1Hr and stained with antibodies diluted in PBT+4% NGS, except for the pHluorin surface assay, which used no detergent and MetOH-free PFA. Antibodies used were: mouse anti-Slit-C (c555.6D, DSHB, 1:100), mouse anti-cMyc (9E10, 1:1000), rabbit anti-cMyc (Sigma c3956, 1:1000), rabbit anti-GFP (Invitrogen #A11122, 1:1000), rabbit anti-HA (Covance, 1:1000), rabbit anti-*d*Rab5 (abcam 31261,1:1000), rabbit anti-*d*Rab7 (Tanaka & Nakamura 2008, 1:3000), rabbit anti-Sos (SantaCruz C23 1:500), Cy3 goat anti-mouse (Jackson Immunoresearch, 1:1000), and Alexa488 goat anti-rabbit (Molecular Probes, 1:500). Coverslips were mounted in Aquamount. 0.252μM totalZ confocal stacks were collected using a Leica TCS SP5 confocal microscope at 63X and zoom3 and processed with FIJI and hand-calculations in Excel.

*Quantification*: The morphological profiles of S2R+ cells were generated by binary thresholding the signal from Slit or Myc (Robo-Cterm epitope tag), then we manually defined a region of interest cropping out the variably sized cell cortices and computed the total pixel area of the process (FIJI histogram: count-mode), and averaged across many cells for each genotype to compute average process area. For the Sholl analysis a manually drawn ray defined the center of the cell with a starting radius manually defined starting after the cell cortex and continuing until the maximal radius of the process field (with any intervening cells cleared from the background) was entered into FIJI Sholl plugin. The resulting number of intersections from multiple cells were

concatenated onto a common radius scale in Excel and the average number of intersections for each radius/genotype was plotted, only for the radii for which more than one cell had process field. For colocalization analysis a region of interest around the processes was defined and in Robo-C/Rab5 signal was subtracted Myc -80, Rab5 -15 across the whole image, then the average Mander's Overlap Coefficient from FIJI Coloc2 algorithm in the Slit-only condition for Slit-Rab5, or the ratio of SlitCM/Control CM for RoboMyc-Rab5, from representative cells (n's indicated in histograms).

Embryos: Dechorionated, formaldehyde-fixed, methanol-devitellinized *Drosophila* embryos were fluorescently stained using standard methods. The following antibodies were used in this study: FITC-conjugated goat anti-HRP (Jackson # 123-095-021, 1:250), mouse anti-Fasciclin-II/mAb 1D4 [Developmental Studies Hybridoma Bank, (DSHB), 1:100], mouse anti-βgal (DSHB, 1:150), Alexa-488 conjugated goat-anti-HRP (Jackson #123-605-021 1:100), Cy3-conjugated goat anti-mouse (Jackson #115-165-003, 1:1000), Alexa-488-conjugated goat anti-rabbit (Molecular Probes #A11008, 1:500). Embryos were filleted and mounted in 70%glycerol/1XPBS and imaged on Leica TCS SP5 at 63X with a zoom of 1.7. Images were processed using FIJI.

**Biochemistry**

Control and Slit CM were boiled for 10' in 2X SDS Loading Buffer. Proteins were resolved by SDS Page and transferred to nitrocellulose and incubated with anti-Slit-C (C555-6D) 1:100 overnight at 4°C in PBS/0.05% Tween-20/5% non-fat dry milk. Blots were incubated with HRP-conjugated anti-mouse secondary antibody for 1 hour at RT and signal was detected using ECL Prime (Amersham).

**Robo Endocytosis Figures**

**Figure 2.1: Genetic interactions between Clathrin-dependent endocytosis, and endocytic trafficking genes, and *slit* and *robo***

**Chance_Figure 1**

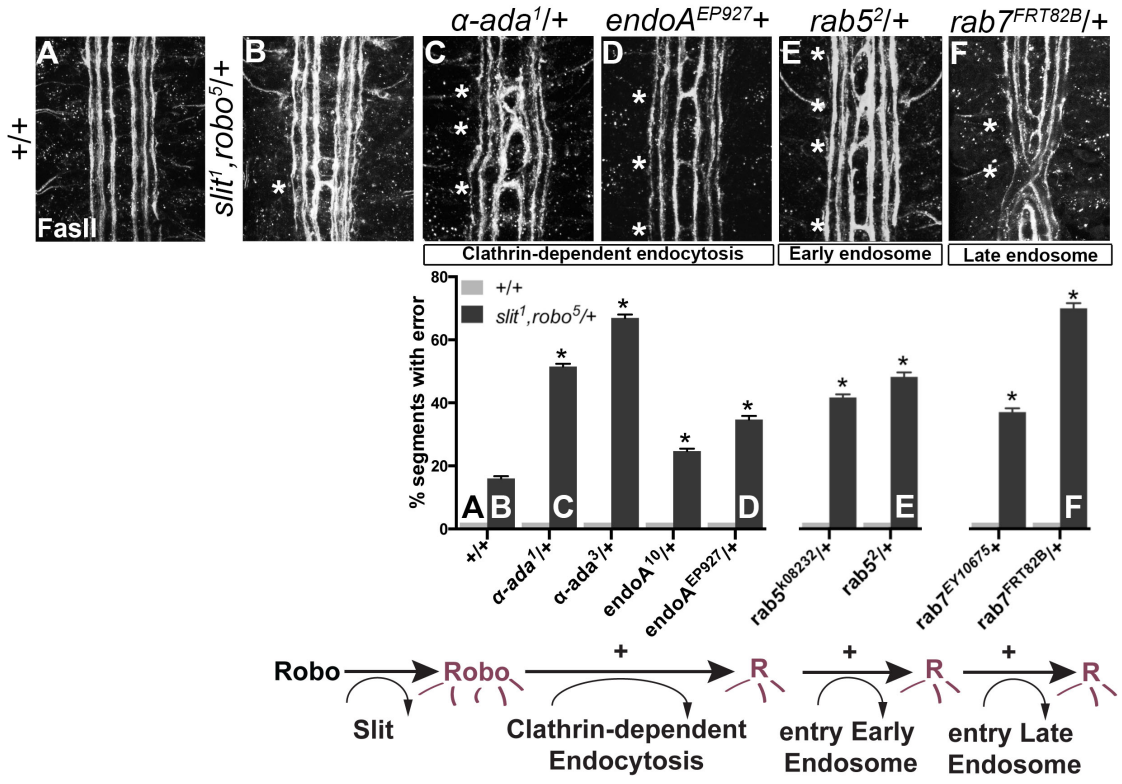

**Figure 2.1: Genetic interactions between Clathrin-dependent endocytosis, and endocytic trafficking genes, and *slit* and *robo***

(A) An ipsilateral subset of axons in the ventral nerve cord of *WT* stage 16 *Drosophila* embryos are stained with a monoclonal antibody (mAb) to FasciclinII (FasII), and quantified in the histogram below as having 0% error in the number of embryonic segments with fascicles crossing the midline. (B) Double heterozygous *slit, robo* embryos have a mild loss-of-repulsion phenotype (induction of ectopic crossing events in 16% of embryonic segments). Inhibiting Clathrin-dependent endocytosis by removing one copy of either *α-adaptin* or *endophilinA* in the *slit,robo/+* background enhances the number of crossing defects (C, D), as does inhibiting either entry into the early endosome by removing one copy of *rab5* (E), or entry into the late endosome by removing one copy of *rab7* (F). These genetic enhancements of the *slit,robo/+*, but not of the *+/+,* ectopic crossing frequency are statistically significant (*, indicates $p<0.0001$) by two-way ANOVA, Sidak's 95% Confidence Interval. Error bars indicate standard error of the mean. (+/+ n (number of segments)=121, $slit^{1},robo^{5}$/+: 132; $\alpha$-$ada^{1}$/+ 121, $\alpha$-$ada^{1}$/ $slit^{1},robo^{5}$ 99; $\alpha$-$ada^{3}$/+ 121, $\alpha$-$ada^{3}$/ $slit^{1},robo^{5}$ 154; $endoA^{10}$/+ 121, $slit^{1},robo^{5}$/+; $endoA^{10}$/+ 154; $endoA^{EP927}$/+ 121, $slit^{1},robo^{5}$/+; $endoA^{EP927}$/+ 121; $rab5^{k08232}$/+ 121, $slit^{1},robo^{5}/rab5^{k08232}$ 154; $rab5^{2}$/+ 121, $slit^{1},robo^{5}/rab5^{2}$ 121; $rab7^{EY10675}$/+ 121, $slit^{1},robo^{5}$/+; $rab7^{EY10675}$/+ 176; $rab7^{FRT82B}$/+ 121, $slit^{1},robo^{5}$/+; $rab7^{FRT82B}$/+ 154.)

**Figure 2.2: Genetic interactions between Dominant-Negative Transgenes for Clathrin-dependent endocytosis, and endocytosis through the late endosome, and slit**

***Chance_Figure 2***

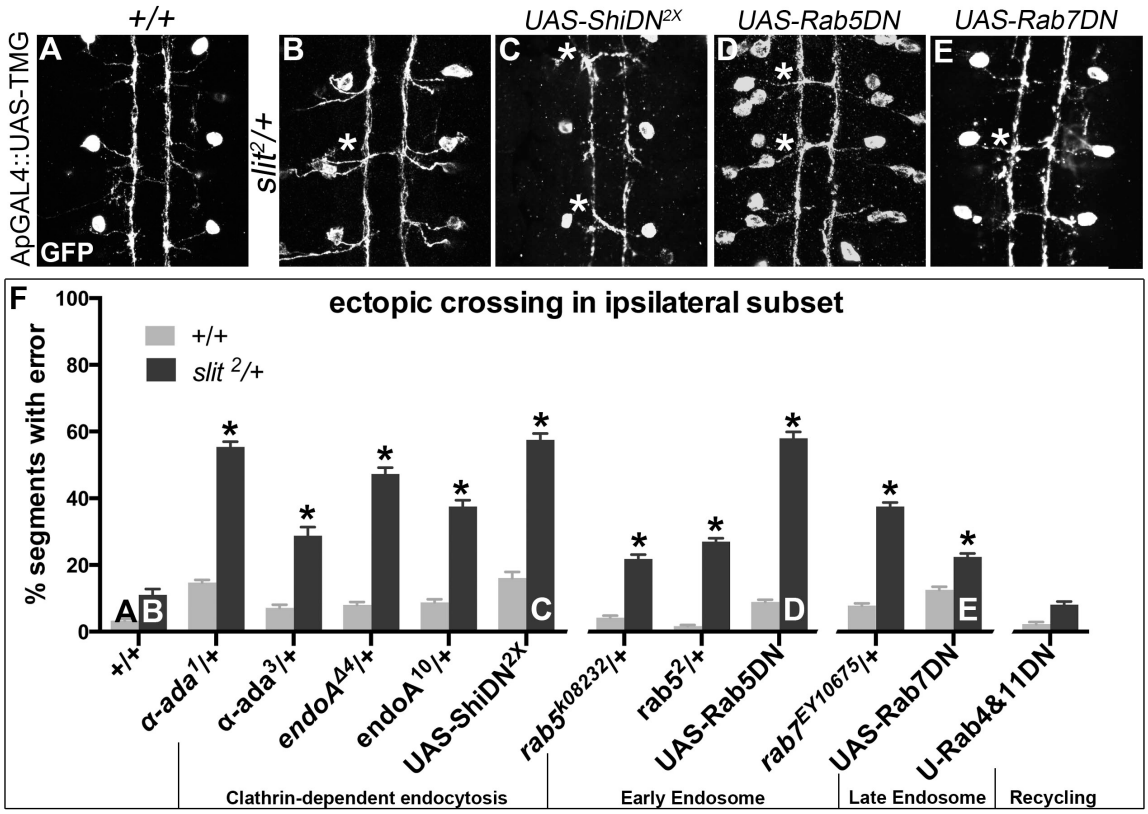

**Figure 2.2: Genetic interactions between Dominant-Negative Transgenes for Clathrin-dependent endocytosis, and endocytosis through the late endosome, and *slit***

A more restricted ipsilateral subset of axons are genetically labeled with Tau-Myc-GFP transgene to highlight their microtubules and therefore axonal projection patterns. (A) In stage 16 WT embryos the two Ap axon fascicles on either side of the midline project ipsilaterally in all embryonic segments (3 shown here, 8 abdominal scored). (B) In animals where one copy of *slit* has been removed, a partial loss of repulsion phenotype results with 11% of segments exhibiting ectopic crossing events (indicated by *). (C) Inhibiting Clathrin-dependent endocytosis in a WT background by adding in Dominant-Negative (DN) transgenes to Shibire, the fly homolog to Dynamin, causes ectopic crossing errors in the Ap axons. (D) Inhibiting entry into the early endosome by expressing DN-Rab5 Transgene causes ectopic crossing, which enhances the background level present in *slit* heterozygotes. (E) Inhibiting entry into the late endosome with DN-Rab7 transgene expression also causes loss of repulsion, which enhances the background level of crossing in *slit* heterozygotes. (F) Histogram: Inhibiting entry into the recycling endosome does not enhance the background crossing in *slit* heterozygotes. These genetic enhancements are statistically significant (*, indicates $p<0.0001$)) by two-way ANOVA, Sidak's 95% Confidence Interval. Error bars indicate standard error of the mean.

(+/+ n (number of segments)=112, $slit^2$/+: 104; $\alpha\text{-}ada^1$/+ 320, $\alpha\text{-}ada^1$/ $slit^2$ 112; $\alpha\text{-}ada^3$/+ 112, $\alpha\text{-}ada^3/slit^2$ 80; $endoA^{\Delta 4}$/+ 88, $slit^2$/+; $endoA^{\Delta 4}$/+ 112; $endoA^{10}$/+136, $slit^2$/+; $endoA^{10}$/+ 120; *UAS-ShiDN*/+;UAS-ShiDN/+ 112, $slit^2$/UAS-ShiDN; *UAS-ShiDN*/+ 80; $rab5^{k08232}$/+ 144, $slit^2/rab5^{k08232}$ 110; $rab5^2$/+ 232, $slit^2/rab5^2$ 152; UAS-Rab5DN/+ 168, $slit^2$/+; UAS-Rab5DN/+ 88; $rab7^{EY10675}$/+ 128, $slit^2$/+; $rab7^{EY10675}$/+ 112; UAS-Rab7DN/+

128, *slit*$^{2}$/+; UAS-Rab7DN/+ 152; *UAS-Rab4DN*/+;UAS-Rab11DN/+ 128, *slit*$^{2}$/UAS-Rab4DN; *UAS-Rab11DN*/+ 136.) See also Supplemental Figure1.

**Figure 2.3: Clathrin-dependent endocytosis from the cell surface through the early and late endosome positively regulate Robo signaling in vitro**

Chance_Figure3

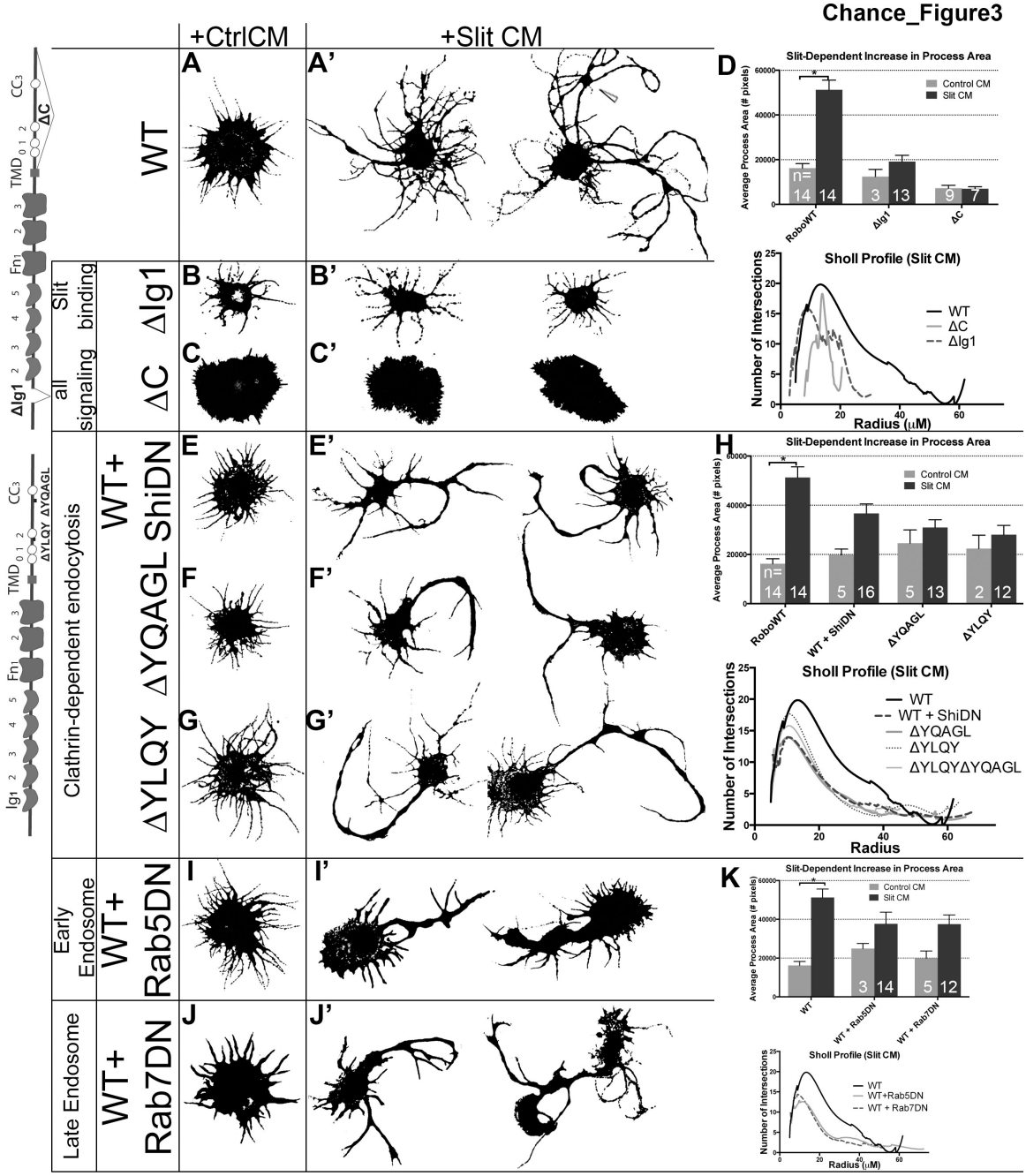

**Figure 2.3: Clathrin-dependent endocytosis from the cell surface through the early and late endosome positively regulate Robo signaling *in vitro***

Morphological profiles of Drosophila embryonic cells bath treated for 10' with Conditioned Media (CM) from cells either expressing empty vector ("Control", A-C, E-G, I-J), or secreting Slit (A-C', E-G', I-J'). Cells expressing WT Robo that are treated with Control CM show a baseline level of process generation (A) that are more branched and elaborated if Slit treated, with two representative examples shown in (A'). This change is quantified as an increase in the average process area of multiple cells in the histogram, which is statistically significant by Two-way ANOVA, Sidak's 95% Confidence Interval (n's denoted on histogram). Error bars indicate standard error of the mean (D: n's displayed on each bar). The Sholl analysis profile below reflects process field complexity as a function of the cells' radii for cells treated with Slit CM (WT n=13, ΔC n=5, ΔIg1 n=8). (B) Cells that express Robo missing their Slit-binding motif (ΔIg1), do not elaborate processes in response to Slit treatment (B'), and show a smaller total process area, and a drop in the process field maximum radius in the Sholl profile (D). (C) Cells expressing Robo that lacks the ability to signal (ΔC-terminus) show short processes that don't branch or elaborate in response to Slit treatment (C', D, E, E'). Inhibiting Clathrin-dependent endocytosis directly by cotransfection of WT Robo with DN-Shibire, the fly homolog of Dynamin, causes no change in the average process area of cells treated with Control CM but a defect in process elaboration in response to Slit treatment as compared to WT alone (A'), quantified as a decrease in the total process area in cells treated with Slit CM and a downward shift in the Sholl profile (H: ShiDN n=13, ΔYQAGL n=13, ΔYQAGL n=12, ΔYLQYΔYQAGL n=10).

(F, G) Cells expressing Robo carrying deletions of either of two motifs predicted to be required for binding to AP-2, the Clathrin-adaptor complex expressed on the surface of

cells, look similar to cells in (E'). (I, J) Inhibiting entry into the early (I'), or late (J') endosome by co-expression of DN-Rab5, or DN-Rab7, respectively, with WT Robo causes a decrease in total process area, and a downward shift in the Sholl profile (K: Rab5DN n=14, Rab7DN n=13). See also Supplemental Fig. 2.

**Figure 2.4: Clathrin-dependent Endocytosis is required for removal of Robo from the cell surface**

**Chance_Fig4:**

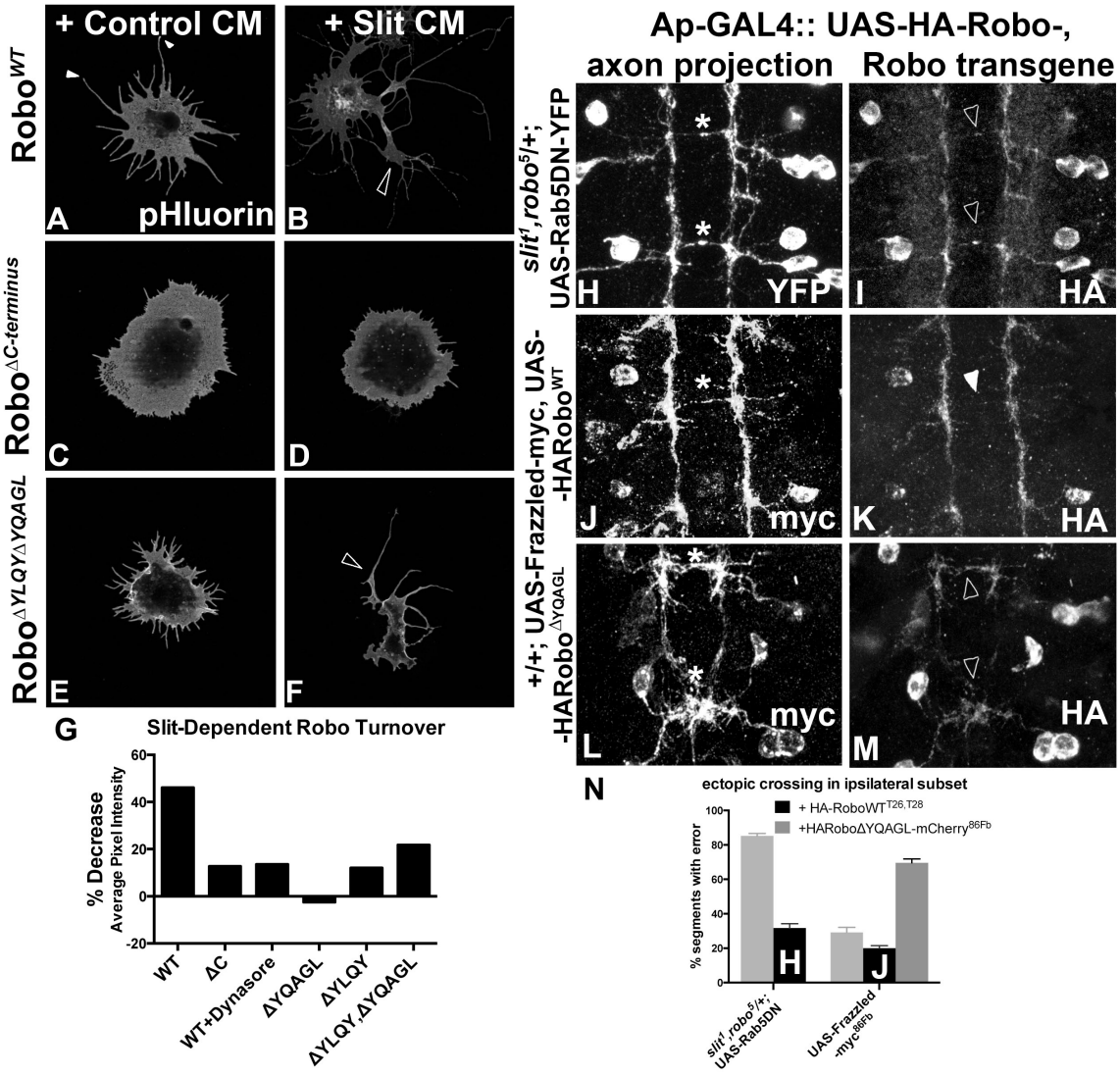

**Figure 2.4: Clathrin-dependent Endocytosis is required for removal of Robo from the surface**

An N-terminal pH sensitive tag on Robo (A-F) reveals the pool of Robo expressed on the surface of S2R+ cells after 2' of conditioned media (CM) bath-treatment. S2R+ cells treated with CM from cells expressing Slit (B) as opposed to empty vector (A) show a decrease in surface levels of Robo, quantified in (G) as a percent decrease in average pixel intensity value of processes in (B) as compared to (A). (C, D) Inhibiting Robo signaling by deleting the entire C-terminus shunts the Slit-dependent reduction in average pixel intensity value of surface Robo, leading to a smaller percentage decrease in (G). (E, F) Deleting both of Robo's putative AP-2 motifs abrogates the Slit-dependent reduction in surface receptor levels, leading to a smaller % decrease in average pixel intensity in (G). (H-M) The ectopic crossing events of a normally ipsilateral subset of axons in the ventral nerve cord of Stage 16 *Drosophila* embryos are induced by either manipulating entry to the early endosome with expression of DN-Rab5 transgene (H), or by overexpression of an attractive guidance receptor, Frazzled (J, L). Robo transgene is mislocalized to the ectopically crossing segments of axons in embryos defective for endocytic trafficking (I) but not in those with excessive attractive guidance (K), despite the similarity in strength of ectopic crossing phenotype (N). In contrast, Robo transgene defective for AP-2 binding is mislocalized to the ectopically crossing segments of axons (M) in the same gain of attraction background (L). See also Supplemental Fig. 3.

**Figure 2.5: Slit induces Robo colocalization with Rab5 in cell processes**

Chance_Fig5

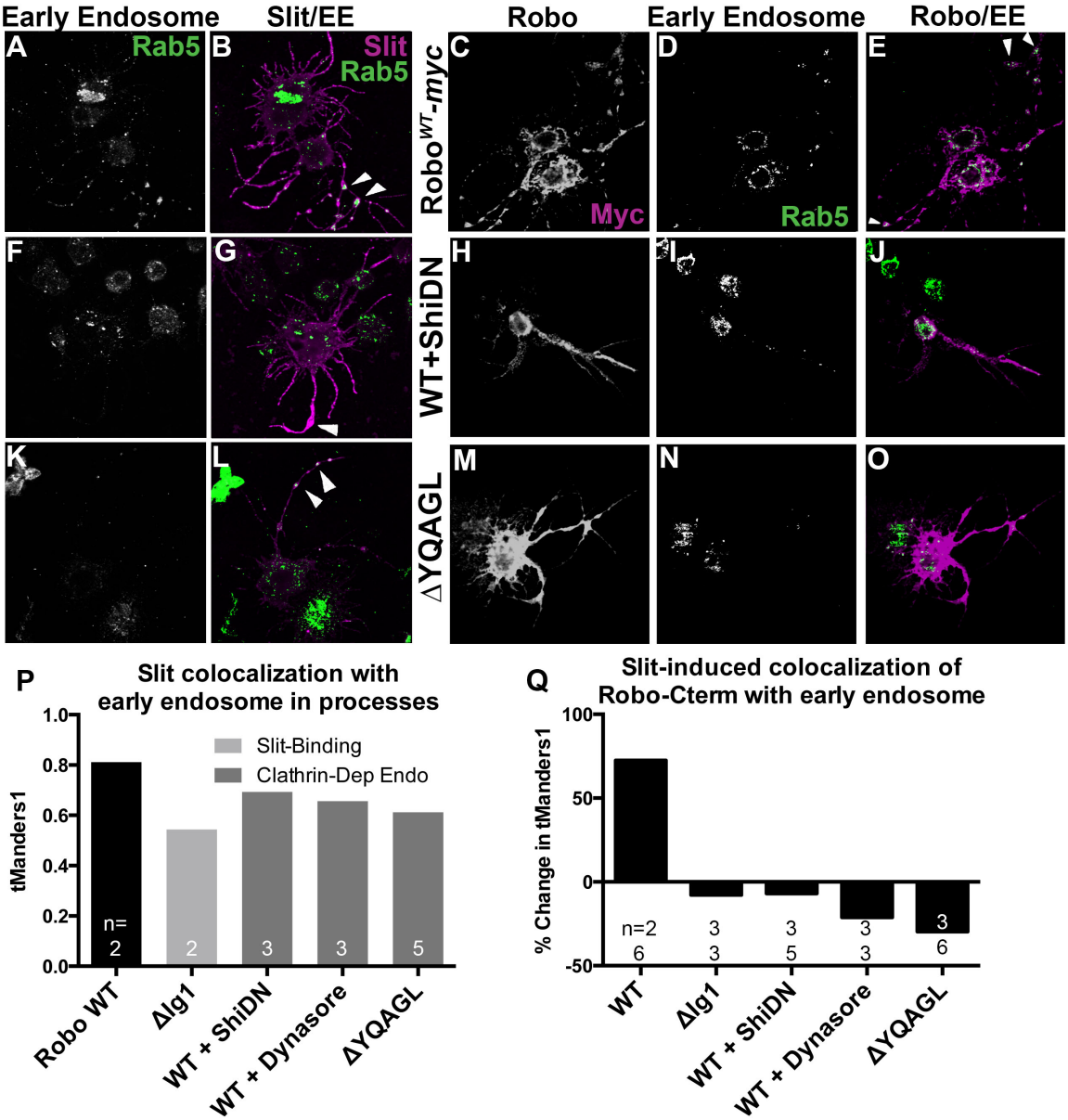

**Figure 2.5: Slit induces Robo colocalization with Rab5 in cell processes**

S2R+ cells expressing Robo and treated with SlitCM were fixed at an earlier timepoint (2') and stained for endogenous Rab5, a marker of the early endosome, (A, D, F, I, K, N) and either bound Slit ligand (B, G, L), or Robo's C-terminal tag (C, H, M). Cells with Slit bound to processes show covariance between ligand and early endosome signal (B, P (n=# cells indicated below histogram bar)). This colocalization is reduced either by reducing Slit-binding (ΔIg1 in P), or by inhibiting Clathrin-dependent endocytosis globally with DN-Shibire (F, G), or the Dynamin inhibitor Dynasore (P), or by deleting Robo's AP-2-binding motifs (K, L). Treatment with Slit CM induces colocalization between Robo and Rab5 in processes as compared to cells treated with Control CM, quantified as a percent increase of thresholded Mander's Overlap Coefficient between Slit and Control CM (E, Q). Inhibiting Clathrin-dependent endocytosis by coexpression with DN-Shibire (H-J), use of Dynasore, or deleting AP-2 adaptor motifs (M-O), or inhibiting Slit-binding by deleting the first Ig domain, causes a loss of Slit-dependent colocalization between Robo C-terminus and the early endosome in processes, quantified as the percent change in colocalization between Slit and Control CM. The percentage change switches from positive to negative (Q (n's for Ctrl CM on top, Slit CM on bottom). See also Supplemental Fig. 4.

**Figure 2.6: Robo Endocytosis is required for Sos recruitment in vitro**

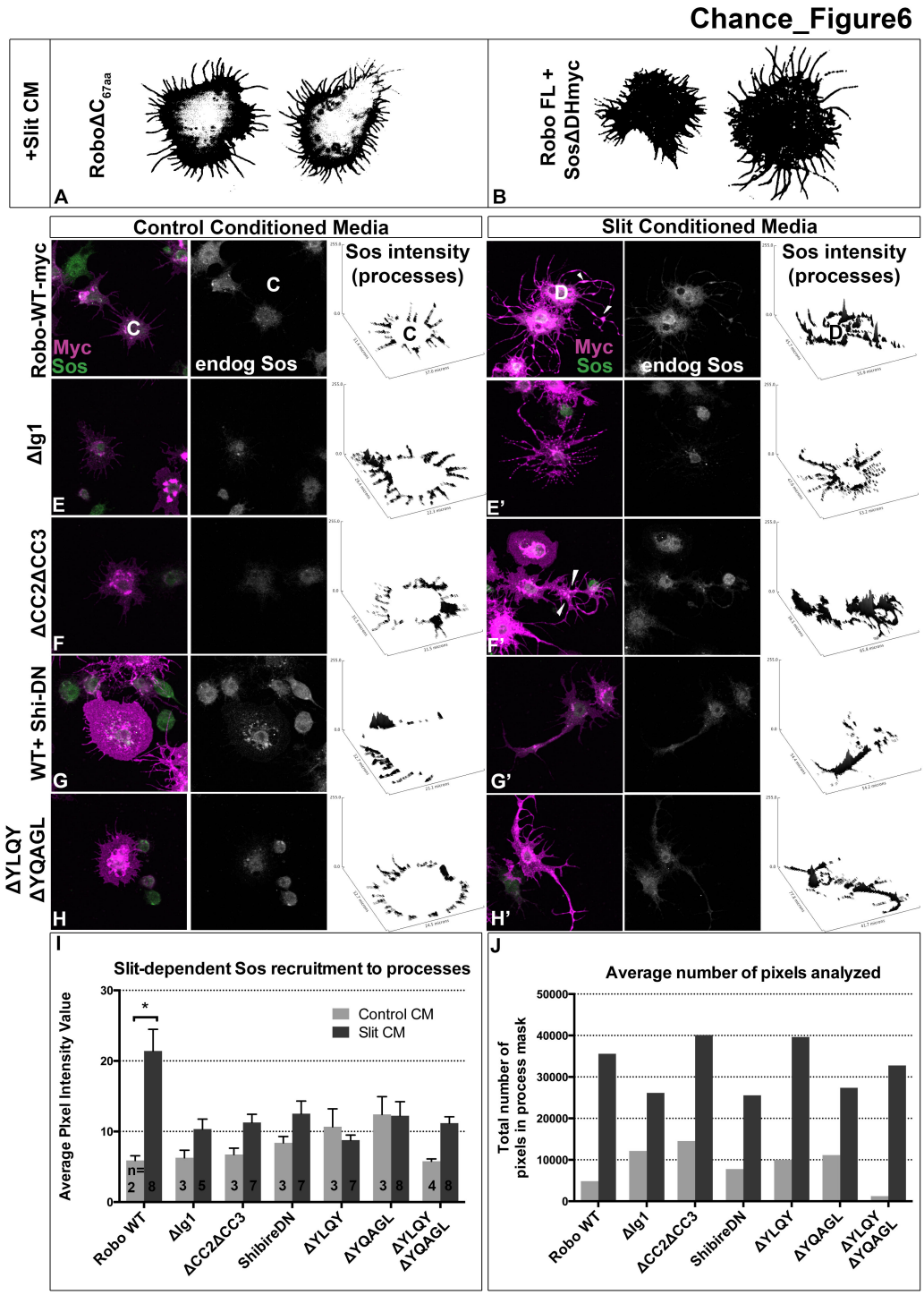

**Figure 2.6: Robo Endocytosis is required for Sos recruitment *in vitro***

Co-expression of a version of Son of Sevenless dominant-negative for its RacGEF activity (B) inhibits spreading and branching of processes in response to Slit CM as effectively as deleting Robo's entire C-terminus (A). Feature extraction of the pixel intensity of endogenous Sos in processes reveals recruitment of Sos to processes in Slit (D) versus Control CM (C) treatment. The increase in Sos signal in processes in response to Slit seen in $Robo^{WT}$-expressing cells, quantified in the histogram as a statistically significant increase (*) in average signal intensity (I, n's displayed on histogram), is missing in cells expressing Robo$\Delta$Ig1 (E, E'). Cells expressing a Robo$\Delta$CC2$\Delta$CC3 receptor that can't bind Ena or Dock, required for Sos binding (F, F') also show impaired recruitment of endogenous Sos to processes, as do conditions inhibiting endocytosis (G-H'), despite comparable number of pixels (process area) analyzed (J). Statistical significance quantified by two-way ANOVA, Sidak's 95% Confidence Interval. Error bars indicate standard error of the mean.

**Figure 2.7: Endocytosis motifs are required for ectopic repulsion in vivo**

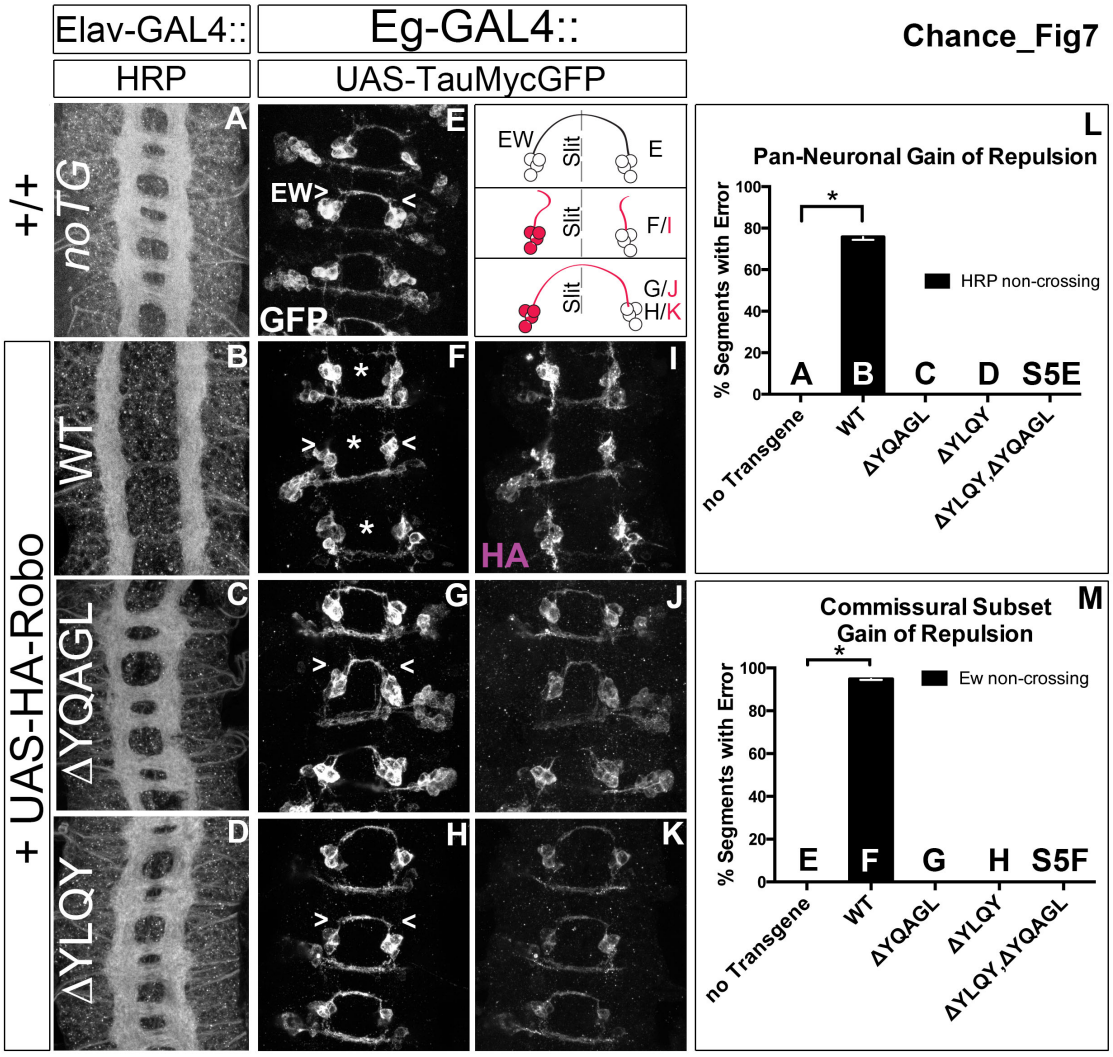

**Figure 2.7: Endocytosis motifs are required for ectopic repulsion *in vivo***

The projection pattern of all axons of the ventral nerve cord of late stage 14 *Drosophila* embryos are imaged with HRP (A-D) and the fascicles of the Eg commissural subset are imaged with a Tau-myc-GFP transgene (E-H). (A) In wild-type embryos, all segments (3 shown here) have two horizontal commissures, which are quantified as 0% of segments with error in the histogram (L n=88). (B) Overexpressing wild-type Robo transgene in all neurons causes gain of repulsion from midline Slit, resulting in a loss of commissures in 76% of embryonic segments (L, n=99). In contrast, overexpressing similar levels of Robo transgene that is missing its AP-2 binding motifs (C, D) can not signal ectopic repulsion from the midline, with all segments projecting in a commissural pattern indistinguishable from embryos without transgene (L ΔYQAGL n=152, ΔYLQY n=136, ΔYLQYΔYQAGL n=88). (E) The Ew commissural subset of axons, schematized on the right, cross the midline in each embryonic segment, quantified as 0% error in (M, n=88). (F) Expressing wild-type Robo transgene (I) specifically in the Ew commissural subset of axons is sufficient to cause ectopic repulsion, with loss of projection across the midline (schematized in dotted gray) in 96% of embryonic segments (M, n=99). In contrast, expressing either RoboΔYQAGL (G, J) or RoboΔYLQY (H, K) does not cause ectopic repulsion of the Ew projection pattern, with a 0% error in (M, ΔYQAGL n=152, ΔYLQY n=136, ΔYLQYΔYQAGL n=88). Error bars indicate standard error of the mean. See also Supplemental Fig. 5.

**Figure 2.8: Robo Endocytosis is required for axon guidance *in vivo***

**Chance_Fig8**

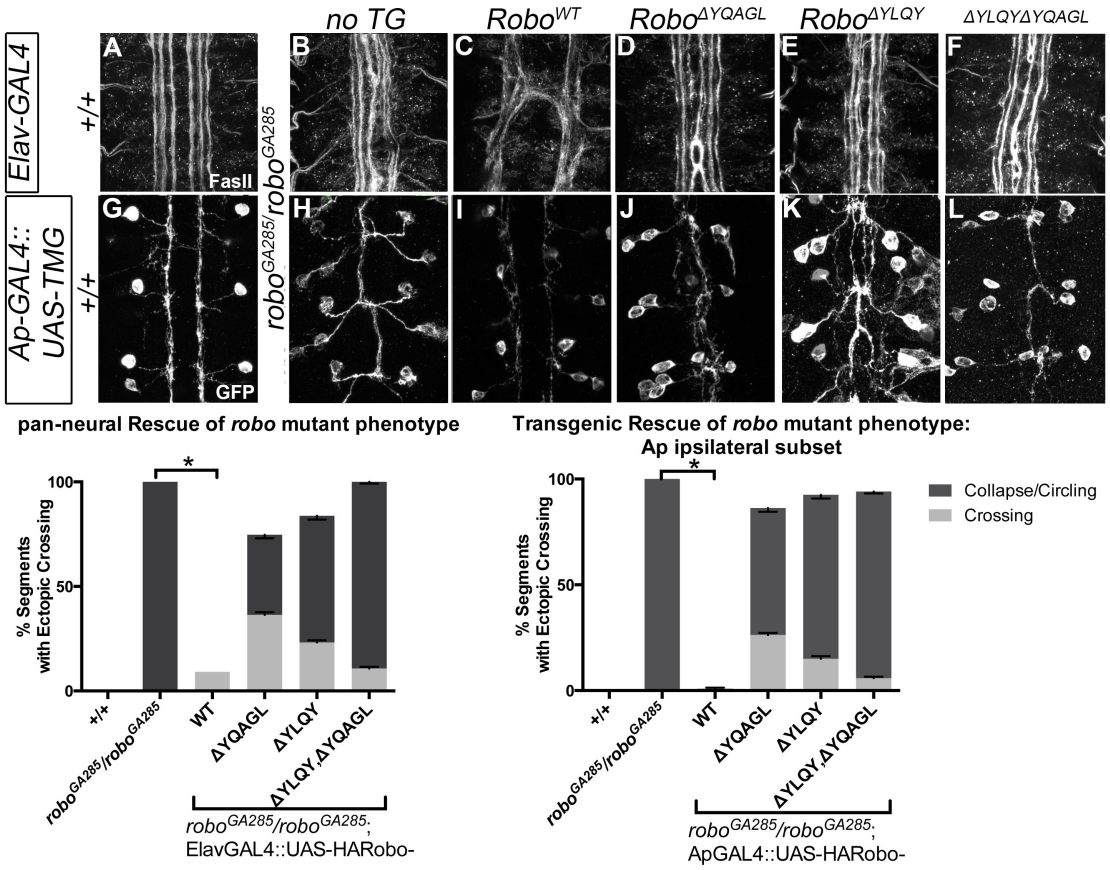

**Figure 2.8: Robo Endocytosis is required for axon guidance *in vivo***

Two ipsilateral subsets of axons are imaged in Stage 17 *Drosophila* embryos- the FasII+ axons with a monoclonal antibody to FasII (A-F) and the Ap axons (G-L) with a GFP antibody detecting Tau-Myc-GFP transgene. In wild-type embryos these ipsilateral subsets project on either side of the midline, with three fascicles on either side for FasII (A) and one fascicle on either side for Ap (G). In *robo* mutant embryos, the two medial-most of the FasII+ fascicles (B) and both of the Ap fascicles (H) collapse onto the midline, scored as 100% of embryonic segments having ectopic collapse/circling events. Expressing wild-type Robo transgene is sufficient to restore repulsive signaling and therefore rescue the crossing defects in the FasII+ axons (C, +/+ n=121, $robo^{GA285}/robo^{GA285}$ n=121, $robo^{GA285}/robo^{GA285}$;ElavGAL4/UAS-Robo$^{WT}$ n=121) and the Ap axons (I +/+ n=120, $robo^{GA285}/Ap,\ robo^{z1772}$ n=120, $robo^{GA285}/Ap,\ robo^{z1772}$;UAS-RoboWT n=80). In contrast, expressing RoboΔYQAGL (D, J), RoboΔYLQY (E, K), or RoboΔYQAGL ΔYLQY (F, L) is not sufficient to rescue the ectopic crossing events, with a large portion of embryonic segments carrying severe errors (crossing/circling events represented by dark gray) remaining. Dark gray indicates a qualitatively more severe crossing error, light gray indicates a less severe crossing error, with the stacked histogram bar height indicating total % of embryonic segments with loss-of-repulsion errors for each genotype. Error bars indicate standard error of the mean. ($robo^{GA285}/robo^{GA285}$; ElavGAL4/UAS-Robo$^{\Delta YQAGL}$ n=154, $robo^{GA285}/robo^{GA285}$; ElavGAL4/UAS-Robo$^{\Delta YLQY}$ n=99, $robo^{GA285}/robo^{GA285}$; ElavGAL4/UAS-Robo$^{\Delta YLQY\Delta YQAGL}$ n=121. $robo^{GA285}/ApGAL4,\ robo^{z1772}$;UAS-Robo$^{\Delta YQAGL}$ n=80, $robo^{GA285}/ApGAL4,\ robo^{z1772}$;UAS-Robo$^{\Delta YLQY}$ n=120, $robo^{GA285}/ApGAL4,\ robo^{z1772}$;UAS-Robo$^{\Delta YLQY\Delta YQAGL}$ n=136.)

**Figure 2.9: A model for how Endocytosis might contribute to Robo signaling**

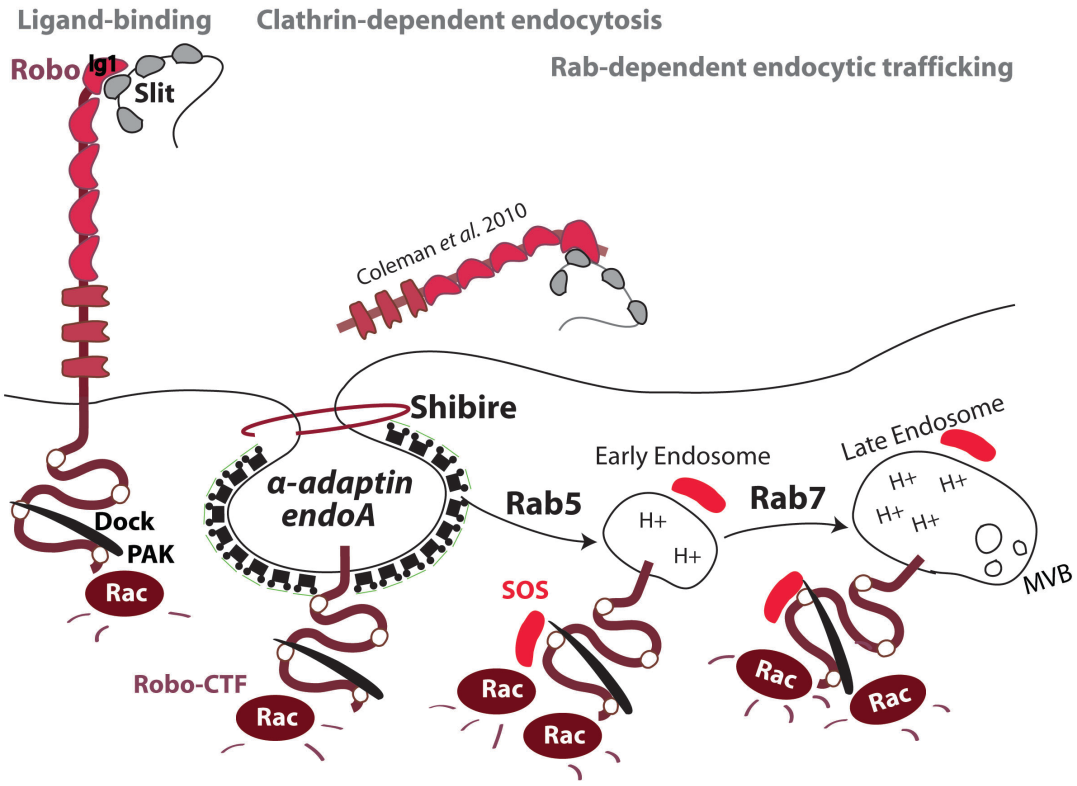

**Figure 2.9: A model for how Endocytosis might contribute to Robo signaling**

Following ectodomain binding to Slit, Pak and Dock are recruited to the Conserved Cytoplasmic (CC) Domains #2 & 3 within Robo's C-terminus, and contingently upon Dock-binding Son of Sevenless (Sos) is recruited to the activation complex, to induce Rac activation (Fan *et al.* 2003, Yang *et al.* 2006). Juxtamembrane extracellular cleavage by the ADAM Metalloprotease Kuz is required for recruitment of Sos (Coleman *et al.* 2010). Both Clathrin-dependent endocytosis and endocytic trafficking into the early endosome are required for Sos recruitment to the Robo receptor, potentially gated by spatial access to PI3K Kinase activity of Sos's Pleckstrin Homology Domain in the early endosome, leading to a stronger activation of Rac in the early endosome than that by Pak alone.

**Figure 2.10: Endocytosis positively regulates Slit-Robo repulsion, not Frazzled-mediated attraction**

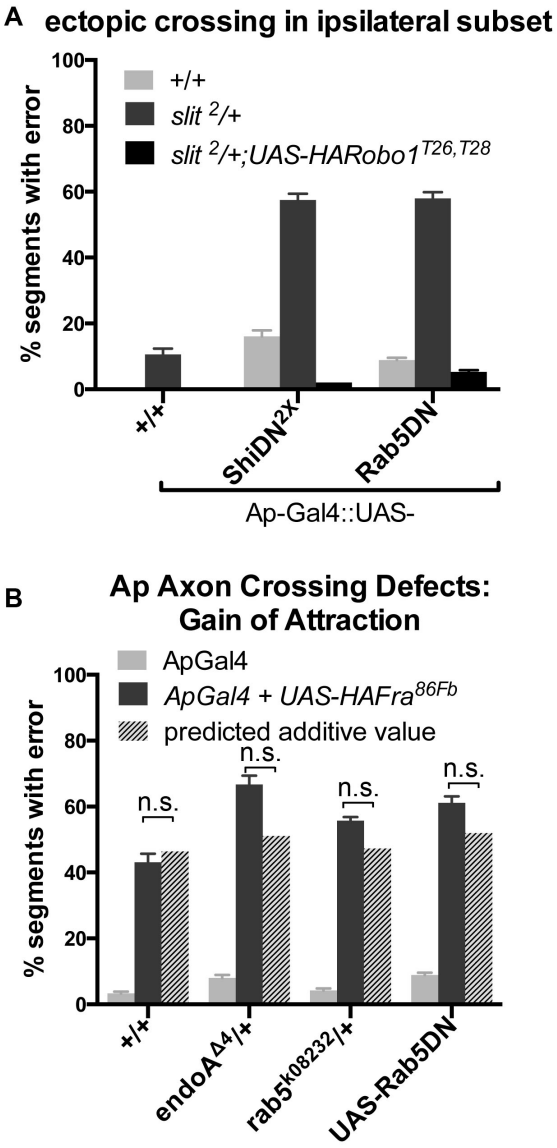

**Figure 2.10: Endocytosis positively regulates Slit-Robo repulsion, not Frazzled-mediated attraction**
A: Expression of UAS-HA-Robo transgenes specifically in the Ap subset of neurons rescues the defects caused by overexpression of ShibireDN and Rab5DN in *slit*$^{2}$/+ heterozygotes. B: Reducing the dosage of endocytic trafficking genes do not enhance (not statistically significant, n.s.) the ectopic crossing errors induced by enhanced midline attraction resulting from ectopic expression of the attractive guidance receptor Frazzled beyond the predicted percentage crossing frequency from an additive interaction in the Ap neurons. Error bars indicate standard error of the mean.

**Figure 2.11: Endocytosis positively regulates Robo signaling in vitro**

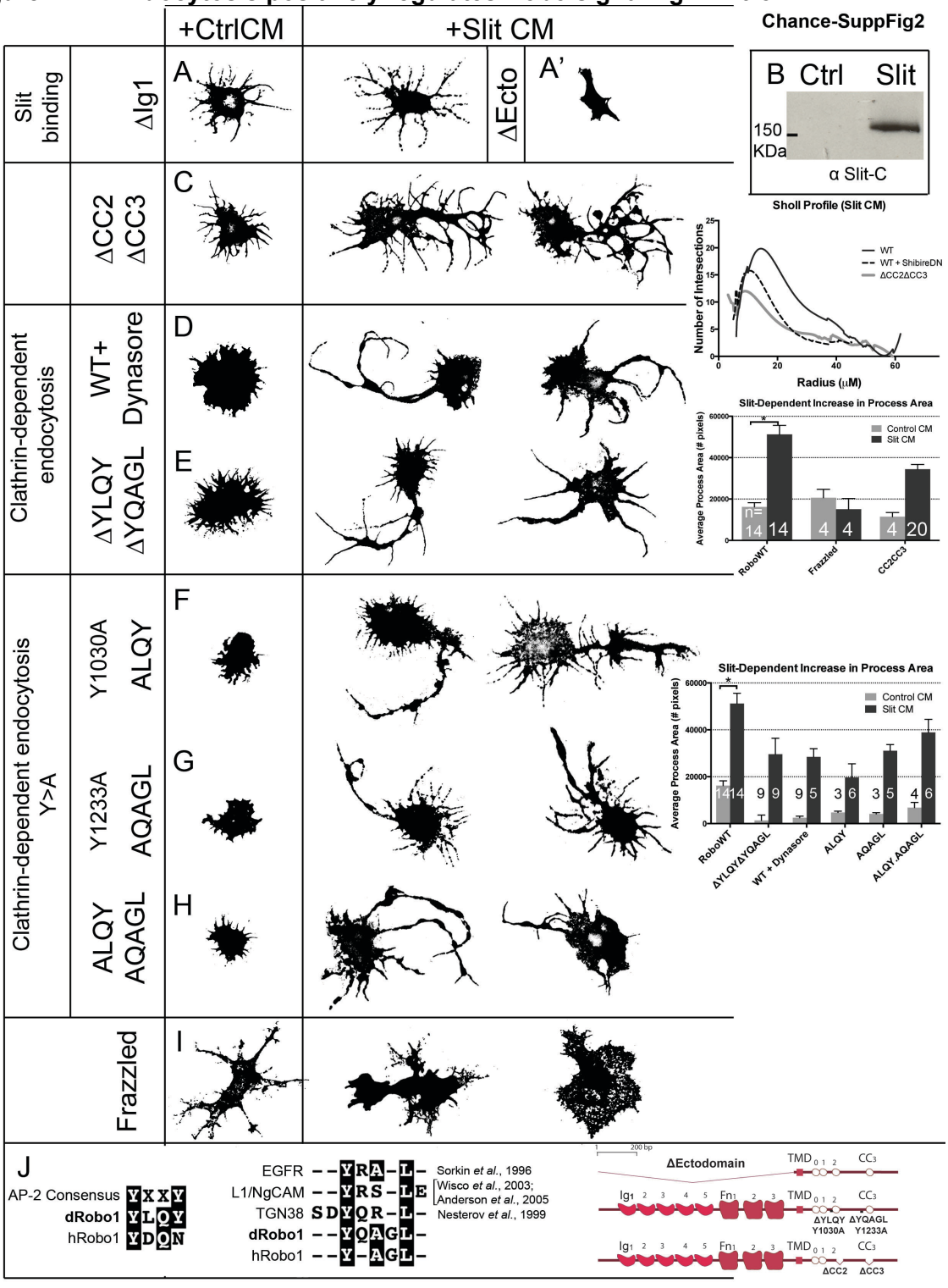

**Figure 2.11: Endocytosis positively regulates Robo signaling *in vitro***

Representative examples of the morphological profiles of Drosophila embryonic cells transfected with Robo and bath-treated for 10' with Control CM or Slit CM are displayed. (A) Cells that express Robo deficient for Slit-binding by deletion of the first Ig domain, or by deletion of the entire ectodomain (A', schematized in domain structure cartoon below) do not elaborate processes as much (A) or at all (A') in response to Slit treatment. (C) Robo missing its CC2 and CC3 domains, required for Rac activation, display a qualitatively distinct class of impaired process elaboration. There is an increase in the number of short branches, but the total process area and therefore Sholl profile is shunted as compared to WT-expressing cells (Sholl n=11). Inhibiting Clathrin-dependent endocytosis either directly by treatment with 20μM Dynasore, a dynamin inhibitor (D), or by deleting its AP-2 binding motifs together (E), or point-mutating the catalytic tyrosines each singly (F, G) or both together (H) leads to the same qualitative type of spreading behavior. In all cases, there is a reduction in process branching, which is quantified as a reduction in the process area in Slit-CM treated cells and a downward shift in the Sholl profile (quantified on the right) as compared to WT-expressing cells. Deleting both AP-2 motifs together results in a smaller maximal process radius. (I) Expression of the attractive guidance receptor Frazzled causes S2R+ cells to spread in a qualitatively distinct manner with more lamellipodial-appearing spreading that does not respond to Slit-CM treatment. J: Box-shade alignments of amino acid sequence of the identified AP-2 adaptor motifs show sequence conservation between *Drosophila* Robo1 and Human Robo1, and the originating sequences, suggesting conservation of function throughout phylogeny. Domain structure diagrams show the location of the putative AP-2-binding motifs, and the other variants assayed here, within *Drosophila* Robo1.

**Figure 2.12: Slit-dependent Robo endocytosis occurs upstream of Sos recruitment**

**Chance_Supp Fig. 3**

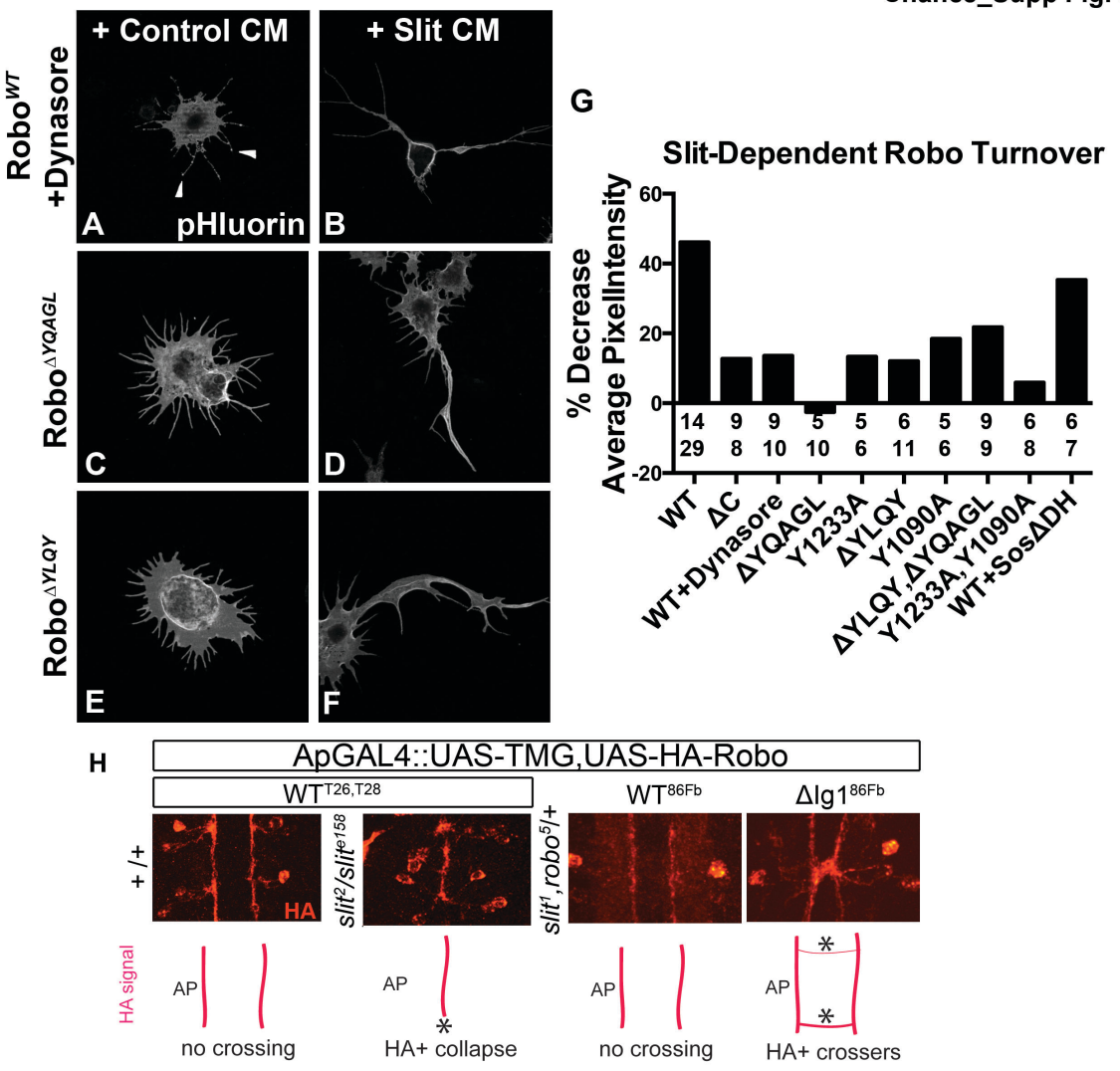

**Figure 2.12: Slit-dependent Robo endocytosis occurs upstream of Sos recruitment**

A-F: Surface Robo signal in S2R+ cells is isolated by a pH sensitive GFP tag, pHluorin, on Robo's ectodomain. In cells treated with the Dynamin inhibitor Dynasore, Robo is still expressed on the tips of processes in Control CM conditions (arrowheads, A), but the downregulation of surface signal in response to Slit treatment seen with WT-Robo expressing cells is blunted and surface Robo remains high (B, G). Disrupting Robo's AP-2 binding motifs singly does not affect the average pHluorin signal intensity in Control CM conditions (C, E), but inhibits the reduction in Slit CM conditions (D, F) seen in WT-Robo expressing cells, resulting in a reduced % decrease in average signal intensity (G). Point-mutating the catalytic tyrosines of the AP-2 motifs singly or together also reduces the Slit-dependent decrease in surface Robo signal, while inhibiting Sos-mediated activation of Rac by co-expressing Son-of-sevenless missing its Dbl Homology domain does not affect surface Robo levels (G). Number of cells analyzed are indicated on the histogram (top number, n from Control CM, bottom number, Slit CM). (H) Signal from an HA epitope tag on Robo's ectodomain expressed in the ipsilateral Ap subset of neurons is imaged by immunostaining in Stage 16 Drosophila embryos. Inhibiting Slit by either creating slitmutant/hypomorph embryos or by deleting Robo's Slit-binding domain ($\Delta$Ig1) causes mislocalization of Robo to ectopically collapsed or crossing portions of axons, respectively.

**Figure 2.13: Slit colocalization with Rab5 persists over 10' in vitro**

**Chance_Supplemental Fig4**

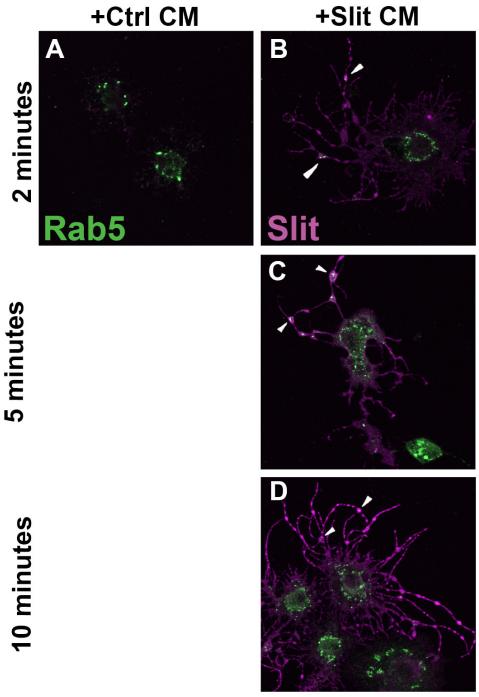

**Figure 2.13: Slit colocalization with Rab5 persists over 10' *in vitro***

Endogenous Rab5 in S2R+ Robo-expressing cells bath-treated with Control CM (A) or Slit CM for 2' (B), 5' (C) or 10' (D). Slit antibody staining is specific for cells treated with Slit CM (B-D), and Rab5 is recruited to processes in cells that have bound Slit. At all three timepoints Slit and Rab5 are colocalized in varicosities and branchpoints of elaborating processes (arrowheads, B-D).

**Figure 2.14: Robo missing its AP2 motifs functions as a Dominant-Negative in vivo**

**Chance_SuppFig5**

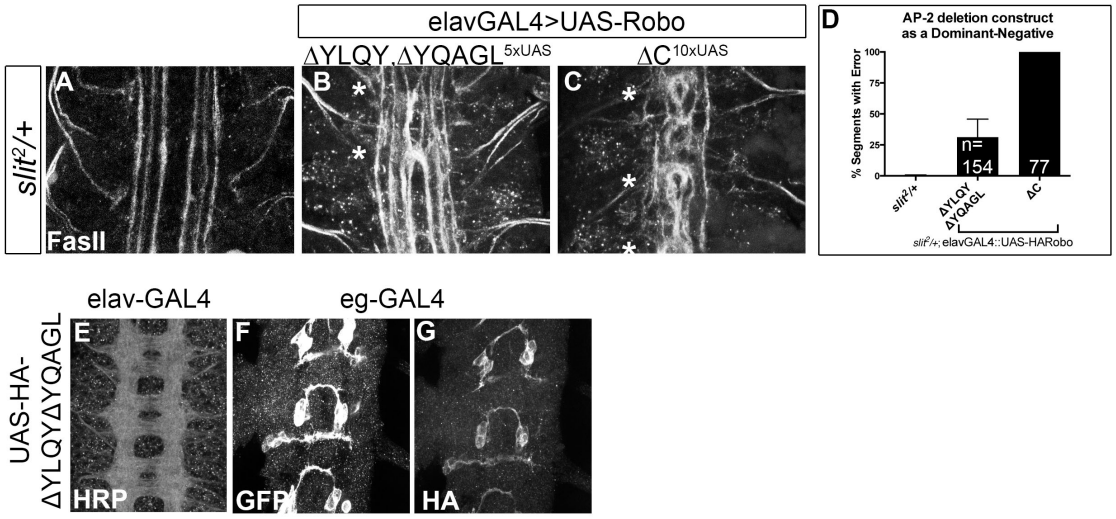

**Figure 2.14: Robo missing its AP2 motifs functions as a Dominant-Negative *in vivo***

In *slit*$^{2}$/+ embryos, Robo missing its entire C-terminus (C) functions as a strong dominant-negative for midline repulsion, inducing an 100% error rate (D) when driven in all neurons, quantified here in the normally-ipsilateral medialmost FasII+ axons (A). Like RoboΔC Robo$^{\Delta YQAGL\Delta YLQY}$ overexpression in all neurons in a partial loss of Slit background causes ectopic crossing (B). (E-G) RoboΔYQAGLΔYLQY can not signal repulsion to cause loss of commissural projection pattern when overexpressed either in all neurons (E), or in the Eg commissural subset (F, G).

# BIBLIOGRAPHY


Anitha A, Nakamura K, Yamada K, Suda S, Thanseem I, Tsujii M, Iwayama Y, Hattori E, Toyota T, Miyachi T et al. 2008. Genetic analyses of roundabout (ROBO) axon guidance receptors in autism. *American journal of medical genetics Part B, Neuropsychiatric genetics : the official publication of the International Society of Psychiatric Genetics* **147B**: 1019-1027.

Bartoe JL, McKenna WL, Quan TK, Stafford BK, Moore JA, Xia J, Takamiya K, Huganir RL, Hinck L. 2006. Protein interacting with C-kinase 1/protein kinase Calpha-mediated endocytosis converts netrin-1-mediated repulsion to attraction. *J Neurosci* **26**: 3192-3205.

Bashaw GJ, Goodman CS. 1999. Chimeric axon guidance receptors: the cytoplasmic domains of slit and netrin receptors specify attraction versus repulsion. *Cell* **97**: 917-926.

Bashaw GJ, Kidd T, Murray D, Pawson T, Goodman CS. 2000. Repulsive axon guidance: Abelson and Enabled play opposing roles downstream of the roundabout receptor. *Cell* **101**: 703-715.

Brose K, Bland KS, Wang KH, Arnott D, Henzel W, Goodman CS, Tessier-Lavigne M, Kidd T. 1999. Slit proteins bind Robo receptors and have an evolutionarily conserved role in repulsive axon guidance. *Cell* **96**: 795-806.

Campbell DS, Holt CE. 2001. Chemotropic responses of retinal growth cones mediated by rapid local protein synthesis and degradation. *Neuron* **32**: 1013-1026.

Chang BS, Katzir T, Liu T, Corriveau K, Barzillai M, Apse KA, Bodell A, Hackney D, Alsop D, Wong ST et al. 2007. A structural basis for reading fluency: white matter defects in a genetic brain malformation. *Neurology* **69**: 2146-2154.

Christoforidis S, Miaczynska M, Ashman K, Wilm M, Zhao L, Yip SC, Waterfield MD, Backer JM, Zerial M. 1999. Phosphatidylinositol-3-OH kinases are Rab5 effectors. *Nature cell biology* **1**: 249-252.

Coleman HA, Labrador JP, Chance RK, Bashaw GJ. 2010. The Adam family metalloprotease Kuzbanian regulates the cleavage of the roundabout receptor to control axon repulsion at the midline. *Development* **137**: 2417-2426.

Cowan CW, Shao YR, Sahin M, Shamah SM, Lin MZ, Greer PL, Gao S, Griffith EC, Brugge JS, Greenberg ME. 2005. Vav family GEFs link activated Ephs to endocytosis and axon guidance. *Neuron* **46**: 205-217.

Das B, Shu X, Day GJ, Han J, Krishna UM, Falck JR, Broek D. 2000. Control of intramolecular interactions between the pleckstrin homology and Dbl homology domains of Vav and Sos1 regulates Rac binding. *J Biol Chem* **275**: 15074-15081.

Diefenbach TJ, Guthrie PB, Stier H, Billups B, Kater SB. 1999. Membrane recycling in the neuronal growth cone revealed by FM1-43 labeling. *J Neurosci* **19**: 9436-9444.

Falk J, Konopacki FA, Zivraj KH, Holt CE. 2014. Rab5 and Rab4 regulate axon elongation in the Xenopus visual system. *J Neurosci* **34**: 373-391.

Fan X, Labrador JP, Hing H, Bashaw GJ. 2003. Slit stimulation recruits Dock and Pak to the roundabout receptor and increases Rac activity to regulate axon repulsion at the CNS midline. *Neuron* **40**: 113-127.

Fukuhara N, Howitt JA, Hussain SA, Hohenester E. 2008. Structural and functional analysis of slit and heparin binding to immunoglobulin-like domains 1 and 2 of Drosophila Robo. *J Biol Chem* **283**: 16226-16234.

Galperin E, Sorkin A. 2003. Visualization of Rab5 activity in living cells by FRET microscopy and influence of plasma-membrane-targeted Rab5 on clathrin-dependent endocytosis. *Journal of cell science* **116**: 4799-4810.

Gonzalez-Gaitan M, Jackle H. 1997. Role of Drosophila alpha-adaptin in presynaptic vesicle recycling. *Cell* **88**: 767-776.

Guichet A, Wucherpfennig T, Dudu V, Etter S, Wilsch-Brauniger M, Hellwig A, Gonzalez-Gaitan M, Huttner WB, Schmidt AA. 2002. Essential role of endophilin A in synaptic vesicle budding at the Drosophila neuromuscular junction. *The EMBO journal* **21**: 1661-1672.

Gupta GD, Swetha MG, Kumari S, Lakshminarayan R, Dey G, Mayor S. 2009. Analysis of endocytic pathways in Drosophila cells reveals a conserved role for GBF1 in internalization via GEECs. *PloS one* **4**: e6768.

Hattori M, Osterfield M, Flanagan JG. 2000. Regulated cleavage of a contact-mediated axon repellent. *Science* **289**: 1360-1365.

Hines JH, Abu-Rub M, Henley JR. 2010. Asymmetric endocytosis and remodeling of beta1-integrin adhesions during growth cone chemorepulsion by MAG. *Nat Neurosci* **13**: 829-837.

Howitt JA, Clout NJ, Hohenester E. 2004. Binding site for Robo receptors revealed by dissection of the leucine-rich repeat region of Slit. *The EMBO journal* **23**: 4406-4412.

Hsouna A, Kim YS, VanBerkum MF. 2003. Abelson tyrosine kinase is required to transduce midline repulsive cues. *J Neurobiol* **57**: 15-30.

Hu H, Li M, Labrador JP, McEwen J, Lai EC, Goodman CS, Bashaw GJ. 2005. Cross GTPase-activating protein (CrossGAP)/Vilse links the Roundabout receptor to Rac to regulate midline repulsion. *Proc Natl Acad Sci U S A* **102**: 4613-4618.

Hutson LD, Chien CB. 2002. Pathfinding and error correction by retinal axons: the role of astray/robo2. *Neuron* **33**: 205-217.

Itofusa R, Kamiguchi H. 2011. Polarizing membrane dynamics and adhesion for growth cone navigation. *Molecular and cellular neurosciences* **48**: 332-338.

Janes PW, Saha N, Barton WA, Kolev MV, Wimmer-Kleikamp SH, Nievergall E, Blobel CP, Himanen JP, Lackmann M, Nikolov DB. 2005. Adam meets Eph: an ADAM substrate recognition module acts as a molecular switch for ephrin cleavage in trans. *Cell* **123**: 291-304.

Jekely G, Sung HH, Luque CM, Rorth P. 2005. Regulators of endocytosis maintain localized receptor tyrosine kinase signaling in guided migration. *Dev Cell* **9**: 197-207.

Johnson KG, Ghose A, Epstein E, Lincecum J, O'Connor MB, Van Vactor D. 2004. Axonal heparan sulfate proteoglycans regulate the distribution and efficiency of the repellent slit during midline axon guidance. *Curr Biol* **14**: 499-504.

Jurney WM, Gallo G, Letourneau PC, McLoon SC. 2002. Rac1-mediated endocytosis during ephrin-A2- and semaphorin 3A-induced growth cone collapse. *J Neurosci* **22**: 6019-6028.

Kamiguchi H, Lemmon V. 2000. Recycling of the cell adhesion molecule L1 in axonal growth cones. *J Neurosci* **20**: 3676-3686.

Kapfhammer JP, Raper JA. 1987. Collapse of growth cone structure on contact with specific neurites in culture. *J Neurosci* **7**: 201-212.

Keleman K, Rajagopalan S, Cleppien D, Teis D, Paiha K, Huber LA, Technau GM, Dickson BJ. 2002. Comm sorts robo to control axon guidance at the Drosophila midline. *Cell* **110**: 415-427.

Keleman K, Ribeiro C, Dickson BJ. 2005. Comm function in commissural axon guidance: cell-autonomous sorting of Robo in vivo. *Nat Neurosci* **8**: 156-163.

Kidd T, Bland KS, Goodman CS. 1999. Slit is the midline repellent for the robo receptor in Drosophila. *Cell* **96**: 785-794.

Kidd T, Brose K, Mitchell KJ, Fetter RD, Tessier-Lavigne M, Goodman CS, Tear G. 1998a. Roundabout controls axon crossing of the CNS midline and defines a novel subfamily of evolutionarily conserved guidance receptors. *Cell* **92**: 205-215.

Lanahan AA, Hermans K, Claes F, Kerley-Hamilton JS, Zhuang ZW, Giordano FJ, Carmeliet P, Simons M. 2010. VEGF receptor 2 endocytic trafficking regulates arterial morphogenesis. *Dev Cell* **18**: 713-724.

Lanier LM, Gates MA, Witke W, Menzies AS, Wehman AM, Macklis JD, Kwiatkowski D, Soriano P, Gertler FB. 1999. Mena is required for neurulation and commissure formation. *Neuron* **22**: 313-325.

Li G, D'Souza-Schorey C, Barbieri MA, Roberts RL, Klippel A, Williams LT, Stahl PD. 1995. Evidence for phosphatidylinositol 3-kinase as a regulator of endocytosis via activation of Rab5. *Proc Natl Acad Sci U S A* **92**: 10207-10211.

Lin KT, Sloniowski S, Ethell DW, Ethell IM. 2008. Ephrin-B2 induced cleavage of EphB2 receptor is mediated by matrix metalloproteinases to trigger cell repulsion. *J Biol Chem*.

Liu Z, Patel K, Schmidt H, Andrews W, Pini A, Sundaresan V. 2004. Extracellular Ig domains 1 and 2 of Robo are important for ligand (Slit) binding. *Molecular and cellular neurosciences* **26**: 232-240.

Ma L, Tessier-Lavigne M. 2007. Dual branch-promoting and branch-repelling actions of Slit/Robo signaling on peripheral and central branches of developing sensory axons. *J Neurosci* **27**: 6843-6851.

Macia E, Ehrlich M, Massol R, Boucrot E, Brunner C, Kirchhausen T. 2006. Dynasore, a cell-permeable inhibitor of dynamin. *Dev Cell* **10**: 839-850.

Marston DJ, Dickinson S, Nobes CD. 2003. Rac-dependent trans-endocytosis of ephrinBs regulates Eph-ephrin contact repulsion. *Nature cell biology* **5**: 879-888.

Matusek T, Gombos R, Szecsenyi A, Sanchez-Soriano N, Czibula A, Pataki C, Gedai A, Prokop A, Rasko I, Mihaly J. 2008. Formin proteins of the DAAM subfamily play a role during axon growth. *J Neurosci* **28**: 13310-13319.

Moline MM, Southern C, Bejsovec A. 1999. Directionality of wingless protein transport influences epidermal patterning in the Drosophila embryo. *Development* **126**: 4375-4384.

Murray MJ, Whitington PM. 1999. Effects of roundabout on growth cone dynamics, filopodial length, and growth cone morphology at the midline and throughout the neuropile. *J Neurosci* **19**: 7901-7912.

O'Donnell M, Chance RK, Bashaw GJ. 2009. Axon growth and guidance: receptor regulation and signal transduction. *Annu Rev Neurosci* **32**: 383-412.

Ohno H, Stewart J, Fournier MC, Bosshart H, Rhee I, Miyatake S, Saito T, Gallusser A, Kirchhausen T, Bonifacino JS. 1995. Interaction of tyrosine-based sorting signals with clathrin-associated proteins. *Science* **269**: 1872-1875.

Onishi K, Shafer B, Lo C, Tissir F, Goffinet AM, Zou Y. 2013. Antagonistic functions of Dishevelleds regulate Frizzled3 endocytosis via filopodia tips in Wnt-mediated growth cone guidance. *J Neurosci* **33**: 19071-19085.

Ozdinler PH, Erzurumlu RS. 2002. Slit2, a branching-arborization factor for sensory axons in the Mammalian CNS. *J Neurosci* **22**: 4540-4549.

Palamidessi A, Frittoli E, Garré M, Faretta M, Mione M, Testa I, Diaspro A, Lanzetti L, Scita G, Di Fiore PP. 2008. Endocytic trafficking of Rac is required for the spatial restriction of signaling in cell migration. *Cell* **134**: 135-147.

Piper M, Anderson R, Dwivedy A, Weinl C, van Horck F, Leung KM, Cogill E, Holt C. 2006. Signaling mechanisms underlying Slit2-induced collapse of Xenopus retinal growth cones. *Neuron* **49**: 215-228.

Piper M, Salih S, Weinl C, Holt CE, Harris WA. 2005. Endocytosis-dependent desensitization and protein synthesis-dependent resensitization in retinal growth cone adaptation. *Nat Neurosci* **8**: 179-186.

Potkin SG, Turner JA, Guffanti G, Lakatos A, Fallon JH, Nguyen DD, Mathalon D, Ford J, Lauriello J, Macciardi F et al. 2009. A genome-wide association study of schizophrenia using brain activation as a quantitative phenotype. *Schizophrenia bulletin* **35**: 96-108.

Seeger M, Tear G, Ferres-Marco D, Goodman CS. 1993. Mutations affecting growth cone guidance in Drosophila: genes necessary for guidance toward or away from the midline. *Neuron* **10**: 409-426.

Seto ES, Bellen HJ. 2006. Internalization is required for proper Wingless signaling in Drosophila melanogaster. *J Cell Biol* **173**: 95-106.

Shu T, Richards LJ. 2001. Cortical axon guidance by the glial wedge during the development of the corpus callosum. *J Neurosci* **21**: 2749-2758.

Slessareva JE, Routt SM, Temple B, Bankaitis VA, Dohlman HG. 2006. Activation of the phosphatidylinositol 3-kinase Vps34 by a G protein alpha subunit at the endosome. *Cell* **126**: 191-203.

Slovakova J, Speicher S, Sanchez-Soriano N, Prokop A, Carmena A. 2012. The actin-binding protein Canoe/AF-6 forms a complex with Robo and is required for Slit-Robo signaling during axon pathfinding at the CNS midline. *J Neurosci* **32**: 10035-10044.

Sorkin A, Mazzotti M, Sorkina T, Scotto L, Beguinot L. 1996. Epidermal growth factor receptor interaction with clathrin adaptors is mediated by the Tyr974-containing internalization motif. *J Biol Chem* **271**: 13377-13384.

Sorkin A, von Zastrow M. 2009. Endocytosis and signalling: intertwining molecular networks. *Nature reviews Molecular cell biology* **10**: 609-622.

Teis D, Taub N, Kurzbauer R, Hilber D, de Araujo ME, Erlacher M, Offterdinger M, Villunger A, Geley S, Bohn G et al. 2006. p14-MP1-MEK1 signaling regulates endosomal traffic and cellular proliferation during tissue homeostasis. *J Cell Biol* **175**: 861-868.

Tojima T, Itofusa R, Kamiguchi H. 2010. Asymmetric clathrin-mediated endocytosis drives repulsive growth cone guidance. *Neuron* **66**: 370-377.

Vaccari T, Lu H, Kanwar R, Fortini ME, Bilder D. 2008. Endosomal entry regulates Notch receptor activation in Drosophila melanogaster. *J Cell Biol* **180**: 755-762.

van Bergeijk P, Adrian M, Hoogenraad CC, Kapitein LC. 2015. Optogenetic control of organelle transport and positioning. *Nature* **518**: 111-114.

van der Bliek AM, Redelmeier TE, Damke H, Tisdale EJ, Meyerowitz EM, Schmid SL. 1993. Mutations in human dynamin block an intermediate stage in coated vesicle formation. *J Cell Biol* **122**: 553-563.

Wang KH, Brose K, Arnott D, Kidd T, Goodman CS, Henzel W, Tessier-Lavigne M. 1999. Biochemical purification of a mammalian slit protein as a positive regulator of sensory axon elongation and branching. *Cell* **96**: 771-784.

Whitford KL, Marillat V, Stein E, Goodman CS, Tessier-Lavigne M, Chedotal A, Ghosh A. 2002. Regulation of cortical dendrite development by Slit-Robo interactions. *Neuron* **33**: 47-61.

Williams ME, Wu SC, McKenna WL, Hinck L. 2003. Surface expression of the netrin receptor UNC5H1 is regulated through a protein kinase C-interacting protein/protein kinase-dependent mechanism. *J Neurosci* **23**: 11279-11288.

Wisco D, Anderson ED, Chang MC, Norden C, Boiko T, Folsch H, Winckler B. 2003. Uncovering multiple axonal targeting pathways in hippocampal neurons. *J Cell Biol* **162**: 1317-1328.

Yang L, Bashaw GJ. 2006. Son of sevenless directly links the Robo receptor to rac activation to control axon repulsion at the midline. *Neuron* **52**: 595-607.

Yoo S, Kim Y, Noh H, Lee H, Park E, Park S. 2011. Endocytosis of EphA receptors is essential for the proper development of the retinocollicular topographic map. *The EMBO journal* **30**: 1593-1607.

Zimmer M, Palmer A, Kohler J, Klein R. 2003. EphB-ephrinB bi-directional endocytosis terminates adhesion allowing contact mediated repulsion. *Nature cell biology* **5**: 869-878.

# CHAPTER 3: Proteolytic Processing regulates signaling from the Roundabout receptor


## Abstract

Understanding how an individual growth cone deploys its guidance receptors to make guidance choices is critical to learning how proper wiring is established in development. Roundabout (Robo) is one such guidance receptor that mediates repulsion from its ligand Slit in both humans and *Drosophila*. As with other guidance receptors, Robo influences guidance by modulating intracellular cytoskeletal dynamics. Little is known about how Robo receptor signaling is activated and how the timing and duration of this signaling is controlled. Here we present genetic and biochemical evidence supporting a role for proteolytic processing and receptor trafficking in regulating Slit-Robo repulsive signaling in the *Drosophila* embryonic ventral nerve cord. We have previously found that Kuzbanian (Kuz), an ADAM protease, is required for (1) the normal localization and expression of Robo protein, and (2) Robo proteolysis that positively regulates repulsive guidance (Coleman et al 2010). Here we present evidence that after Kuz-dependent cleavage activates Robo, γ-Secretase catalyzes a second cleavage that likely acts to limit the duration of signaling from the activated Robo C-terminal fragment. We present data that (1) show γ-secretase can cleave Robo *in vitro* and (2) suggest that γ-Secretase negatively regulates repulsive signaling *in vitro* and *in vivo*. Taken together, these data suggest that proteolytic processing provides a mechanism for the precise temporal control over the activity of the Robo guidance receptor.

We are also investigating a role for the interplay between endocytosis and proteolysis of Robo. In commissural axons, Robo expression on the growth cone is

normally prevented prior to midline crossing; this is reflected in the exclusion of Robo protein from the commissural portion of axons as they cross. Surprisingly, we find that in *kuz* and *slit* mutants that have ectopic midline projections due to loss of repulsion, Robo is mislocalized to the crossing portions of axons. This raises the possibility that Robo internalization by cleavage or endocytosis may be essential for repulsive signaling. We are currently testing for a link between Robo cleavage and endocytosis in mediating axon repulsion at the midline.

## Introduction

*Drosophila roundabout* (*robo*) is a member of a conserved gene family with demonstrated importance in midline guidance in humans (Jen et al. 2004) that was originally identified in a genetic screen in the embryonic nerve cord of *Drosophila* for a similar role in midline guidance (Seeger et al. 1993; Kidd et al. 1998a; Kidd et al. 1998b). Robo is an IgCAM guidance receptor that mediates repulsion from the midline in response to its ligand Slit (Brose et al. 1999b; Kidd et al. 1999b); *robo* mutants exhibit ectopic entry of normally-ipsilateral axons into the midline zone, and re-entry into the same region by post-crossing contralateral axons, thereby creating hallmark circular axon paths resembling roadway roundabouts.

Given that it is the array of guidance receptors expressed on the surface of the growth cone that influences guidance decisions made at choicepoints, it is not surprising that a variety of investigations have revealed the importance of molecules exerting control over receptor surface expression for guidance (see Chapter 1). In the case of

Robo, the impact of the spatiotemporal pattern of surface expression is evidenced by the role of *commissureless (comm)* in gating Robo delivery to the growth cone plasma membrane, such that the times when Robo is sequestered from delivery by *comm* are the times in which growth cones are able to ignore Slit and cross the midline (Seeger et al. 1993; Kidd et al. 1998a; Keleman et al. 2002; Keleman et al. 2005; Gilestro 2008). Until now this receptor sorting mechanism has been assumed to provide the primary means by which Robo trafficking regulates midline repulsion. More recently, we have provided evidence in our lab that the *kuzbanian (kuz)* metalloprotease also regulates the spatial patterns of Robo protein and, in contrast to Comm, positively regulates repulsive guidance (Coleman et al. 2010).

The endogenous expression pattern of Robo throughout the embryonic ventral nerve cord is characterized by commissural exclusion and longitudinal enrichment (Kidd et al. 1998a). This pattern of commissural exclusion is observed for all three Robo proteins even when they are over-expressed (Rajagopalan et al. 2000). Interestingly, this Robo-free commissural pattern is abolished in embryos that are defective for *kuz* function (Schimmelpfeng et al. 2001; Coleman et al. 2010). *kuz* mutant embryos also display an axon guidance phenotype similar to that in *robo* mutant embryos; impaired midline repulsion (Coleman et al 2010). The striking association between a phenotype resembling *robo* loss-of-function (ectopic midline crossing by normally-ipsilateral axons) and failure to exclude Robo1 protein from the midline-traversing segments of axons suggests that *kuz* activity is necessary for Robo's ability to sense Slit, and further suggest the possibility that following Kuz activity, Robo is cleared from the plasma membrane.

**A Kuzbanian-catalyzed juxtamembrane cleavage of Robo is required for its repulsive guidance activity in vivo**

*kuz* is a metalloprotease that was identified by a genetic screen in our lab for molecules involved in Slit/Robo-mediated midline repulsion (Coleman et al 2010). Ectopic midline crossing of ipsilateral interneurons, a hallmark of defective midline repulsion, is observed in both *kuz* zygotic mutant embryos and in embryos where both *slit* and *kuz* activity are partially reduced (Schimmelpfeng et al. 2001; Coleman et al. 2010). This dose-dependent interaction supports the idea that Kuz is a positive regulator of Slit-Robo signaling.

*kuz* was originally discovered for its role in the Notch pathway, where it cleaves Notch in response to binding of its ligand Jagged, leading to the creation of an ectodomain and a C terminal fragment (CTF) (Rooke et al. 1996; Pan and Rubin 1997b). Like Notch, Robo is a substrate for Kuzbanian-mediated juxtamembrane cleavage both *in vitro* and *in vivo* (Figure 3.1B). Co-transfection of *kuz* enhances the abundance of an ~120 KDa N-terminal fragment of Robo in S2R+ cells, consistent with its identity as an ectodomain generated by juxtamembrane cleavage. Expressing a N-terminal tagged transgene of Robo panneuronally results in the production of a full-length receptor and a N-terminal fragment of similar size to that observed in the *in vitro* ectodomain shedding assay, showing that juxtamembrane cleavage of Robo can occur *in vivo*. Some evidence that the *in vivo* cleavage product is catalyzed by *kuz* comes from dose-dependance on Kuz function: adding a WT Kuz transgene enhances the abundance of this fragment, while a dominant negative Kuz transgene (missing its prodomain and metalloprotease domain) reduces its abundance. To test whether this juxtamembrane

cleavage contributes to midline repulsion, we assayed whether an uncleavable version of Robo (Figure 3.1B, top), a chimeric receptor with Fra identity at its predicted cleavage site (Figure 3.1A) could rescue the *robo* mutant phenotype *in vivo (*Figure 3.1D). In *robo* mutants, the medial-most of the normally ipsilateral FasII-positive fascicles ectopically enter into and circle within the midline, and the ipsilateral apterous (ap) axon tracts collapse onto the midline. Expressing a WT Robo transgene in all neurons mostly rescues ectopic circling of the medial-most FasII+ fascicle, and completely rescues the Apterous ectopic crossing (quantified on right). However, expressing two independent Robo-U transgenes does not rescue either FasII circling or the collapse of the two apterous fascicles on to the midline. This defect in Robo signaling is not likely due to any defect in ligand-binding caused structural changes caused by the chimeric receptor, as Slit-binding is qualitatively intact in S2R+ cells (Figure 3.1C). These observations, along with the biochemical evidence for Kuz-dependent generation of Robo fragments, strongly suggest that Kuz-mediated cleavage of Robo is necessary for repulsive signaling.

**Robo clearance from commissural segments is correlated with repulsion**

Another clue about Kuz's mechanism of action comes from a puzzling phenomenon in *kuz* loss-of-function embryos. Compared to heterozygotes (Figure 3.2A, whose midline guidance phenotype is equivalent to WT), *kuz* mutants, like *slit* hypomorphs (Figure 3.2E), have reduced midline repulsion, as evidenced by the ectopic entry of axons into the midline area, which results in thinner longitudinal and thicker commissural segments of axons (Figure 3.2C). What is surprising here is that in spite of

this loss of repulsive activity**,** there is a paradoxical increase in repulsive receptor protein levels (Figure 3.2G), concomitant with mislocalization of Robo to the midline-traversing segments of axons. Normally Robo is excluded from commissures (Figure 3.2B), even when expressed at high levels (Rajagopalan et al. 2000), but in *kuz* mutants and *slit* hypomorphs, surface Robo is mislocalized to the commissural segments of axons (carrots, Figure 3.2D,F). To look with more spatial resolution at this phenomenon we used the GAL4-UAS system to test whether N-terminally tagged Robo is retained on single fascicles of axons exhibiting loss-of-repulsion defects in *slit* and *kuz* loss-of-function embryos. We find that there is a correlation between loss of repulsion, and retained Robo receptor on both ectopically crossing, normally ipsilateral Ap axons (Figure 3.2I), as well as on commissural Eg axons (Figure 3.2H). These *in vivo* observations provide evidence for a mechanistic link between clearance from axons and signaling, but also raise the question of how a cleavage event that leaves a membrane-bound signaling fragment could lead to removal of this fragment from the cell surface.

### γ-Secretase catalyzes Robo cleavage and negatively regulates Slit-Robo signaling

Insight from Kuz's role in other signaling pathways implicates a putative subsequent cleavage event for Robo. Many ADAM10/Kuz substrates, like Notch and APP, undergo processive proteolytic cleavage whereby the metalloprotease-mediated ectododomain shedding event is constitutively followed by a *gamma*-secretase mediated intramembrane proteolysis, which generates a soluble intracellular domain, or ICD (Beel and Sanders 2008; van Tetering et al. 2009). In the case of DCC this second cleavage evidently promotes receptor clearance, as surface accumulation is enhanced in *Ps1* mutant primary mouse neuron cultures (Parent et al. 2005). That this event follows a

metalloprotease shedding event is likely; inhibiting the first cleavage event by application of metalloprotease inhibitors to dorsal spinal cord explant cultures from rat results in higher DCC levels (Galko and Tessier-Lavigne 2000). Given the observation of higher levels of membrane retained Robo in *kuz* mutants, it is possible that Kuz's activating cleavage allows Robo turnover by a subsequent *gamma*-secretase mediated cleavage event (Selkoe and Wolfe 2007). It is likely that turnover of Robo CTF by such a second cleavage would occur not at the surface but following entry into an endocytic compartment, which we showed positively regulates Robo signaling (Chapter 2). Presenilin, the catalytic member of the *gamma*-Secretase complex, prefers the acidic environment of the endosome to perform its cleavages; inhibition of Clathrin-dependent endocytosis by expression of Shibire-DN wing and eye imaginal disc fly extracts abrogates the generation of Notch ICD as well as does direct application of a *gamma*-Secretase inhibitor (Vaccari et al. 2008).

If this proteolytic cascade indeed underlies *kuz* mutant embryos' commissural clearance defect, then one would predict that we could detect a dependence on Presenilin activity of the conversion of Robo CTF to Robo ICD. Others have demonstrated such a dependency in the case of human Robo; Robo CTF conversion into ICD in transfected HEK293T cells is inhibited by treatment with the *gamma*-secretase inhibitor L-685,458 (Seki et al. 2010). I have found that there is a ~60 KDa C-terminal Robo fragment whose abundance is enhanced by both cotransfection of Kuz, and inhibition of gamma-secretase activity (Compound E, a *gamma*-secretase inhibitor) in *Drosophila* cell lysates. The fact that the abundance of this fragment is increased when *kuz* activity is limited (Figure 3.3A) and reduced when *gamma*-Secretase activity is inhibited (Figure 3.3B) is consistent with its identity as a Robo CTF. There is also a ~58

KDa fragment whose abundance is enhanced by treatment with a proteasomal inhibitor, consistent with its identity as an ICD that is degraded quickly (Figure 3.3B). The sizes at which these fragments run in SDS-PAGE analysis match both their predicted molecular weights (with 6XMyc tags, CTF: 63KDa, ICD: 59KDa) and their respective engineered cleavage products based on predicted cleavage sites. Finally, their abundance is enhanced by treatment with Slit CM as compared to Control CM in S2R+ cells suggesting a ligand-dependency to the second cleavage event.

*Gamma*-Secretase is a multi-molecular complex, consisting of Presenilin Enhancer 2 (*pen-2*), Anterior Pharynx Defective 1 (*aph-1)*, Nicastrin (*nct)*, and Presenilin (*psn*). Nicastrin is thought to recognize the ectodomain remnants of sheddase substrate CTF's -not by consensus sequence but by size. Presenilin provides the enzymatic activity by its catalytic aspartic acid residues in an aqueous pore within the plane of the membrane. This cleavage event is thought to be constitutive upon access to sheddase substrate by Nicastrin, and only dependent on the pH-sensitivity of the cleavage mechanism. To test for a functional contribution of γ-Secretase activity to the Slit/Robo pathway *in vivo*, I generated embryos that were heterozygous for *slit,robo* and homozygous for *presenilin* (and *aph-1*, and *nct*) and tested for genetic interactions between members of the γ-secretase complex and the Slit/Robo pathway. I detect a decrease in the number of ectopic crossing events in FasII-positive ipsilateral fascicles (Figure 3.4A). This genetic suppression is statistically significant by the Student's unpaired t-test for two heteroallelic combinations (Figure 3.4B). The same polarity of regulation is observed in the more restricted ipsilateral subset of Ap axons (Figure 3.4C). In embryos mutant for *psn,* the intermediate loss of repulsion in *slit* heterozygous embryos alone is suppressed. Additionally, the even stronger ectopic crossing

phenotype observed in *slit* heterozygous embryos that also express Rab5DN, which inhibits entry to the early endosome (Chapter 2), are also suppressed in *psn* mutants. These observations are consistent with a model in which Presenilin negatively regulates Slit-Robo mediated midline guidance. *psn* mutant embryos do not have a midline guidance phenotype on their own, but, likely due to its role in Notch-regulated neurogenesis, *presenilin* exhibits one of the highest levels of maternal deposition of mRNA, strongly suggesting that embryos that are zygotically null for *psn* are not completely defective for Presenilin function.

To directly test whether gamma-Secretase negatively regulates Slit-dependent Robo activation, we turned to a newly established *in vitro* activation assay (see Figure 2.3). Application of a *gamma*-Secretase inhibitor to Robo-transfected S2R+ cells (Figure 3.5B) enhances the increase in branching and process length over that observed in WT Robo alone (Figure 3.5A). The *gamma*-Secretase inhibitor-induced enhancement of Robo-transfected S2R+ process generation effect is so obvious that I noticed it as a novice in the lab before I was focusing on this cellular behavior as anything of interest. The enhancement of process length is consistent with our genetic interaction results that implicate *gamma*-Secretase as a negative regulator of Slit-Robo signaling, and a model in which Presenilin catalyzes an inactivating cleavage of Robo. If we are inhibiting a second cleavage that normally inactivates Robo signaling then we would expect to see a prolonged time-course in which activated Robo can stimulate what we know to be Rac-based cytoskeletal motility that underlies process growth, as co-expression of Sos missing its RacGEF domain blocks Slit-dependent process elaboration (Figure 2.6). The *gamma*-Secretase modulation of this behavior is still a preliminary result without quantification, but consistently across two trials I am seeing cells that can no longer be captured in the field size I used to image many cells over the past couple of years. To

give you a better sense of this I have included representative WT Robo expressing Slit CM-treated cells from the same experimental trial in (Figure 3.5A, same trial as 3.5B,D). Applying this same *gamma*-Secretase inhibitor to cells expressing Robo missing its AP-2 adaptor motifs (see Figure 2.3, Figure 3.5D) are indistinguishable from those untreated with the drug (Figure 3.5C), missing the increase in branching and length resulting from drug treatment observed in WT-Robo expressing cells. Taking this analysis to be similar to epistasis of *endocytosis* and *transmembrane cleavage* on the common substrate of Robo, we propose that endocytosis is epistatic to transmembrane cleavage, consistent with the second cleavage event occurring downstream of endocytosis.

This is consistent with the dependence of Notch ICD generation on Clathrin-dependent endocytosis (Vaccari et al. 2008; Gupta et al. 2009). The dependence of Presenilin activity on endocytic trafficking may be explained by the spatial restriction of *gamma*-Secretase complex localization or activity to the acidic late endosome. Nicastrin has been demonstrated to localize to the lysosome (Pasternak et al. 2003), and the NGF treatment-dependent conversion of p75 CTF into ICD occurs in the sub-cellular fraction-derived compartment of endosomes in PC12 cells (Urra et al. 2007). If Robo's cleavage by Presenilin releases the ICD into the lysosome for degradation, thereby terminating its signaling, this would explain how the turnover of Robo protein depends on Kuz's activating cleavage and why we see a negative regulatory role for *psn* in *in vivo* genetic interactions and *in vitro* activation.

If the second cleavage event serves to terminate signaling from an activated CTF then we would expect that the cleavage product would have no repulsive activity. Consistent with this model, the engineered ICD displays neither cell spreading (or process generation) activity when expressed either in S2R+ cells (Figure 3.5F,G) nor midline guidance activity when expressed transgenically in the *Drosophila* embryo.

Over-expressing an insert of C-terminal epitope-tagged ICD, that is inserted into the same chromosomal site – and therefore not subject to positional-induced expression level differences- as the Full-length, *wild-type* Robo analyzed in (Figure 2.7), is not sufficient to signal repulsion from the midline either in all neurons or in the Eg commissural subset (data not shown). Similarly, the same insert is not able to rescue loss of midline repulsion in either the FasII or Ap+ axons in *robo* mutant embryos, in contrast to full-length Robo Transgene (data not shown, compared to Figure 2.8). Robo ICD's lack of ability to signal to the cytoskeleton of S2R+ cells or navigating growth cones are not due to any obvious effects on protein localization as the ICD construct is detected by immunostaining uniformly throughout a given S2R+ cell, and in axon fascicles when expressed in subsets of neurons(data not shown).

Interestingly driving expression of Robo CTF in S2R+ cells (Figure 3.5E) confers slightly more cortical spreading capacity than does expressing ICD, but this effect is modest comparing cortical size of cells expressing Robo missing its first Ig domain or even the entire C-terminus. This indicates that Robo ectodomain beyond the first 9 amino acids from the TMD confers some signaling capacity to Robo. This might reflect a requirement for Robo ectodomain in either a low level of auto-activation by self-association between high concentrations of receptors, or a conformational change that is enhanced by ligand-binding, as occurs in the Notch pathway (Kopan and Ilagan 2009). Future work with ectodomain swaps or serial ectodomain deletions in this assay may be able to shed insight into this question. This may also simply reflect the speed with which the constitutive cleavage of a CTF into an ICD occurs, if indeed the second cleavage event is inactivating for this assay. Regardless, Robo ICD's lack of repulsive signaling capacity when overexpressed along with endogenous Robo in the embryo rules out a

model for ICD function in which it serves as a positive feedback loop effector in ligand-induced receptor activation, as is the case for Eph ICD (Georgakopoulos et al. 2006).

**Robo juxtamembrane cleavage is required for Robo activation, and occurs upstream of Slit-binding**

To more directly test for the polarity of regulation provided by the first ectodomain shedding event we turned to the same *in vitro* Slit-dependent Robo activation assay just described. ADAM10 metalloproteases both catalyze the cleavage of and contribute to the signaling of other axon guidance molecules, often in a ligand-dependent manner (Galko and Tessier-Lavigne 2000; Hattori et al. 2000; Janes et al. 2005; Georgakopoulos et al. 2006; Litterst et al. 2007); reviewed in (Beel and Sanders 2008)). It was previously demonstrated that KuzDN co-expression abrogates the Slit-dependent recruitment of Sos to the Robo receptor in HEK293T cells (Coleman et al 2010), and that the juxtamembrane region of Robo is required for repulsive midline guidance.

Here, using finer molecular genetic manipulations than the original RoFraRo (Robo-U, Figure 3.1), we again provide evidence that Robo's juxtamembrane region is required for its activation *in vitro*. Expressing versions of Robo where the entire 55aa juxtamembrane domain between its FN3 and TMD is deleted (Figure 3.6B), or versions with two smaller deletions encompassing the putative Kuz cleavage site on dRobo1 (Figure 3.6C,D) inhibits the Slit-dependent process elaboration seen in cells expressing WT Robo (Figure 3.6A). Unlike a human Robo juxtamembrane deletion that included part of the FNIII domain (Seki et al 2010), this deletion is expressed in cells, as assayed by immunostaining for a C-terminal epitope tag. Importantly, adding back human

Robo1's JM Domain (33amino acids, Figure 3.6E) restores the process elaboration response, consistent with a restoration of the activating cleavage, suggesting that this cleavage site is interchangeable and therefore conserved across phyla.

The crystal structure of human Robo1 reveals a beta-bulge (an electron-dense region) that is predicted to provide steric hindrance to hRobo1's ADAM10 cleavage site Glutamine888-Glutamine889. A point mutation to an aspartic acid residue that is predicted to destabilize the beta-bulge has been demonstrated to enhance the abundance of Robo ectodomain from transiently transfected HEK293T cells (Barak et al. 2014). To test whether this may have an effect on *Drosophila* Robo activation, I assayed the effect of the analogous point mutation on the process elaboration response to Slit. Slit-CM-treated cells expressing this construct appear to have an increase in process length (Figure 3.6F), a feature which reflects Robo activation, as the maximal Sholl radius is decreased in cells expressing Robo missing its entire C terminus or Slit-binding region (Figure 2.3). What is surprising is that combining this point mutation with a deletion of the Ig1 domain results in cells that look qualitatively like ΔIg1 (Figure 3.6G), but that have an increase in process length (Figure 3.6H). Whether this difference can be accounted for by the amount of Robo that is still able to bind Slit (there is still a very faint amount of Slit detectable by immunostaining on cells expressing Robo ΔIg1, as compared to cells expressing CTF, or no Robo at all), or that the cleavage is occurring upstream of Slit binding but is still required for activation is not known. A piece of evidence supporting the latter hypothesis is that ectodomain is still shed into the media from S2R+ cells expressing Robo missing its Ig1 domain. Further, Robo that is missing both its juxtamembrane domain and its Ig1 domain look more like ΔJM, whereas those that are missing their Ig1 domain and treated with the Clathrin-dependent endocytosis

inhibitor Dynasore look more like ΔIg1 alone (data not shown). One significant caveat to any conclusions about ordering ligand-binding and Kuzbanian-mediated proteolysis from this assay alone is that we have never been able to detect any Slit-dependency of ectodomain shedding from S2R+ or HEK293T cells in our lab. We can detect enhancement or abrogation by co-transfection with WT or DN-Kuz, respectively. This may reflect that the cleavage event indeed occurs before Slit binding, or it may reflect a shortcoming of our reduced complexity *in vitro* system.

Barak et al. propose a mechanism for *in vivo* Robo activation in which the mechanical tension generated by the force between a migrating growth cone and its tethering to the ECM by Robo-Slit-binding overcomes the intramolecular interactions stabilizing Robo's JM beta-bulge to induce a conformational change that allows ADAM10 access to its cleavage site on Robo. This model does accommodate the need for repulsion from an initially 'adhesive' event, implicated by others in repulsive guidance, however the relative avidities of the proposed protein-protein(-sulfate) interactions have not been quantified and therefore this model, though informed by that from other pathways (Notch and Ephrin) is unverified. A more lucid conclusion from this *in vitro* activation assay is that endocytosis and juxtamembrane cleavage both contribute to Robo activation as deleting both the juxtamembrane and the AP-2 adaptor motifs (Chapter 2) lead to a strong abrogation of process generation (Figure 3.6J) that is indistinguishable from deleting the entire C-terminus (Figure 3.6K). This evidence argues against a simple passive model in which Kuz-mediated cleavage or endocytosis are passive agents required for release of a migrating growth cone, but instead argue for a requirement for Robo internalization in the activation of cytoskeletal dynamics. Future work will have to be performed to elucidate the mechanics of Robo activation *in vivo*.

Taking the smallest juxtamembrane deletion identified to have reduced Robo activation (Figure 3.6D), and reduced CTF/ICD generation in S2R+ cells here (Figure 3.7C), I assayed its ability to induce gain of repulsion. Unlike over-expressing a juxtamembrane manipulation that does not affect ectodomain shedding in S2R+ cells (Figure 3.7A), that is sufficient to induce thinning commissures and thickened longitudinals, Robo missing its HKK residues does not display gain of repulsion, despite comparable expression levels, as assayed by HA antibody signal in (Figure 3.7B vs. A). There does also appear to be some commissural signal of transgene, like that in *kuz* mutants or in over-expressed Robo-U (Coleman et al 2010), consistent with membrane-bound, inactivated Robo retained on the segments of axons as they ignore repulsive cue within the midline. This construct gives worse rescue than WT Robo when expressed in the ipsilateral Ap axons of *robo* mutants (Figure 3.7D). Whether this trend holds up across multiple inserts and in the full array of assays utilized in Figures 2.7 and 2.8 remains to be tested.

## Discussion

The *in vivo* paradoxical correlation between increase in repulsive receptor levels and decreased midline repulsion suggest that Kuz positively regulates (1) repulsive guidance, (2) exclusion of Robo from commissures, and (3) a reduction in Robo protein levels. Together with the biochemical analysis, we can conclude that the mechanism of Kuz's action in repulsive guidance is juxtamembrane cleavage of Robo, which somehow couples exclusion of Robo from commissures to repulsive signaling. This suggests that

somehow this cleavage event is both necessary for activation of Robo (and therefore repulsion) and linked to clearance from commissural segments of axons. We provide evidence that this cleavage event may occur upstream of Slit-binding, not refuting that it is required for Robo's activation, but future work is required to provide a formal decision on the relative order of these two events *in vivo.*

The correlation between clearance from axons and signaling is consistent with internalization into a given growth cone that we demonstrated is provided by Slit-dependent Robo endocytosis in Chapter 2. The *in vitro* S2R+ Robo activation assay corroborates that a juxtamembrane cleavage provided by the ADAM10 metalloprotease Kuzbanian is required for its repulsive signaling *in vivo.* We also demonstrate that this process, combined with Robo endocytosis, can fully account for all Robo signaling as assayed by process elaboration provided by the C-terminus. Finally, we presented evidence supporting a model in which a second, inactivating *gamma*-Secretase mediated cleavage of Robo shortens the time-course of signaling from an activated, internalized receptor fragment.

**A Presenilin-mediated inactivating cleavage of Robo**

Given that the Uncleavable Robo *in vivo* rescue data predict Kuz to be performing an activating cleavage, a subsequent cleavage might serve to shorten the time course of activation, thereby providing evidence for an attenuation of signaling from an activated guidance receptor. Metalloproteases have been shown to both cleave and contribute to the signaling of other axon guidance molecules. For example, Kuz-mediated cleavage of ephrin-A2 allows for repulsion from an initial point of adhesion with its cognate EphA receptor (Janes et al. 2005; Atapattu et al. 2012). The signaling role of

the second, constitutive *gamma*-Secretase-mediated cleavage is not conserved between pathways; for example, in the case of Notch the ICD acts as a transcriptional regulator (Mumm et al. 2000), in the case of Ephrin-B it acts as a local signaling molecule to positively regulate phosphorylation of uncleaved ligands (Georgakopoulos et al. 2006).

In our system we have shown that *gamma*-Secretase provides a negative regulatory cleavage event to Robo signaling both at the midline and in a ligand-dependent cytoskeletal readout *in vitro*. Our *in vitro* Robo activation and *in vivo* genetic interactions are consistent with *gamma*-Secretase negatively regulating Slit-Robo midline repulsion and Slit-dependent process elaboration, respectively. If *gamma*-Secretase's cleavage of Robo occurs in the multi-vesicular bodies of the late endosome, then releasing a soluble ICD into the topology-reversed lysosomal compartment would passively lead to turnover of Robo protein levels. That Kuzbanian's activating cleavage would gate this second cleavage event provides an explanation for how and why the juxtamembrane cleavage that is required for Robo signaling is coupled with turnover of protein levels. We predict that the Kuzbanian-mediated Robo cleavage product, the CTF, if already afforded Dock recruitment by Slit-binding when generated from Full-length receptor (as opposed to engineered CTF which is incapable of Slit-binding) would signal as it trafficks through endocytic pathways until its solubilization into the MVB's. Degradation of Robo ICD in the lysosome would curtail the time-course of signaling from a receptor that has lost the spatial fidelity to the original location of its activating ligand at the surface of the cell.

Future work to further elucidate the relative order and interplay between endocytosis and proteolytic regulation of Robo activation dynamics should shed insight onto the contribution of these pathways to Robo-mediated midline repulsion.

## Materials and Methods

### Genetics

The following Drosophila mutant alleles were used: *robo*$^{GA285}$, *robo*$^{z1772}$, *robo*$^{5}$, *slit*$^{1}$, *slit*$^{2}$, *slit*$^{e158}$, *kuz*$^{e29}$, *kuz*$^{H143}$, *psn*$^{12}$, *psn*$^{145}$, *psn*$^{227}$, *nct*$^{EY}$, *aph-1*$^{D35}$. The following transgenes were used: P[UASp-YFP-Rab5.S25N]35. The following transgenic flies were generated by BestGene Inc (Chino Hills, CA) using ΦC31-directed site-specific integration into landing sites at cytological position 86F8 (controlling for expression level effects from chromosomal position): P*[5xUAS-RoboICDKozak-6xmyc]86Fb, P[GAL4-elav.L]3 (elav-GAL4), eg*$^{MZ360}$ *eg-GAL4* (Ito *et al.* 1995), *ap-GAL4* (Calleja *et al.* 1996), eg-GAL4. All crosses were carried out at 25°C. Embryos were genotyped using balancer chromosomes carrying *lacZ* markers or by the presence of epitope-tagged transgenes.

### Molecular Biology

*pUAST cloning:* The RoboICDKozak coding sequences were cloned into a pUAST vector (p5UASTAttB) including 5xUAS and an attB site for ΦC31-directed site-specific integration. All p5UASTattB constructs include identical heterologous 5' UTR and signal sequences (derived from the Drosophila wingless gene) and a C-terminal 6×myc tag. The pUAST-3xHA-RoboΔHKK-6xMyc transgenic lines were created by standard transgenic methods without control over chromosomal insertion site. Robo domain deletion variants created for this study were generated by PCR and include the following amino acids (numbers refer to Genbank reference sequences AAF46887 [Robo]: Robo$^{\Delta Ig1}$ (153-1395) (Evans et al 2014), Robo$^{\Delta C}$ (56-950) (Evans et al 2014), Robo$^{\Delta YLQY}$

$^{\Delta YQAGL}$ (1090-1093; 1233-1237), Robo$^{\Delta(Juxtamembrane)}$ (862-916), Robo$^{JM\ D>A}$ (863), Robo$^{\Delta DINPTTHKK}$ (900-908), Robo$^{\Delta HKK}$ (906-908), Robo$^{\Delta Juxtamembrane}$ (862-916), Robo$^{humanRobo1\ swap}$ (865-897 of hRobo). All Robo constructs used in the *in vitro* S2R+ activation assay were cloned into the 5xUAS-AttB plasmid containing 3xHA(N) and 6xMyc(C) tags, or 3xHA no C-terminal Tag (Barry Dickson, shuttled into p5AttB here), Robo ΔEcto/CTF (3xHA/6xMyc) was created by PCR using the following primers: tatataCGCTAGCatg**ACCACTGACTACCTATCTGGACC,** tcgggtggctattgggatgc. RoboΔYLQY was created using the following primers: TTGTCAAATCCAAC**CCGGTTGAACCGATCA,**TGATCGGTTCAACCGG**GTTGGATTT GACAA**; ΔYQAGL: CAGCCAGCGAG**AATGCAGCG,** CGCTGCATTCTCGCTGGCTG; RoboΔ(JM):**TGGACCTTACTCCAAACCGATATCACTATTC**TACCTATCTGGACCGTG GCTAATGG,CCATTAGCCACGGTCCAGATAGGTA**GAATAGTGATATCGGTTTGGAG TAAGGTCCA;** RoboΔDINPTTHKK: CATACCACCTGGC**ACCACTGACTACC,** GGTAGTCAGTGGTGCCAGGTGGTATG;RoboΔHKK:GACATTAATCCCACCACT**ACCA CTGACTACCTATCT,** AGATAGGTAGTCAGTGGTAGTGGTGGGATTAATGTC; RoboJM$^{D>A}$ : TCACTATTCATGG**c**CCCCACCCAT,ATGGGTGGGGgCCATGAATAGTGA ; Robo ICD:tatataCGCTAGCatg**CATCAAATGACCAAGGAATTGGGTC,**

TAGATCTGGTGGTTGGAGGAGGTC=RKC179; RoboICDKozak:tatatata**GAATTCcacc**atgCATCAAATGACCAAGGAATTGGGTC, (RKC179), cloned into vector 192 (BmtI-less backbone, see Chapter2 Materals & Methods); RoboCTF: CGCTAGCTTAGAT**ACCACTGACTACCTATCTGGACC, (RKC179).**

**Immunofluorescence and Imaging**

*in vitro* Robo activation assay: *Drosophila* S2R+ cells were cultured at 25°C in Schneider's media plus 10% FBS and 1% Penicillin-Streptomycin. To assay for Slit response, cells were plated on acid-etched, poly-L-lysine coated coverslips in duplicate in six-well plates (Robo-expressing cells) at a density of $1\text{-}2\times10^6$ cells/mL, and transfected with 0.25ug of p5AttB construct and pMT-GAL4/2mL Schneider's (a one-day lag between CM and Robo cells) using Effectene transfection reagent (Qiagen). GAL4 expression was induced with 0.5 mM $CuSO_4$ for 24 hours, then Slit-Conditioned Media (CM) was collected and concentrated from cells transfected with empty pUAST vector or Slit. Robo-transfected cells were incubated with CM on an orbital shaker at room temperature for 10 minutes, then fixed for 10 minutes at RT in 4% PFA. Cells were rinsed with 1XPBS, permeabilized with PBS+0.1% Triton X-100 (PBT) for 2 minutes, then blocked for 1Hr and stained with antibodies diluted in PBT+4% NGS. Antibodies used were: mouse anti-Slit-C (c555.6D, DSHB, 1:100), mouse anti-cMyc (9E10, 1:1000), rabbit anti-cMyc (Sigma c3956, 1:1000), rabbit anti-GFP (Invitrogen #A11122, 1:1000), rabbit anti-HA (Covance, 1:1000), Cy3 goat anti-mouse (Jackson Immunoresearch, 1:1000), and Alexa488 goat anti-rabbit (Molecular Probes, 1:500). Coverslips were mounted in Aquamount. 0.252μM totalZ confocal stacks were collected using a Leica TCS SP5 confocal microscope at 63X and zoom3 and processed with FIJI and hand-calculations in Excel.

Embryos: Dechorionated, formaldehyde-fixed, methanol-devitellinized *Drosophila* embryos were fluorescently stained using standard methods. The following antibodies were used in this study: FITC-conjugated goat anti-HRP (Jackson # 123-095-021, 1:250), mouse anti-Fasciclin-II/mAb 1D4 [Developmental Studies Hybridoma Bank, (DSHB), 1:100], rabbit anti-GFP (Invitrogen #A11122), 1:1000, mouse anti-HA (1:1000),

mouse anti-βgal (DSHB, 1:150), Alexa-488 conjugated goat-anti-HRP (Jackson #123-605-021 1:100), Cy3-conjugated goat anti-mouse (Jackson #115-165-003, 1:1000), Alexa-488-conjugated goat anti-rabbit (Molecular Probes #A11008, 1:500). Embryos were filleted and mounted in 70%glycerol/1XPBS and imaged on Leica TCS SP5 at 63X with a zoom of 1.7. Images were processed using FIJI.

**Biochemistry**

Robo ectodomain: S2R+ cell conditioned media/supernantant was boiled for 10' in 2X SDS Loading Buffer. Robo CTF/ICD: S2R+ cell lysates were lysed in TBS-V with NP40. Robo ectodomain from embryos: embryos were lysed with TBS-V with NP40 and immunopreciptated with mouse-anti-HA to detect full-length and ectodomain products from UAS-HA-Robo-myc p5 AttB inserts into the 86Fb chromosomal site. Proteins were resolved by SDS Page and transferred to nitrocellulose and incubated with anti-HA (Covance 1:1000) or anti-Myc (9E10 1:1000) overnight at 4°C in PBS/0.05% Tween-20/5% non-fat dry milk. Blots were incubated with HRP-conjugated anti-mouse secondary antibody for 1 hour at RT and signal was detected using ECL Prime (Amersham).

## Robo proteolytic processing figures

### A Kuzbanian-catalyzed juxtamembrane cleavage of Robo is required for its repulsive guidance activity *in vivo*

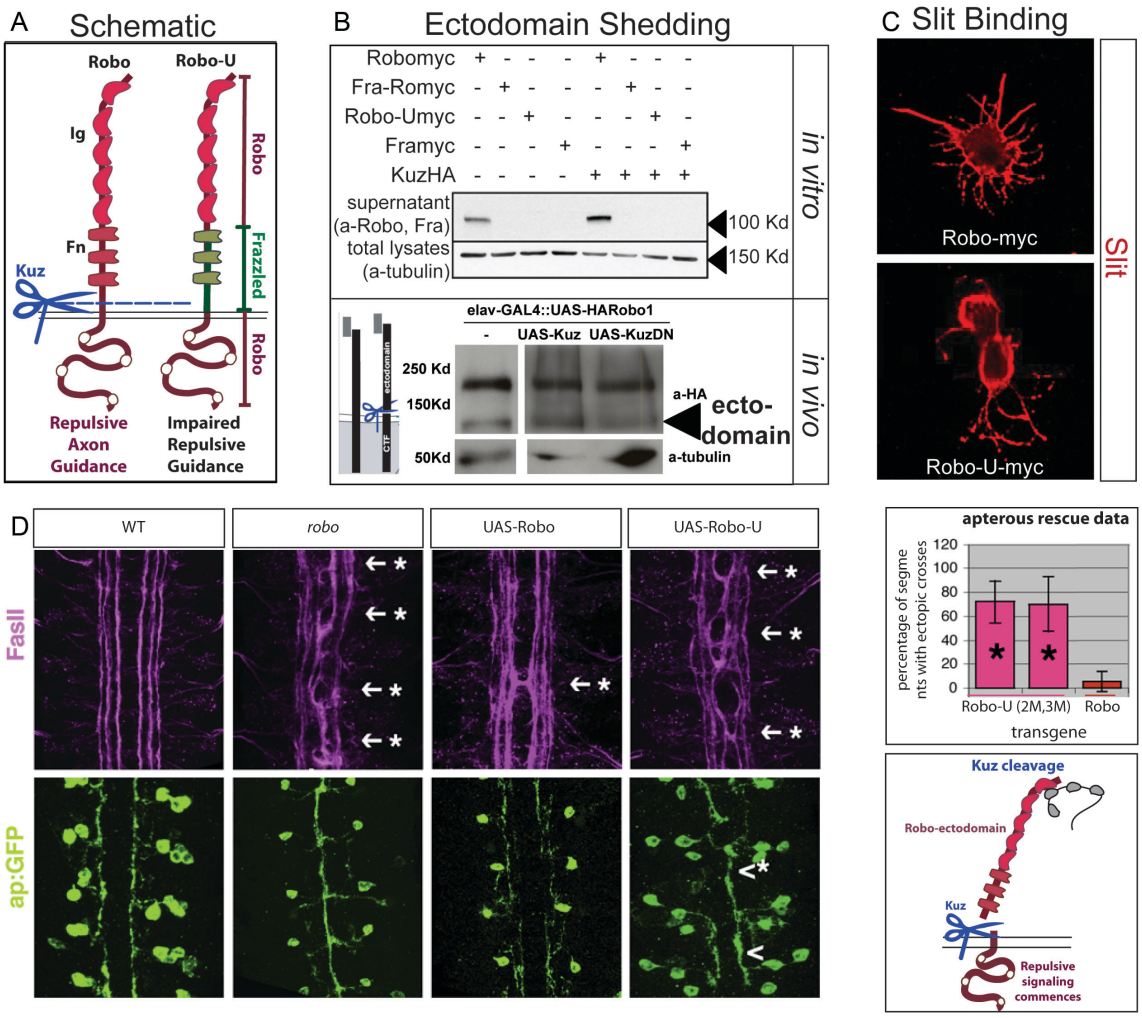

**Figure 3.1: A kuzbanian-catalyzed juxtamembrane cleavage of Robo is required for its repulsive guidance activity in vivo**
*A-C:* Robo is cleaved by Kuzbanian metalloprotease, chimeric Ro-Fra-Ro (Robo-U) is not.

B. The *kuzbanian* metalloprotease enhances shedding of an N-terminal Robo fragment in S2R+ cells, and has a dose-dependent effect on the same fragment of Robo transgene in embryos. A chimeric version of Robo ("Robo-U"), lacking Robo identity at its putative cleavage site (blue dotted line), is uncleavable by Kuz in an *in vitro* assay (A,B). Robo-U's juxtamembrane Frazzled identity does not affect its ligand-binding (Slit signal on S2R+ cells expressing indicated receptors, C).

D. Kuz-mediated Robo cleavage is important for repulsive guidance

*robo* null embryos show ectopic entry of the medial-most of the normally ipsilateral FasII-positive fascicles into, and collapse of the ipsilateral apterous (Ap) axons onto, the midline. Expressing a WT Robo transgene in neurons largely rescues ectopic circling of the medialmost FasII fasicle, and completely rescues apterous ectopic collapse (quantified on right). Expressing two independent Robo-U transgenes does not rescue either FasII or apterous ectopic crossing (quantified on right). These data provide strong evidence that Kuz-mediated cleavage of Robo is important for repulsive guidance in vivo.

(Figure adapted from Coleman *et al.* 2010- Experiments in B *in vitro* and D were performed by Hope Coleman, Experiments in B *in vivo* and C were performed by RKC. All schematics were created by RKC.)

**Robo clearance from commissural segments is correlated with repulsion**

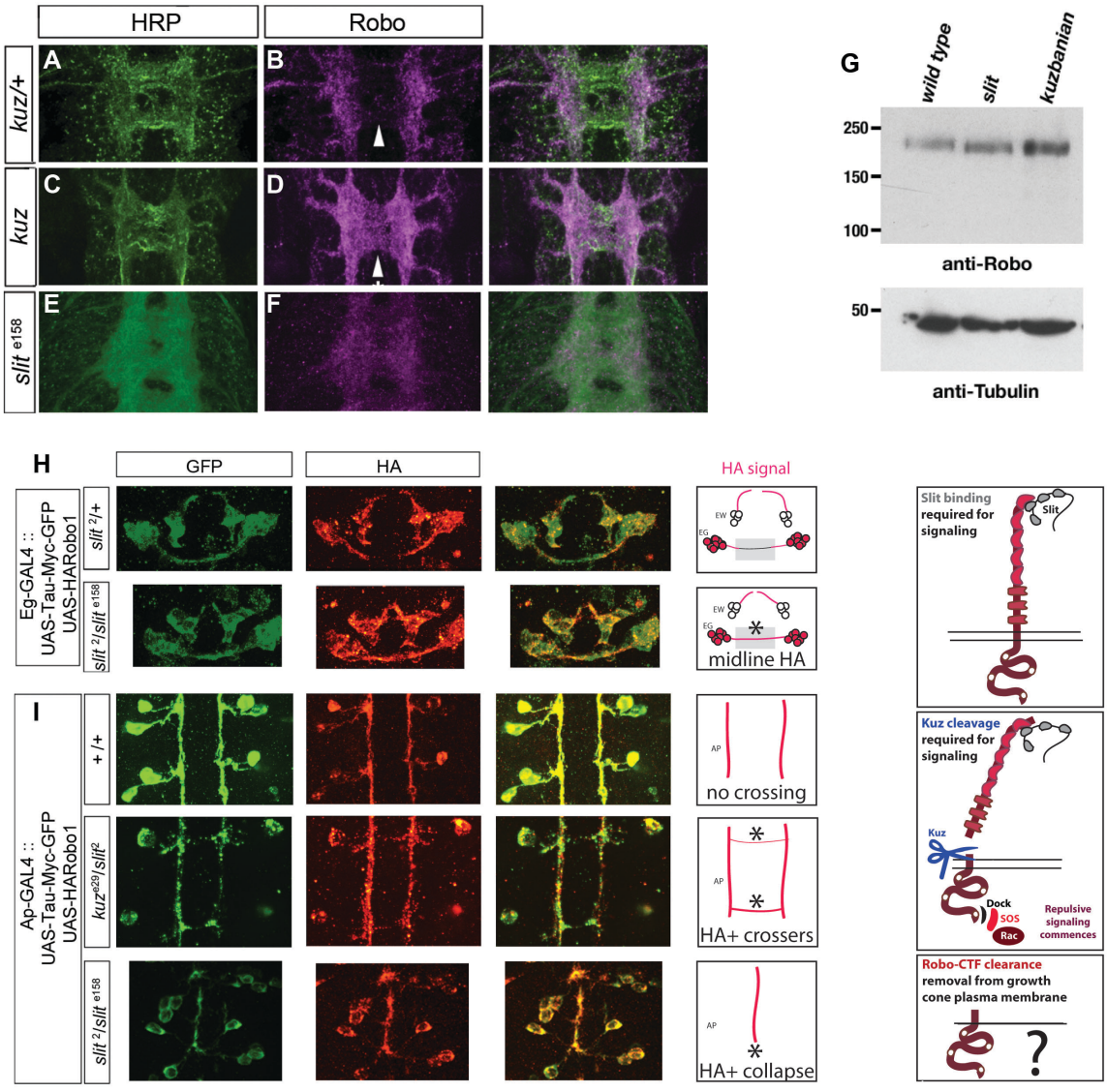

**Figure 3.2: Robo clearance from commissural segments is correlated with repulsion**

A-F*:* Stage 14 *Drosophila* embryos are stained with either HRP, marking all neurons, or 13C9, detecting endogenous Robo protein levels. B and D were stained before fixation, reflecting surface Robo distribution while F reflects signal from both intra- and extra-cellular Robo. *kuzbanian* mutant and *slit* hypomorphic embryos display Robo protein mislocalized to the commissural segments of axons.

H-I: The projection pattern of the Eg commissural subset of axons(H) and the ipsilateral Apterous subset of axons (I) are labeled with a GFP-tagged microtubule transgene. An N-terminal epitope tag on Robo is imaged in red and schematized on the right in pink. ku*zbanian* and *slit* are required for repulsive guidance and clearance of Robo transgene from axon fascicles. In a commissural subset of axons in *slit* hypomorphs, there is a displacement towards the midline, with ectopically retained HA-Robo signal (H). In *slit* mutants, the normally ipsilateral Ap axon fascicles that collapse onto the midline express HARobo signal (Figure 3.2I). In *slit/kuz* transheterozygotes, there are subtle crossing events, that, also bear HA signal.

(Figure adapted from Coleman *et al.* 2010- Experiments in A-D; G were performed by Greg Bashaw. All others were performed by RKC.)

**Figure 3.3*: gamma*-Secretase catalyzes Robo cleavage *in vitro***

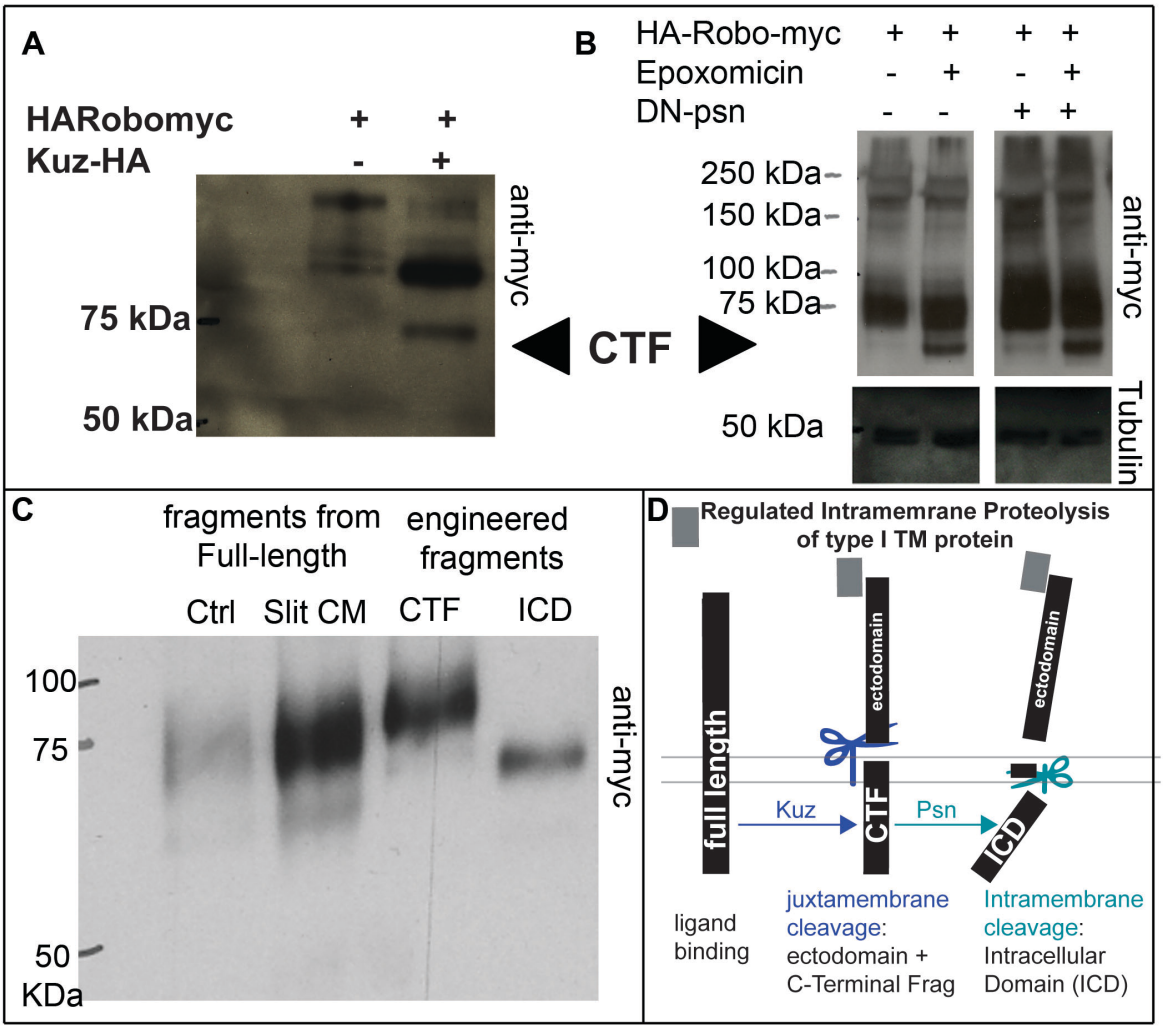

**Figure 3.3: *gamma*-Secretase catalyzes Robo cleavage in vitro**

A-C: Antibody signal to C-terminal epitope tag on Robo from Western Blots of samples from S2R+ cell lysates transiently transfected with Robo are displayed.

D: The schematic illustrates processive proteolysis of a full-length receptor into an ectodomain and CTF by Kuz/ADAM10, and subsequent γ-Secretase-mediated cleavage of membrane-bound CTF into a soluble ICD.

SDS-PAGE analysis of S2R+ cell lysates reveals two C-terminal fragments of Robo. The abundance of a ~60KDa C-terminal fragment is enhanced either by enhancing Kuz function by co-transfection with WT Kuz (A), or by inhibition of *gamma*-Secretase activity by co-transfection with UAS-Presenilin-DN (B). The generation of these fragments from full-length receptor is enhanced by Slit Conditioned Media treatment (C, lane 2 as compared to lane 1), and they run at the same size as engineered Robo missing its ectodomain (CTF), and that which starts after the Transmembrane domain (ICD). Note that the size-matched ICD generated from full-length Robo also displays Slit-sensitive abundance.

**Figure 3.4: gamma-Secretase complex genes genetically interact with the Slit/Robo pathway**

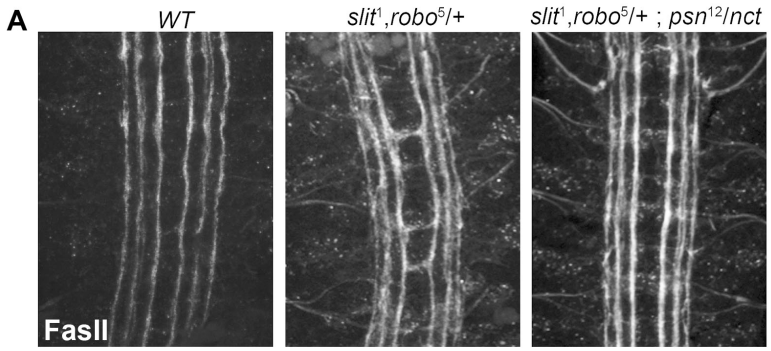


| Genotype | (embryos)/ segments scored | % FasII crossing defects | Statistics unpaired t-test |
|---|---|---|---|
| slit$^{1}$,robo$^{5}$/+ | (12)/132 | 22.7 | -- |
| slit$^{1}$,robo$^{5}$/+;psn$^{145}$/psn$^{12}$ | (22)/242 | 4.1 | p<0.0005 |
| slit$^{1}$,robo$^{5}$/aph-1$^{D35}$; psn$^{12}$/+ | (23)/253 | 12.6 | -- |
| slit$^{1}$,robo$^{5}$/+;nct/psn$^{12}$ | (48)/528 | 6.5 | p<0.005 |
| slit$^{1}$,robo$^{5}$/+;nct/psn$^{227}$ | (11)/110 | 6.4 | -- |

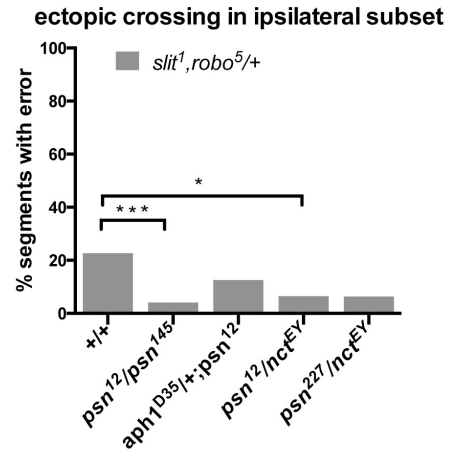


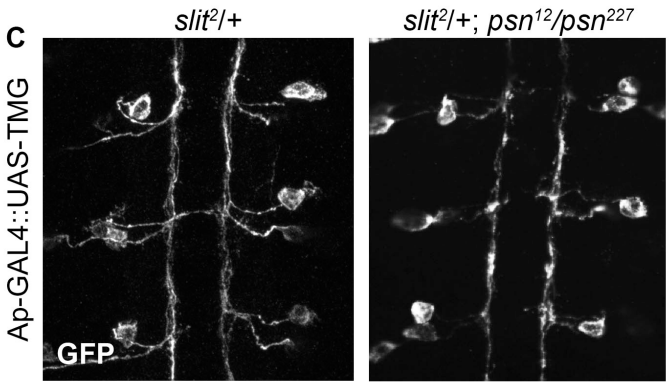


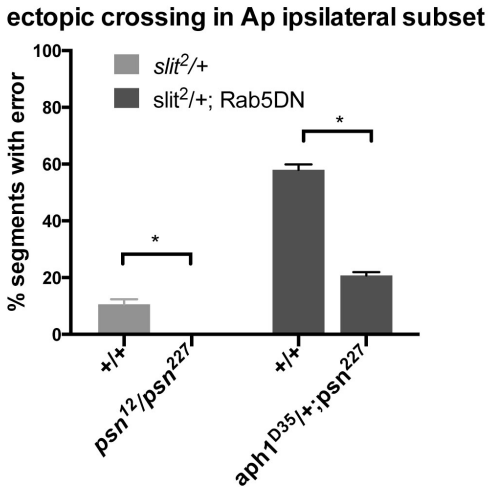

**Figure 3.4*: gamma*-Secretase complex genes genetically interacts with the Slit/Robo pathway**

(A) An ipsilateral subset of axons in the ventral nerve cord of stage 16 *Drosophila* embryos are stained with a monoclonal antibody (mAb) to FasciclinII (FasII). Double heterozygous *slit, robo* embryos have a mild loss-of-repulsion phenotype (induction of ectopic crossing events in 22% of embryonic segments). Inhibiting *gamma*-Secretase activity by removing heteroallelic combinations of members of its complex *presenilin (psn), nicastrin (nct) or anterior pharynx 1 (aph-1)* suppresses the crossing defects to 0%. These suppressions are statistically significant by the Student's Unpaired t-test when indicated by *'s (B).

C: A more restricted ipsilateral subset of axons are genetically labeled with Tau-Myc-GFP transgene to highlight their microtubules and therefore axonal projection patterns. In stage 16 WT embryos the two Ap axon fascicles on either side of the midline project ipsilaterally in all embryonic segments. In animals where one copy of *slit* has been removed, a partial loss of repulsion phenotype results with 11% of segments exhibiting ectopic crossing events (indicated by *). In embryos that also express DN-Rab5, inhibitng early endosome entry, in the same background the crossing errors are enhanced. Inhibiting *gamma*-Secretase by introducing two mutant *psn alleles* in first background, and one allele each of *aph-1* and *psn*, suppresses the ectopic crossing errors to 0%, and 22%, respectively (D).

**Figure 3.5: *gamma*-Secretase negatively regulates Robo signaling**

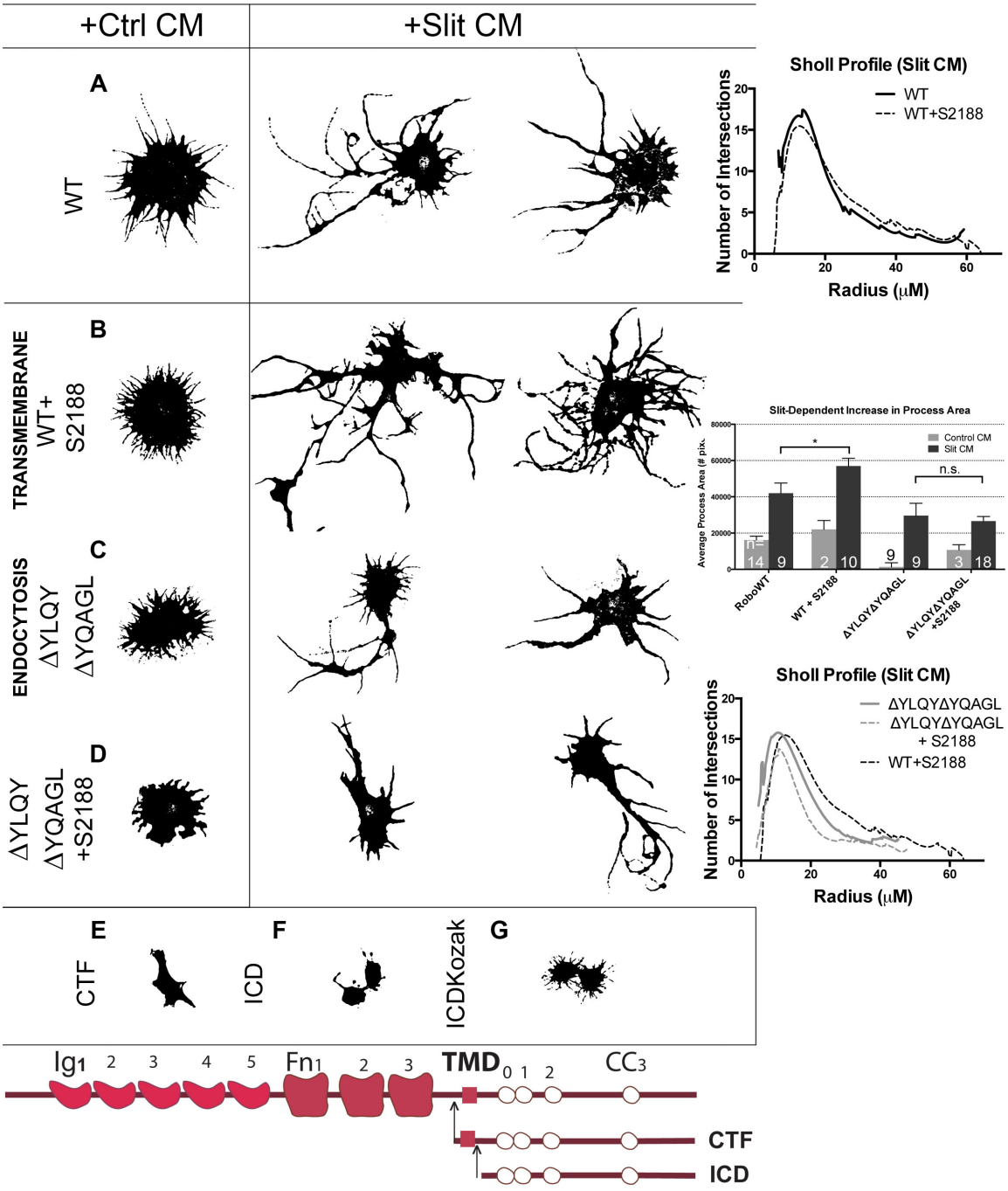

**Figure 3.5: gamma-Secretase negatively regulates Robo signaling**

Morphological profiles of Drosophila embryonic cells bath treated for 10' with Conditioned Media (CM) from cells either expressing empty vector ("Control"), or secreting Slit. A: Cells expressing WT Robo that are treated with Control CM show a baseline level of process generation that are more branched and elaborated if Slit treated, with two representative examples for Slit CM shown. B: Cells expressing WT treated with 20μM of the *gamma*-Secretase inhibitor S2188 (Wolfe et al. 1998) show enhancement of process length and branching seen in A; displayed cells are determined to be representative from two trials. In contrast, cells expressing Robo missing its AP-2 binding motifs (Figure 2.3,C) do not show sensitivity to S2188 by enhancement of process length or branching upon treatment with the same drug (D). E-G: Cells expressing engineered C-terminal fragments of Robo to approximate *kuzbanian* and *presenilin*-mediated cleavages are not responsive to SlitCM treatment. Cells expressing engineered Robo CTF (E, containing 9 amino acids N-terminal to the Transmembrane Domain) exhibit low levels of spreading behavior. Cells expressing Robo ICD (F, soluble), or the ICD with a Kozak sequence (G), do not show the cortical spreading behavior that Robo-CTF+ cells do, but do show a very low basal process generation above untransfected cells.

**Figure 3.6: Juxtamembrane Robo cleavage required for its signaling occurs upstream of Slit-binding in vitro**

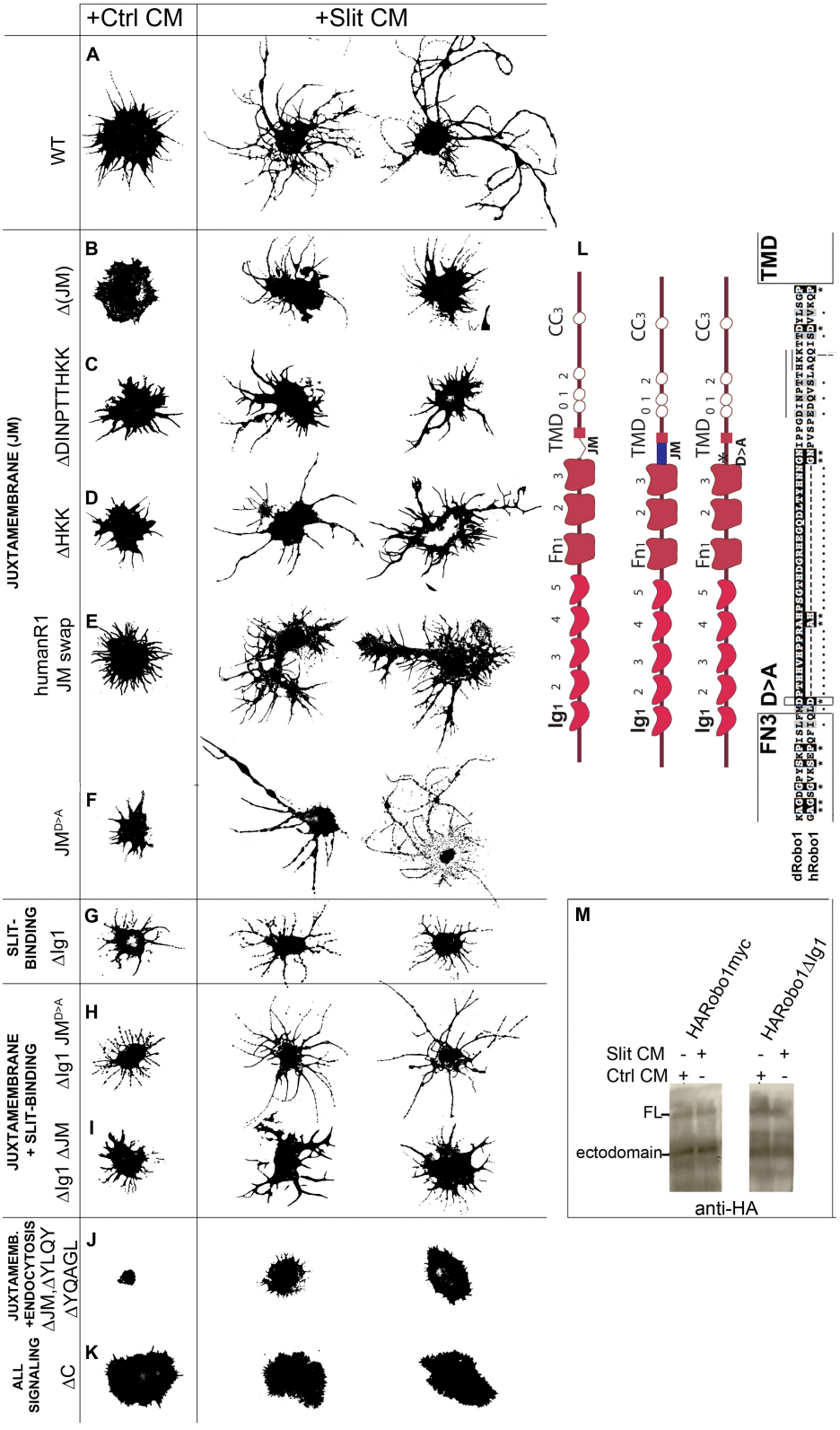

**Figure 3.6: Juxtamembrane Robo cleavage required for its signaling occurs upstream of Slit-binding in vitro**

Morphological profiles of Drosophila embryonic cells bath treated for 10' with Conditioned Media (CM) from cells either expressing empty vector ("Ctrl CM"), or secreting Slit. A: Cells expressing WT Robo that are treated with Control CM show a baseline level of process generation that are more branched and elaborated if Slit treated, with two representative examples for Slit CM shown. B-F: Manipulations to Robo's juxtamembrane domain, illustrated in domain structure diagrams and in more detail in the box-shade sequence alignment between *Drosophila* and *Human* Robo1 in (L) are assayed for effect on process elaboration behavior. B: Cells expressing Robo with its entire JuxtaMembrane (JM), the 55 amino acid stretch between the third FibroNectin Domain (FNIII) and the TransMembrane Domain (TMD), deleted show a reduction in process branching behavior, consistently across many trials (not quantified). C,D: Finer, nested deletions of 9 (C) and 3 (D) amino acids encompassing the predicted *d*Robo1 Kuzbanian cleavage site (aligned with *h*Robo1's Q-Q cleavage site indicated by the dotted line in the box shade alignment in L) also inhibit Slit-dependent process elaboration. E: Swapping in *human*Robo1's juxtamembrane domain is sufficient to restore a process branching response to Slit treatment. F: Point-mutating an aspartic acid residue at the very N-terminus of the JuxtaMembrane domain, homologous to the one shown by others to enhance the abundance of *Human* Robo ectodomain shed from transiently transfected HEK293T cells (Barak et al 2014), show an increase in process length in response to Slit CM treatment as compared to WT Robo-expressing cells. G: Cells missing their first ImmunoGlobulin (Ig) domain, required for Slit-binding in *Human* Robo1 (Fukuhara et al. 2008; Hohenester 2008) show a decrease in process field maximal radius and a characteristic 'beaded string' process morphology. H: Cells

expressing Robo missing its Ig1 and bearing the JM D>A point mutation are of a qualitative type that is an amalgamation of those with either manipulation singly; they have the beaded string process morphology of ΔIg1 with the increase of JM D>A in process length over just ΔIg1 alone. I: In contrast, cells missing both their Ig1 Domain and JM domain do not bear the qualitative type of processes that the ΔIg1 alone expressing cells do; instead they resemble ΔJM alone. M: Western blots of conditioned media from cells expressing either WT or ΔIg1 Robo-expressing cells both reveal Robo ectodomain (HA+ Fragment at ~120KDa), demonstrating that Kuz-mediated juxtamembrane cleavage is not affected in this assay by deletion of Robo's Slit-binding domain. J: Cells missing both their JM Domain and their AP-2 Binding motifs show strong complete abrogation of process elaboration response to Slit CM-treatment, rendering them indistinguishable from those expressing Robo missing it's entire C-terminus (K).

**Figure 3.7: Robo ICD generation requires *kuz*-mediated juxtamembrane cleavage**

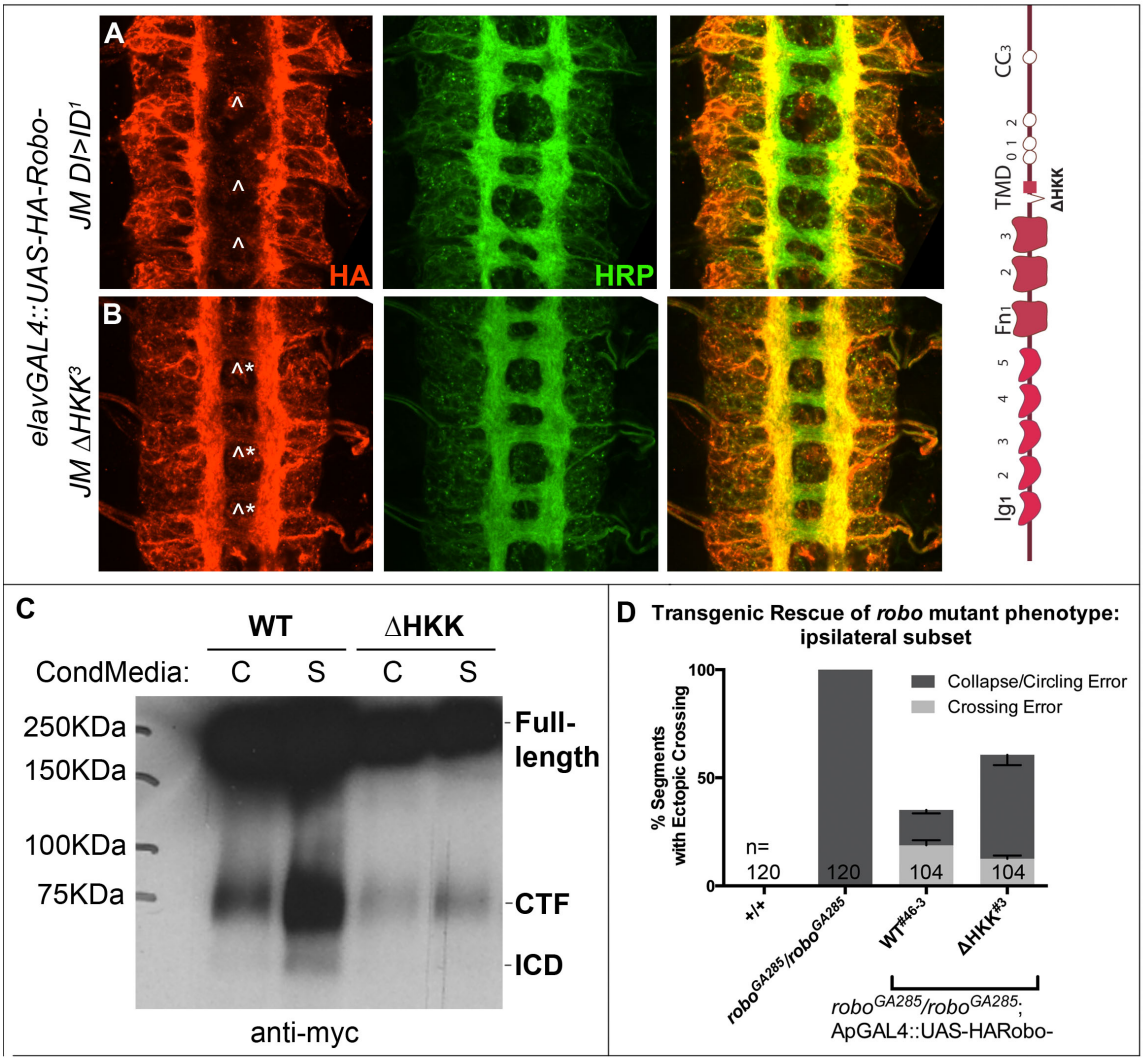


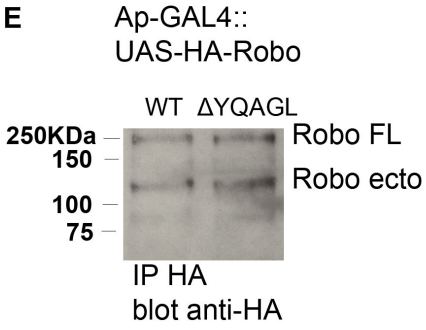

**Figure 3.7: Robo ICD generation requires kuz-mediated juxtamembrane cleavage**

A-B: The nerve cords of Stage late 14 *Drosophila* embryos are stained with HRP to reveal the entire neuropil scaffold (all neurons in green), and HA to reveal the spatial pattern of Robo transgene overexpressed in all neurons (N-terminal tag, red). A: Robo expressing a double point mutation that is sufficient to cause gain of repulsion in all neurons, and displays ectodomain shedding in embryos (data not shown) and therefore taken to function as a WT receptor is excluded from the commissural segments of axons. B: Robo missing its putative Kuz cleavage motif, that contributes to receptor activation (Figure 3.6D), does not cause appreciable thinning of the commissures and is faintly mislocalized to the commissural segments of axons (asterisks). C: Western blots of S2R+ lysates stained for Robo's C-terminal epitope tag preliminarily reveal that there is a shunting of the Slit CM-dependent increase in CTF upon deletion of the same 3 amino acid motif shown in B. D: One transgenic insertion is less effective than WT at rescuing the ectopic crossing defects in *robo* mutant embryos when transgenically expressed in the Ap ipsilateral subset of axons, as compared to one WT Robo insert. E: Immunopreciptations of N-terminal epitope tag on Robo transgenes expressed in the Apterous ipsilateral subset of axons using the GAL4-UAS system are blotted with antibody to the same HA tag. The abundance of the ectodomain fragment (120KDa) is not reduced in Robo constructs defective for AP-2 binding and therefore Clathrin-dependent endocytosis, as compared to WT, consistent with Kuzbanian-mediated juxtamembrane cleavage occurring upstream of endocytosis.

**Figure 3.8: A Model detailing Proteolytic Processing cascade and endocytic trafficking's contributions to Robo's activation dynamics**

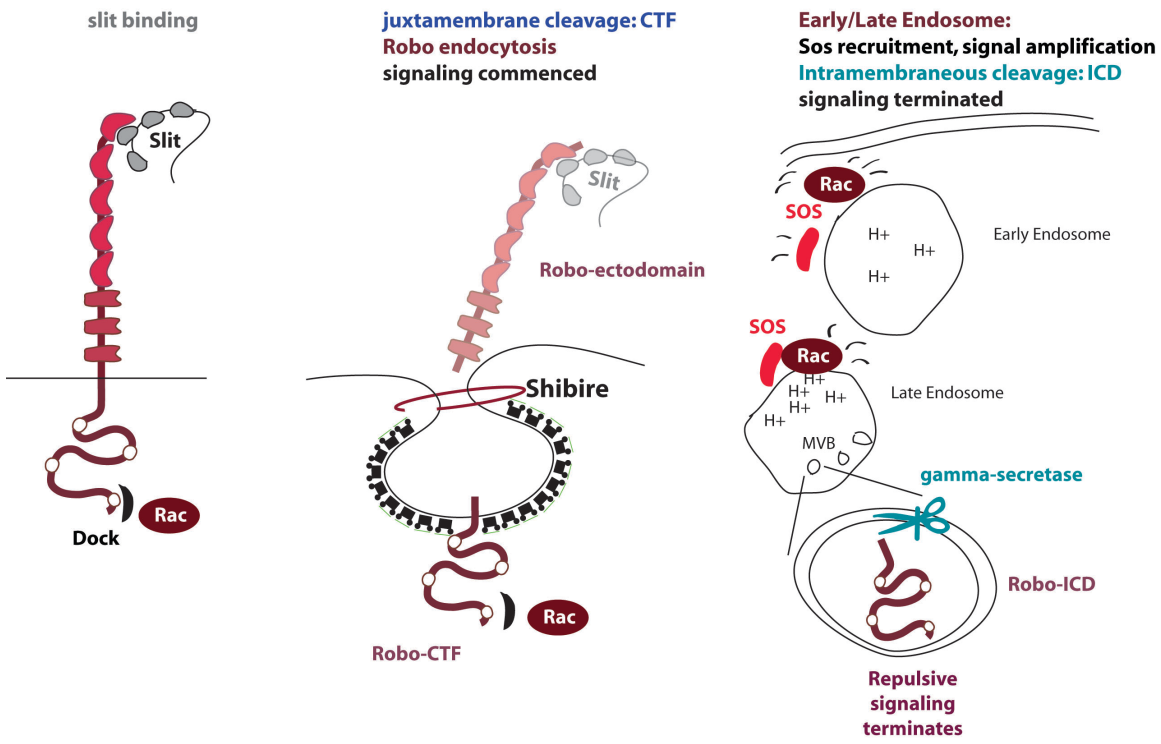

**Figure 3.8: A Model detailing Proteolytic Processing cascade and endocytic trafficking's contributions to Robo's activation dynamics**

Upon Slit-binding Robo is activated; the adaptor protein Dreadlocks (Dock) is recruited to Robo's CC2 and CC3 motifs, which in turn activated PAK and consequently initiates Rac activation (Fan et al. 2003). Juxtamembrane cleavage of Robo by Kuzbanian (Kuz) is required for both Robo activation *in vitro* and midline repulsion *in vivo* (Coleman et al. 2010). This cleavage event may occur after Slit-binding, but all evidence indicates that it is still required for Robo signaling output. Robo endocytosis occurs following juxtamembrane Kuz cleavage, as Robo defective for endocytosis still effectively generates Robo ectodomain in the embryo. Juxtamembrane proteolysis and Clathrin-dependent endocytosis cooperate to account for all the Robo activation provided by Robo's C-terminus *in vitro*. The correlation between retained surface Robo and decreased activation in Kuz-inhibited conditions may be explained by both internalization into the growth cone of Robo as well as the subsequent *gamma*-Secretase-mediated cleavage that allows its degradation, after entry into the late endosome, into the multivesicular bodies of the mature late endosome bound for lysosomal degradation.

## BIBLIOGRAPHY


Anitha, A., Nakamura, K., Yamada, K., Suda, S., Thanseem, I., Tsujii, M., Iwayama, Y., Hattori, E., Toyota, T., Miyachi, T. et al. 2008. Genetic analyses of roundabout (ROBO) axon guidance receptors in autism. *American journal of medical genetics Part B, Neuropsychiatric genetics : the official publication of the International Society of Psychiatric Genetics* **147B**(7): 1019-1027.

Atapattu, L., Saha, N., Llerena, C., Vail, M.E., Scott, A.M., Nikolov, D.B., Lackmann, M., and Janes, P.W. 2012. Antibodies binding the ADAM10 substrate recognition domain inhibit Eph function. *J Cell Sci* **125**(Pt 24): 6084-6093.

Bai, G., Chivatakarn, O., Bonanomi, D., Lettieri, K., Franco, L., Xia, C., Stein, E., Ma, L., Lewcock, J.W., and Pfaff, S.L. 2011. Presenilin-dependent receptor processing is required for axon guidance. *Cell* **144**(1): 106-118.

Barak, R., Lahmi, R., Gevorkyan-Airapetov, L., Levy, E., Tzur, A., and Opatowsky, Y. 2014. Crystal structure of the extracellular juxtamembrane region of Robo1. *J Struct Biol* **186**(2): 283-291.

Bartoe, J.L., McKenna, W.L., Quan, T.K., Stafford, B.K., Moore, J.A., Xia, J., Takamiya, K., Huganir, R.L., and Hinck, L. 2006. Protein interacting with C-kinase 1/protein kinase Calpha-mediated endocytosis converts netrin-1-mediated repulsion to attraction. *J Neurosci* **26**(12): 3192-3205.

Bashaw, G.J. and Goodman, C.S. 1999. Chimeric axon guidance receptors: the cytoplasmic domains of slit and netrin receptors specify attraction versus repulsion. *Cell* **97**(7): 917-926.

Bashaw, G.J., Kidd, T., Murray, D., Pawson, T., and Goodman, C.S. 2000. Repulsive axon guidance: Abelson and Enabled play opposing roles downstream of the roundabout receptor. *Cell* **101**(7): 703-715.

Beel, A.J. and Sanders, C.R. 2008. Substrate specificity of gamma-secretase and other intramembrane proteases. *Cell Mol Life Sci* **65**(9): 1311-1334.

Bhat, K.M., Gaziova, I., and Krishnan, S. 2007. Regulation of axon guidance by slit and netrin signaling in the Drosophila ventral nerve cord. *Genetics* **176**(4): 2235-2246.

Brose, K., Bland, K.S., Wang, K.H., Arnott, D., Henzel, W., Goodman, C.S., Tessier-Lavigne, M., and Kidd, T. 1999a. Slit proteins bind Robo receptors and have an evolutionarily conserved role in repulsive axon guidance. *Cell* **96**(6): 795-806.

Butler, S.J. and Dodd, J. 2003. A role for BMP heterodimers in roof plate-mediated repulsion of commissural axons. *Neuron* **38**(3): 389-401.

Campbell, D.S. and Holt, C.E. 2001. Chemotropic responses of retinal growth cones mediated by rapid local protein synthesis and degradation. *Neuron* **32**(6): 1013-1026.

Chang, B.S., Katzir, T., Liu, T., Corriveau, K., Barzillai, M., Apse, K.A., Bodell, A., Hackney, D., Alsop, D., Wong, S.T. et al. 2007. A structural basis for reading fluency: white matter defects in a genetic brain malformation. *Neurology* **69**(23): 2146-2154.

Charron, F., Stein, E., Jeong, J., McMahon, A.P., and Tessier-Lavigne, M. 2003. The morphogen sonic hedgehog is an axonal chemoattractant that collaborates with netrin-1 in midline axon guidance. *Cell* **113**(1): 11-23.

Chen, J.H., Wen, L., Dupuis, S., Wu, J.Y., and Rao, Y. 2001. The N-terminal leucine-rich regions in Slit are sufficient to repel olfactory bulb axons and subventricular zone neurons. *J Neurosci* **21**(5): 1548-1556.

Christoforidis, S., Miaczynska, M., Ashman, K., Wilm, M., Zhao, L., Yip, S.C., Waterfield, M.D., Backer, J.M., and Zerial, M. 1999. Phosphatidylinositol-3-OH kinases are Rab5 effectors. *Nature cell biology* **1**(4): 249-252.

Coleman, H.A., Labrador, J.P., Chance, R.K., and Bashaw, G.J. 2010. The Adam family metalloprotease Kuzbanian regulates the cleavage of the roundabout receptor to control axon repulsion at the midline. *Development* **137**(14): 2417-2426.

Cowan, C.W., Shao, Y.R., Sahin, M., Shamah, S.M., Lin, M.Z., Greer, P.L., Gao, S., Griffith, E.C., Brugge, J.S., and Greenberg, M.E. 2005. Vav family GEFs link activated Ephs to endocytosis and axon guidance. *Neuron* **46**(2): 205-217.

Das, B., Shu, X., Day, G.J., Han, J., Krishna, U.M., Falck, J.R., and Broek, D. 2000. Control of intramolecular interactions between the pleckstrin homology and Dbl homology domains of Vav and Sos1 regulates Rac binding. *J Biol Chem* **275**(20): 15074-15081.

Dickson, B.J. 2002. Molecular mechanisms of axon guidance. *Science* **298**(5600): 1959-1964.

Diefenbach, T.J., Guthrie, P.B., Stier, H., Billups, B., and Kater, S.B. 1999. Membrane recycling in the neuronal growth cone revealed by FM1-43 labeling. *J Neurosci* **19**(21): 9436-9444.

Egea, J. and Klein, R. 2007. Bidirectional Eph-ephrin signaling during axon guidance. *Trends Cell Biol* **17**(5): 230-238.

Falk, J., Konopacki, F.A., Zivraj, K.H., and Holt, C.E. 2014. Rab5 and Rab4 regulate axon elongation in the Xenopus visual system. *J Neurosci* **34**(2): 373-391.

Fan, X., Labrador, J.P., Hing, H., and Bashaw, G.J. 2003. Slit stimulation recruits Dock and Pak to the roundabout receptor and increases Rac activity to regulate axon repulsion at the CNS midline. *Neuron* **40**(1): 113-127.

Fukuhara, N., Howitt, J.A., Hussain, S.A., and Hohenester, E. 2008. Structural and functional analysis of slit and heparin binding to immunoglobulin-like domains 1 and 2 of Drosophila Robo. *J Biol Chem* **283**(23): 16226-16234.

Galko, M.J. and Tessier-Lavigne, M. 2000. Function of an axonal chemoattractant modulated by metalloprotease activity. *Science* **289**(5483): 1365-1367.

Galperin, E. and Sorkin, A. 2003. Visualization of Rab5 activity in living cells by FRET microscopy and influence of plasma-membrane-targeted Rab5 on clathrin-dependent endocytosis. *Journal of cell science* **116**(Pt 23): 4799-4810.

Garbe, D.S. and Bashaw, G.J. 2004. Axon guidance at the midline: from mutants to mechanisms. *Crit Rev Biochem Mol Biol* **39**(5-6): 319-341.

Gatto, G., Morales, D., Kania, A., and Klein, R. 2014. EphA4 receptor shedding regulates spinal motor axon guidance. *Curr Biol* **24**(20): 2355-2365.

Georgakopoulos, A., Litterst, C., Ghersi, E., Baki, L., Xu, C., Serban, G., and Robakis, N.K. 2006. Metalloproteinase/Presenilin1 processing of ephrinB regulates EphB-induced Src phosphorylation and signaling. *EMBO J* **25**(6): 1242-1252.

Gilestro, G.F. 2008. Redundant mechanisms for regulation of midline crossing in Drosophila. *PLoS One* **3**(11): e3798.

Gonzalez-Gaitan, M. and Jackle, H. 1997. Role of Drosophila alpha-adaptin in presynaptic vesicle recycling. *Cell* **88**(6): 767-776.

Guichet, A., Wucherpfennig, T., Dudu, V., Etter, S., Wilsch-Brauniger, M., Hellwig, A., Gonzalez-Gaitan, M., Huttner, W.B., and Schmidt, A.A. 2002. Essential role of endophilin A in

synaptic vesicle budding at the Drosophila neuromuscular junction. *The EMBO journal* **21**(7): 1661-1672.
Gupta, G.D., Swetha, M.G., Kumari, S., Lakshminarayan, R., Dey, G., and Mayor, S. 2009. Analysis of endocytic pathways in Drosophila cells reveals a conserved role for GBF1 in internalization via GEECs. *PloS one* **4**(8): e6768.
Hattori, M., Osterfield, M., and Flanagan, J.G. 2000. Regulated cleavage of a contact-mediated axon repellent. *Science* **289**(5483): 1360-1365.
Hines, J.H., Abu-Rub, M., and Henley, J.R. 2010. Asymmetric endocytosis and remodeling of beta1-integrin adhesions during growth cone chemorepulsion by MAG. *Nat Neurosci* **13**(7): 829-837.
Hohenester, E. 2008. Structural insight into Slit-Robo signalling. *Biochem Soc Trans* **36**(Pt 2): 251-256.
Howitt, J.A., Clout, N.J., and Hohenester, E. 2004. Binding site for Robo receptors revealed by dissection of the leucine-rich repeat region of Slit. *The EMBO journal* **23**(22): 4406-4412.
Hsouna, A., Kim, Y.S., and VanBerkum, M.F. 2003. Abelson tyrosine kinase is required to transduce midline repulsive cues. *J Neurobiol* **57**(1): 15-30.
Hu, H., Li, M., Labrador, J.P., McEwen, J., Lai, E.C., Goodman, C.S., and Bashaw, G.J. 2005. Cross GTPase-activating protein (CrossGAP)/Vilse links the Roundabout receptor to Rac to regulate midline repulsion. *Proc Natl Acad Sci U S A* **102**(12): 4613-4618.
Huber, A.B., Kolodkin, A.L., Ginty, D.D., and Cloutier, J.F. 2003. Signaling at the growth cone: ligand-receptor complexes and the control of axon growth and guidance. *Annu Rev Neurosci* **26**: 509-563.
Hutson, L.D. and Chien, C.B. 2002. Pathfinding and error correction by retinal axons: the role of astray/robo2. *Neuron* **33**(2): 205-217.
Itofusa, R. and Kamiguchi, H. 2011. Polarizing membrane dynamics and adhesion for growth cone navigation. *Molecular and cellular neurosciences* **48**(4): 332-338.
Janes, P.W., Saha, N., Barton, W.A., Kolev, M.V., Wimmer-Kleikamp, S.H., Nievergall, E., Blobel, C.P., Himanen, J.P., Lackmann, M., and Nikolov, D.B. 2005. Adam meets Eph: an ADAM substrate recognition module acts as a molecular switch for ephrin cleavage in trans. *Cell* **123**(2): 291-304.
Jekely, G., Sung, H.H., Luque, C.M., and Rorth, P. 2005. Regulators of endocytosis maintain localized receptor tyrosine kinase signaling in guided migration. *Dev Cell* **9**(2): 197-207.
Jen, J.C., Chan, W.M., Bosley, T.M., Wan, J., Carr, J.R., Rub, U., Shattuck, D., Salamon, G., Kudo, L.C., Ou, J. et al. 2004. Mutations in a human ROBO gene disrupt hindbrain axon pathway crossing and morphogenesis. *Science* **304**(5676): 1509-1513.
Johnson, K.G., Ghose, A., Epstein, E., Lincecum, J., O'Connor, M.B., and Van Vactor, D. 2004. Axonal heparan sulfate proteoglycans regulate the distribution and efficiency of the repellent slit during midline axon guidance. *Curr Biol* **14**(6): 499-504.
Jurney, W.M., Gallo, G., Letourneau, P.C., and McLoon, S.C. 2002. Rac1-mediated endocytosis during ephrin-A2- and semaphorin 3A-induced growth cone collapse. *J Neurosci* **22**(14): 6019-6028.
Kamiguchi, H. and Lemmon, V. 2000. Recycling of the cell adhesion molecule L1 in axonal growth cones. *J Neurosci* **20**(10): 3676-3686.
Kapfhammer, J.P. and Raper, J.A. 1987. Collapse of growth cone structure on contact with specific neurites in culture. *J Neurosci* **7**(1): 201-212.

Keleman, K., Rajagopalan, S., Cleppien, D., Teis, D., Paiha, K., Huber, L.A., Technau, G.M., and Dickson, B.J. 2002. Comm sorts robo to control axon guidance at the Drosophila midline. *Cell* **110**(4): 415-427.

Keleman, K., Ribeiro, C., and Dickson, B.J. 2005. Comm function in commissural axon guidance: cell-autonomous sorting of Robo in vivo. *Nat Neurosci* **8**(2): 156-163.

Kennedy, T.E. 2000. Cellular mechanisms of netrin function: long-range and short-range actions. *Biochem Cell Biol* **78**(5): 569-575.

Kidd, T., Bland, K.S., and Goodman, C.S. 1999a. Slit is the midline repellent for the robo receptor in Drosophila. *Cell* **96**(6): 785-794.

Kidd, T., Brose, K., Mitchell, K.J., Fetter, R.D., Tessier-Lavigne, M., Goodman, C.S., and Tear, G. 1998a. Roundabout controls axon crossing of the CNS midline and defines a novel subfamily of evolutionarily conserved guidance receptors. *Cell* **92**(2): 205-215.

Kidd, T., Russell, C., Goodman, C.S., and Tear, G. 1998b. Dosage-sensitive and complementary functions of roundabout and commissureless control axon crossing of the CNS midline. *Neuron* **20**(1): 25-33.

Kopan, R. and Ilagan, M.X. 2009. The canonical Notch signaling pathway: unfolding the activation mechanism. *Cell* **137**(2): 216-233.

Kullander, K. and Klein, R. 2002. Mechanisms and functions of Eph and ephrin signalling. *Nat Rev Mol Cell Biol* **3**(7): 475-486.

Lanahan, A.A., Hermans, K., Claes, F., Kerley-Hamilton, J.S., Zhuang, Z.W., Giordano, F.J., Carmeliet, P., and Simons, M. 2010. VEGF receptor 2 endocytic trafficking regulates arterial morphogenesis. *Dev Cell* **18**(5): 713-724.

Lanier, L.M., Gates, M.A., Witke, W., Menzies, A.S., Wehman, A.M., Macklis, J.D., Kwiatkowski, D., Soriano, P., and Gertler, F.B. 1999. Mena is required for neurulation and commissure formation. *Neuron* **22**(2): 313-325.

Le Borgne, R. 2006. Regulation of Notch signalling by endocytosis and endosomal sorting. *Curr Opin Cell Biol* **18**(2): 213-222.

Li, G., D'Souza-Schorey, C., Barbieri, M.A., Roberts, R.L., Klippel, A., Williams, L.T., and Stahl, P.D. 1995. Evidence for phosphatidylinositol 3-kinase as a regulator of endocytosis via activation of Rab5. *Proc Natl Acad Sci U S A* **92**(22): 10207-10211.

Lin, K.T., Sloniowski, S., Ethell, D.W., and Ethell, I.M. 2008a. Ephrin-B2 induced cleavage of EphB2 receptor is mediated by matrix metalloproteinases to trigger cell repulsion. *J Biol Chem*.

Litterst, C., Georgakopoulos, A., Shioi, J., Ghersi, E., Wisniewski, T., Wang, R., Ludwig, A., and Robakis, N.K. 2007. Ligand binding and calcium influx induce distinct ectodomain/gamma-secretase-processing pathways of EphB2 receptor. *J Biol Chem* **282**(22): 16155-16163.

Liu, Z., Patel, K., Schmidt, H., Andrews, W., Pini, A., and Sundaresan, V. 2004. Extracellular Ig domains 1 and 2 of Robo are important for ligand (Slit) binding. *Molecular and cellular neurosciences* **26**(2): 232-240.

Lyuksyutova, A.I., Lu, C.C., Milanesio, N., King, L.A., Guo, N., Wang, Y., Nathans, J., Tessier-Lavigne, M., and Zou, Y. 2003. Anterior-posterior guidance of commissural axons by Wnt-frizzled signaling. *Science* **302**(5652): 1984-1988.

Ma, L. and Tessier-Lavigne, M. 2007. Dual branch-promoting and branch-repelling actions of Slit/Robo signaling on peripheral and central branches of developing sensory axons. *J Neurosci* **27**(25): 6843-6851.

Macia, E., Ehrlich, M., Massol, R., Boucrot, E., Brunner, C., and Kirchhausen, T. 2006. Dynasore, a cell-permeable inhibitor of dynamin. *Dev Cell* **10**(6): 839-850.

Marston, D.J., Dickinson, S., and Nobes, C.D. 2003. Rac-dependent trans-endocytosis of ephrinBs regulates Eph-ephrin contact repulsion. *Nature cell biology* **5**(10): 879-888.

Matusek, T., Gombos, R., Szecsenyi, A., Sanchez-Soriano, N., Czibula, A., Pataki, C., Gedai, A., Prokop, A., Rasko, I., and Mihaly, J. 2008. Formin proteins of the DAAM subfamily play a role during axon growth. *J Neurosci* **28**(49): 13310-13319.

Moline, M.M., Southern, C., and Bejsovec, A. 1999. Directionality of wingless protein transport influences epidermal patterning in the Drosophila embryo. *Development* **126**(19): 4375-4384.

Mumm, J.S., Schroeter, E.H., Saxena, M.T., Griesemer, A., Tian, X., Pan, D.J., Ray, W.J., and Kopan, R. 2000. A ligand-induced extracellular cleavage regulates gamma-secretase-like proteolytic activation of Notch1. *Mol Cell* **5**(2): 197-206.

Murray, M.J. and Whitington, P.M. 1999. Effects of roundabout on growth cone dynamics, filopodial length, and growth cone morphology at the midline and throughout the neuropile. *J Neurosci* **19**(18): 7901-7912.

Nichols, J.T., Miyamoto, A., and Weinmaster, G. 2007. Notch signaling--constantly on the move. *Traffic* **8**(8): 959-969.

O'Donnell, M., Chance, R.K., and Bashaw, G.J. 2009. Axon growth and guidance: receptor regulation and signal transduction. *Annu Rev Neurosci* **32**: 383-412.

Ohno, H., Stewart, J., Fournier, M.C., Bosshart, H., Rhee, I., Miyatake, S., Saito, T., Gallusser, A., Kirchhausen, T., and Bonifacino, J.S. 1995. Interaction of tyrosine-based sorting signals with clathrin-associated proteins. *Science* **269**(5232): 1872-1875.

Onishi, K., Shafer, B., Lo, C., Tissir, F., Goffinet, A.M., and Zou, Y. 2013. Antagonistic functions of Dishevelleds regulate Frizzled3 endocytosis via filopodia tips in Wnt-mediated growth cone guidance. *J Neurosci* **33**(49): 19071-19085.

Ozdinler, P.H. and Erzurumlu, R.S. 2002. Slit2, a branching-arborization factor for sensory axons in the Mammalian CNS. *J Neurosci* **22**(11): 4540-4549.

Palamidessi, A., Frittoli, E., Garré, M., Faretta, M., Mione, M., Testa, I., Diaspro, A., Lanzetti, L., Scita, G., and Di Fiore, P.P. 2008. Endocytic trafficking of Rac is required for the spatial restriction of signaling in cell migration. *Cell* **134**(1): 135-147.

Pan, D. and Rubin, G.M. 1997a. Kuzbanian controls proteolytic processing of Notch and mediates lateral inhibition during Drosophila and vertebrate neurogenesis. *Cell* **90**(2): 271-280.

Parent, A.T., Barnes, N.Y., Taniguchi, Y., Thinakaran, G., and Sisodia, S.S. 2005. Presenilin attenuates receptor-mediated signaling and synaptic function. *J Neurosci* **25**(6): 1540-1549.

Pasterkamp, R.J. and Kolodkin, A.L. 2003. Semaphorin junction: making tracks toward neural connectivity. *Curr Opin Neurobiol* **13**(1): 79-89.

Pasternak, S.H., Bagshaw, R.D., Guiral, M., Zhang, S., Ackerley, C.A., Pak, B.J., Callahan, J.W., and Mahuran, D.J. 2003. Presenilin-1, nicastrin, amyloid precursor protein, and gamma-secretase activity are co-localized in the lysosomal membrane. *J Biol Chem* **278**(29): 26687-26694.

Piper, M., Anderson, R., Dwivedy, A., Weinl, C., van Horck, F., Leung, K.M., Cogill, E., and Holt, C. 2006. Signaling mechanisms underlying Slit2-induced collapse of Xenopus retinal growth cones. *Neuron* **49**(2): 215-228.

Piper, M., Salih, S., Weinl, C., Holt, C.E., and Harris, W.A. 2005. Endocytosis-dependent desensitization and protein synthesis-dependent resensitization in retinal growth cone adaptation. *Nat Neurosci* **8**(2): 179-186.

Potkin, S.G., Turner, J.A., Guffanti, G., Lakatos, A., Fallon, J.H., Nguyen, D.D., Mathalon, D., Ford, J., Lauriello, J., Macciardi, F. et al. 2009. A genome-wide association study of schizophrenia using brain activation as a quantitative phenotype. *Schizophrenia bulletin* **35**(1): 96-108.

Rajagopalan, S., Nicolas, E., Vivancos, V., Berger, J., and Dickson, B.J. 2000. Crossing the midline: roles and regulation of Robo receptors. *Neuron* **28**(3): 767-777.

Rooke, J., Pan, D., Xu, T., and Rubin, G.M. 1996. KUZ, a conserved metalloprotease-disintegrin protein with two roles in Drosophila neurogenesis. *Science* **273**(5279): 1227-1231.

Schimmelpfeng, K., Gogel, S., and Klambt, C. 2001. The function of leak and kuzbanian during growth cone and cell migration. *Mech Dev* **106**(1-2): 25-36.

Seeger, M., Tear, G., Ferres-Marco, D., and Goodman, C.S. 1993. Mutations affecting growth cone guidance in Drosophila: genes necessary for guidance toward or away from the midline. *Neuron* **10**(3): 409-426.

Seki, M., Watanabe, A., Enomoto, S., Kawamura, T., Ito, H., Kodama, T., Hamakubo, T., and Aburatani, H. 2010. Human ROBO1 is cleaved by metalloproteinases and gamma-secretase and migrates to the nucleus in cancer cells. *FEBS Lett* **584**(13): 2909-2915.

Selkoe, D.J. and Wolfe, M.S. 2007. Presenilin: running with scissors in the membrane. *Cell* **131**(2): 215-221.

Seto, E.S. and Bellen, H.J. 2006. Internalization is required for proper Wingless signaling in Drosophila melanogaster. *J Cell Biol* **173**(1): 95-106.

Shu, T. and Richards, L.J. 2001. Cortical axon guidance by the glial wedge during the development of the corpus callosum. *J Neurosci* **21**(8): 2749-2758.

Slessareva, J.E., Routt, S.M., Temple, B., Bankaitis, V.A., and Dohlman, H.G. 2006. Activation of the phosphatidylinositol 3-kinase Vps34 by a G protein alpha subunit at the endosome. *Cell* **126**(1): 191-203.

Slovakova, J., Speicher, S., Sanchez-Soriano, N., Prokop, A., and Carmena, A. 2012. The actin-binding protein Canoe/AF-6 forms a complex with Robo and is required for Slit-Robo signaling during axon pathfinding at the CNS midline. *J Neurosci* **32**(29): 10035-10044.

Sorkin, A., Mazzotti, M., Sorkina, T., Scotto, L., and Beguinot, L. 1996. Epidermal growth factor receptor interaction with clathrin adaptors is mediated by the Tyr974-containing internalization motif. *J Biol Chem* **271**(23): 13377-13384.

Sorkin, A. and von Zastrow, M. 2009. Endocytosis and signalling: intertwining molecular networks. *Nature reviews Molecular cell biology* **10**(9): 609-622.

Taniguchi, Y., Kim, S.H., and Sisodia, S.S. 2003. Presenilin-dependent "gamma-secretase" processing of deleted in colorectal cancer (DCC). *J Biol Chem* **278**(33): 30425-30428.

Teis, D., Taub, N., Kurzbauer, R., Hilber, D., de Araujo, M.E., Erlacher, M., Offterdinger, M., Villunger, A., Geley, S., Bohn, G. et al. 2006. p14-MP1-MEK1 signaling regulates endosomal traffic and cellular proliferation during tissue homeostasis. *J Cell Biol* **175**(6): 861-868.

Tojima, T., Itofusa, R., and Kamiguchi, H. 2010. Asymmetric clathrin-mediated endocytosis drives repulsive growth cone guidance. *Neuron* **66**(3): 370-377.

Tomita, T., Tanaka, S., Morohashi, Y., and Iwatsubo, T. 2006. Presenilin-dependent intramembrane cleavage of ephrin-B1. *Mol Neurodegener* **1**: 2.

Urra, S., Escudero, C.A., Ramos, P., Lisbona, F., Allende, E., Covarrubias, P., Parraguez, J.I., Zampieri, N., Chao, M.V., Annaert, W. et al. 2007. TrkA receptor activation by nerve growth factor induces shedding of the p75 neurotrophin receptor followed by endosomal gamma-secretase-mediated release of the p75 intracellular domain. *J Biol Chem* **282**(10): 7606-7615.

Vaccari, T., Lu, H., Kanwar, R., Fortini, M.E., and Bilder, D. 2008. Endosomal entry regulates Notch receptor activation in Drosophila melanogaster. *J Cell Biol* **180**(4): 755-762.

van Bergeijk, P., Adrian, M., Hoogenraad, C.C., and Kapitein, L.C. 2015. Optogenetic control of organelle transport and positioning. *Nature* **518**(7537): 111-114.

van der Bliek, A.M., Redelmeier, T.E., Damke, H., Tisdale, E.J., Meyerowitz, E.M., and Schmid, S.L. 1993. Mutations in human dynamin block an intermediate stage in coated vesicle formation. *J Cell Biol* **122**(3): 553-563.

van Tetering, G., van Diest, P., Verlaan, I., van der Wall, E., Kopan, R., and Vooijs, M. 2009. Metalloprotease ADAM10 is required for Notch1 site 2 cleavage. *J Biol Chem* **284**(45): 31018-31027.

Wang, K.H., Brose, K., Arnott, D., Kidd, T., Goodman, C.S., Henzel, W., and Tessier-Lavigne, M. 1999. Biochemical purification of a mammalian slit protein as a positive regulator of sensory axon elongation and branching. *Cell* **96**(6): 771-784.

Whitford, K.L., Marillat, V., Stein, E., Goodman, C.S., Tessier-Lavigne, M., Chedotal, A., and Ghosh, A. 2002. Regulation of cortical dendrite development by Slit-Robo interactions. *Neuron* **33**(1): 47-61.

Williams, M.E., Wu, S.C., McKenna, W.L., and Hinck, L. 2003. Surface expression of the netrin receptor UNC5H1 is regulated through a protein kinase C-interacting protein/protein kinase-dependent mechanism. *J Neurosci* **23**(36): 11279-11288.

Wisco, D., Anderson, E.D., Chang, M.C., Norden, C., Boiko, T., Folsch, H., and Winckler, B. 2003. Uncovering multiple axonal targeting pathways in hippocampal neurons. *J Cell Biol* **162**(7): 1317-1328.

Wolfe, M.S., Citron, M., Diehl, T.S., Xia, W., Donkor, I.O., and Selkoe, D.J. 1998. A substrate-based difluoro ketone selectively inhibits Alzheimer's gamma-secretase activity. *J Med Chem* **41**(1): 6-9.

Yang, L. and Bashaw, G.J. 2006. Son of sevenless directly links the Robo receptor to rac activation to control axon repulsion at the midline. *Neuron* **52**(4): 595-607.

Yoo, S., Kim, Y., Noh, H., Lee, H., Park, E., and Park, S. 2011. Endocytosis of EphA receptors is essential for the proper development of the retinocollicular topographic map. *The EMBO journal* **30**(8): 1593-1607.

Yoshikawa, S., McKinnon, R.D., Kokel, M., and Thomas, J.B. 2003. Wnt-mediated axon guidance via the Drosophila Derailed receptor. *Nature* **422**(6932): 583-588.

Yu, T.W. and Bargmann, C.I. 2001. Dynamic regulation of axon guidance. *Nat Neurosci* **4 Suppl**: 1169-1176.

Zimmer, M., Palmer, A., Kohler, J., and Klein, R. 2003. EphB-ephrinB bi-directional endocytosis terminates adhesion allowing contact mediated repulsion. *Nature cell biology* **5**(10): 869-878.

Zlatic, M., Li, F., Strigini, M., Grueber, W., and Bate, M. 2009. Positional cues in the Drosophila nerve cord: semaphorins pattern the dorso-ventral axis. *PLoS Biol* **7**(6): e1000135.

# CHAPTER 4: General Conclusions and Future Directions

This work presented in this dissertation was designed to further our understanding of the genetic determinants of anatomical connectivity patterns established in development. It is comprised of basic research into the mechanisms regulating the activity of our axon guidance receptor of interest. This gene, *roundabout*, is both causatively linked to a rare Human genetic disorder (Horizontal Gaze Palsy with Progressive Scoliosis) (Jen et al. 2004) and implicated either directly, or by its signaling partners, by Genome-Wide Association Studies in the pathogenesis of a number of common developmental disorders (schizophrenia, autism, and dyslexia/periventricular nodular heterotopia (Hannula-Jouppi et al. 2005; Chang et al. 2007; Anitha et al. 2008; Potkin et al. 2009a; Bates et al. 2011; Wilson et al. 2011; Gulsuner et al. 2013), which fall into the common-disease, common-variant category, and implicated in the generation of human specific cortical wiring programs (Dennis et al. 2012) (Table 4.1). Understanding the molecular mechanisms regulating the function of this receptor in normal development will improve our understanding of both those neurological disorders that have well-defined anatomical and functional correlates and those with higher incidence levels and therefore relevance to healthcare systems.

Slit is a repulsive guidance cue that activates the Roundabout receptor, expressed on the tips of filopodia of migrating growth cones, which incites retraction of actin-rich filopodia on the short term to ultimately inhibit the eventual cable-like axonal projections marking the track of a previously migrating growth cone from growing into Slit-containing regions. Endocytosis has been implicated in several repulsive guidance pathways to contribute to growth cone or axon guidance behaviors by passively turning

over guidance molecules expressed on the surface to inform the combinatorial array of signaling molecules competent to respond to subsequent cues encountered as the growth cone membrane advances. A requirement for endocytosis has also been implicated in the latter projection pattern readout of growth cone behavior; a correlation between endocytosis of guidance cues and the ligand-dependent growth cone behaviors of collapse or turning has emerged *in vitro* and (2) a requirement for Rac-dependant endocytosis in axon targeting has been evidenced *in vivo.* Here we provide the first mechanistic detail elucidating how the spatial fate of a ligand-bound repulsive guidance cue is gated by endocytic trafficking to activate its downstream cytoskeletal effector Son of Sevenless in the early endosome to affect a novel, but well-validated, cytoskeletal behavior *in vitro*. We identify sequence motifs in the Receptor necessary for both its endocytosis in this Slit-dependent cell motility response *in vitro* to also be required for axon targeting in the well-established axon model system of the fruit fly embryo, providing the first evidence for causation of axon guidance receptor endocytosis to inform its growth cone's behavior by signaling to the cytoskeleton.

This work has been designed to test whether internalization of an axon guidance receptor itself, instead of its downstream effectors, mechanistically contributes to the cytoskeletal dynamics necessary for growth cone behavior by serving as a retrograde cue from the tips of filopodia to the growth cone central domain to inform repulsion from a ligand-containing region. The motivation for this hypothesis was largely formed from the curious co-occurrence of receptor mislocalized to the very regions from which it is failing to signal repulsion in *kuz* loss-of-function embryos (Figure 3.2). We had originally thought that the mechanistic link between repulsive signaling and membrane clearance could be accomplished by either endocytosis or by a proteolytic event that would free the

activated signaling fragment (CTF) from the confines of the plasma membrane to allow it access to the many cytoskeletal components of the growth cone. In fact we learned that both endocytosis and transmembrane cleavage both occur, likely following the first juxtamembrane activating cleavage, but that they confer the opposite polarity of regulation to Slit-Robo signaling. Robo endocytosis is a positive regulator while *gamma*-Secretase provides negative regulation to Robo signaling. We are in the beginning stages of assembling the relative order and contribution of these two proteolytic events and the endocytic trafficking pathway, but based on knowledge from other signaling pathways and evidence we have reported here, we propose the following probable model (Figure 4.1).

We learned from a novel *in vitro* activation assay that Slit binding to Robo does induce local endocytosis of receptor through the early and into the late endosome which gates the recruitment of its validated downstream Rac effector Son of Sevenless. The evidence that the small sequence motifs in Robo's C-terminus that are required for its Clathrin-dependent endocytosis are necessary for established axon guidance behaviors, and that inhibiting both endocytosis and juxtamembrane proteolysis together *in vitro* are sufficient to abrogate the Slit-dependent process elaboration response comprised by Robo's entire C-terminus, strongly argue for the importance of both juxtamembrane proteolysis and endocytosis in Robo's activation.

**Figure 4.1: An integrated model of Robo endocytosis and Proteolysis regulating the spatiotemporal dynamics of receptor signaling**

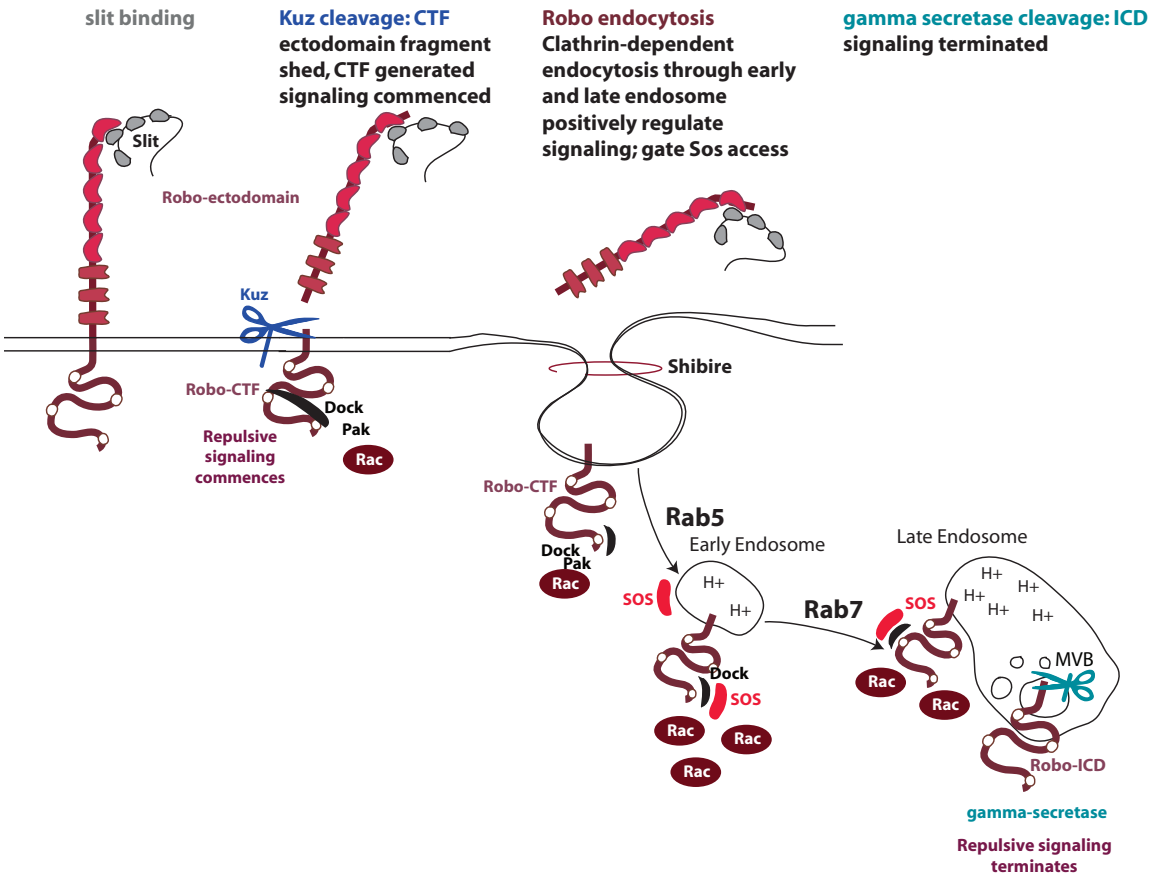

**Figure 4.1: An Integrated Model of Robo endocytosis and proteolysis regulating the spatiotemporal dynamics of receptor signaling**

Upon Slit-binding Robo is activated; the adaptor protein Dreadlocks (Dock) is recruited to Robo's CC2 and CC3 motifs, which in turn activates PAK and consequently initiates Rac activation (Fan et al. 2003). Juxtamembrane cleavage of Robo by Kuzbanian (Kuz) is required for both Robo activation *in vitro* and midline repulsion *in vivo* (Coleman et al. 2010). This cleavage event may occur after Slit-binding, but all evidence indicates that it is still required for Robo signaling output (Figure 3.1D, 3.6B). Robo endocytosis occurs following juxtamembrane Kuz cleavage, as Robo defective for endocytosis still effectively generates Robo ectodomain in the embryo (Figure 3.7E). Juxtamembrane proteolysis and Clathrin-dependent endocytosis cooperate to account for all the Robo activation provided by Robo's C-terminus *in vitro (*Figure 3.6K). The correlation between retained surface Robo and decreased activation in Kuz-inhibited conditions (Figure 3.2) may be explained by both internalization into the growth cone of Robo as well as the subsequent *gamma*-Secretase-mediated cleavage (Selkoe and Wolfe 2007) that allows its degradation, after meeting Sos to evoke further Rac activation in the early and late endosome (Chapter 2), into the multivesicular bodies of the mature late endosome bound for lysosomal degradation.

## Future Directions

### The effect of spatiotemporal dynamics of activated Robo within a growth cone

If indeed endocytosis of Robo serves to expand the spatial range of signaling beyond Ena (Lanier et al. 1999; Matusek et al. 2008) at its originating location in filopodial tips (Kidd et al. 1998a; Slovakova et al. 2012) to affect filopodial retraction from Slit-containing regions (Murray and Whitington 1999; Hutson and Chien 2002), then we would expect to be able to observe a spatiotemporal correlation between Robo at the base of filopodia with the repulsive growth cone behaviors of filopodial retraction, or growth cone collapse/turning within a single growth cone upon encountering Slit. The feasibility of imaging the subcellular resolution of Robo in dissociated *Drosophila* neurons required for such an experiment has recently been demonstrated in dissociated cultures (Katsuki et al. 2009; Slovakova et al. 2012). Similar fluorescent microscopy analysis of individual growth cone filopodial behavior in response to endogenous Slit might also be conducted in an intact, whole-mounted or live, filleted prep (Chen et al. 2009; Featherstone et al. 2009; Figard and Sokac 2011). Combining the genetic manipulations displayed in Chapters 2 & 3 with transgenic fluorescent fusion proteins to track the dynamics of filamentous Actin and Robo in subsets of axons could demonstrate the dependence on Robo mobility- granted by endocytosis or the first proteolytic event- of validated dynamic filopodial behaviors.

First one must demonstrate the established filopodial phenotype in *robo* mutants (Murray and Whitington 1999) still holds in this experimental prep by testing for a difference between *wild-type* and *robo* mutant neurons in filopodial retraction upon either bath treatment of Slit, or midline contact in a filleted prep. Then the fluorescent imaging

conditions need to be calibrated in order to test for a spatiotemporal correlation in Robo (full length, or CTF) translocation from filopodial tip to filopodial base and subsequent retrograde movement within the growth cone with F-actin-imaged growth cone behavior. Next, analysis of the contribution of Clathrin-dependent endocytosis and proteolysis to the above behavior can be assayed by the use of *alpha-adaptin/slit* loss of function genetic manipulations, and the Robo AP-2 adaptor motif deletions in *robo* mutants, and *kuz/slit* loss-of-function and Robo-uncleavable (Juxtamembrane) transgenes ability to rescue *robo* mutants' filopodial retraction defects. One would predict that if juxtamembrane cleavage and endocytosis are both required for the internalization of a motile retrograde cue, then inhibiting either process would cause Robo to stay on the tips of filopodia and never signal to the base of the filopodia to retract or to the growth cone to collapse/turn. In contrast, one would predict that inhibiting Robo's *gamma*-Secretase-mediated inactivating cleavage would cause no defect in the aforementioned process but would instead show prolonged or enhanced repulsive growth cone behavior.

Although some of the early seminal findings on the ability of single filopodial contacts to inform (attractive) growth cone guidance was performed in insect (grasshopper) embryos (O'Connor et al. 1990; Myers and Bastiani 1993), most of our knowledge of growth cone response to extracellular ligands comes from the larger size and control over cue delivery in dissociated neuronal preparations (mollusk- *Aplysia californica* (Suter and Forscher 1998; Lovell and Moroz 2006; Suter 2011) and *Helisoma* (Torreano et al. 2005)), vertebrate – *Xenopus laevis* (Sann et al. 2008; Hines et al. 2010; Lowery et al. 2012; Myers and Gomez 2012), chick (Kapfhammer and Raper 1987b; Kapfhammer and Raper 1987a; Fan and Raper 1995), and mouse (Ma and Tessier-Lavigne 2007)). An alternative, and less risky, approach would be to assess the effect of

Robo endocytosis on the previously validated growth cone responses to Slit of collapse or turning. Studies of vertebrate growth cone behavior have shown that not only is Slit treatment sufficient to induce dissociated Robo-positive axons to branch (Wang et al. 1999a; Ozdinler and Erzurumlu 2002), but also to guide repulsion (Brose et al. 1999b; Nguyen Ba-Charvet et al. 1999; Wu et al. 1999; Niclou et al. 2000; Plump et al. 2002). Determining whether endocytosis is required for the chemo-repulsive effect of Slit on Robo-expressing explant neuronal cultures could be accomplished by testing for a lack of Slit response in human Robo missing its AP-2 binding motifs, as compared to *wild type* human Robo, electroporated in the chick model system. Further mechanistic insight could be gained by examining the sub-cellular resolution of transgenically-expressed C-terminal mCherry-tagged Robo (AP-2 binding defective versus *wild type)* transgenes in single growth cones during the established behavior of collapse in *Xenopus* growth cones (Piper et al. 2006). If endocytosis is required for Robo to meet its downstream Rac effector Sos in the growth cone peripheral domain, then we would expect to find that in growth cones expressing AP-2 binding defective Robo, receptor stays on the tips of filopodia as growth cones ignore Slit and do not collapse. In contrast, our model predicts that in WT-Robo expressing growth cones, the initiation of collapse would not occur until Robo that had previously bound Slit (with a two minute time delay upon contact with a Slit-bearing source), reaches the peripheral domain of the growth cone.

**Determining the contribution of *psn*-mediated Robo cleavage to midline guidance**

A chimeric Presenilin-uncleavable version of Robo, created with a technique verified for other receptors by swapping out its TMD for FasR's (Zampieri et al. 2005), would be predicted by our model to serve as a receptor that has an extended temporal period of signaling once activated by Slit, as it is not subject to an inactivating cleavage. Such a receptor should be assayed for its modulation of the Slit-dependent process generation in the S2R+ Robo activation assay described in Chapters 2 & 3.

Future work to order the proteolytic regulation events and endocytic trafficking events will be assayed in the S2R+ Robo activation assay. The juxtamembrane Robo constructs that evidence reduced process elaboration in response to Slit (ΔJM, ΔDINPTTHKK, ΔHKK, JM D>A) should be assayed for their cleavage capacity, by ability to generate Ectodomain and CTF fragments *in vitro* and their repulsive guidance activity in transgenic rescue assays *in vivo.* These receptor variants should also be assayed for their ability to be cleaved by *gamma*-Secretase, by virtue of generation of an ICD.

**A potential role for extracellular HSPGs in Slit and Robo distribution**

Our findings indicating that Slit-binding does not affect ectodomain shedding *in vitro*, suggest that the Kuz-mediated juxtamembrane cleavage might occur before Slit-binding. These observations are consistent with two earlier reports. First, the lack of dependency of Robo ectodomain generation in S2R+ cells on Slit treatment (Fig3.6M)- that ectodomain exists in the media of Control CM-treated cells and is not enhanced in Slit CM-treated cells, or abolished in cells expressing Robo that can't bind Slit– is

consistent with a finding by others reported before the significance of Robo cleavage had been investigated. The abundance of a Robo C-terminal fragment in lysates of HEK cells requires the presence of its Fibronectin (FN) domains (and presumedly the juxtamembrane domain) but not the five Immunogloblin (Slit-binding (Ig1)) domains, consistent with our findings that the first Ig domain does not inhibit shedding of the ectodomain into S2R+ cell media (Chen et al. 2001). Second, an observation that the spatial pattern of Slit in a whole animal depends on the midline-crossing of axons is consistent with the shedding of Slit-bound Robo ectodomains occurring before Robo (CTF) is endocytosed into the growth cone. In the case of the *Drosophila* midline, Slit protein expressed from midline glia is spread by migrating axons into an expression pattern with a peak at the midline (Zlatic et al. 2009) and two valleys of Slit protein levels along the Medio-Lateral axis (Kidd et al. 1999b; Johnson et al. 2004). Given that 90% of axons normally cross the midline in this system, and the fact that in embryos where axons never cross the midline this lateral distribution of Slit is abolished (Bhat et al. 2007), it is likely that the growth cones crossing the midline are the causative factor. Ectodomain shedding of Robo bound with Slit from migrating growth cones could explain the presence of Slit away from their cells of origin. If the redistribution of Slit indeed represents the population of Slit that has bound and signaled to Robo on navigating growth cones and is in turn shed, this would mean that at least some population of Slit is not internalized into either the navigating growth cone, or the signal-presenting midline glia from which it originated. The lack of Robo-ectodomain/Slit complex endocytosis into midline glia would differentiate Slit/Robo from the Notch pathway in which Delta/Serrate/Lag2 (DSL) ligand internalization by trans-endocytosis contributes to signaling in the ligand-presenting-sending cell (Le Borgne 2006; Nichols et al. 2007).

Given that Heparan Sulfate ProteoGlycans (HSPGs) have been previously demonstrated to contribute to Robo localization (Schulz et al. 2011; Smart et al. 2011), and Robo activation (Seiradake et al. 2009), a future trainee might want to pursue the potential contribution of HSPGs, as implicated in the network of genes not focused on in this work but detailed in (Table 4.2), to the distribution of Slit as well as the clearance of Robo from the commissural segments of axons.

**Table 4.1: Slit/Robo pathway genes associated with variations in Human cortical wiring**

| Human Condition | Anatomical Feature | Human Gene | GWAS Reference |
|---|---|---|---|
| Schizophrenia | Dorsolateral Prefrontal Cortex | *Robo1, Robo2* | (Potkin et al. 2009b) |
| | | *Slit2* | (Brennand and Gage 2011) |
| | | *SrGAP3* | (Wilson et al. 2011) |
| Autism | Dorsolateral Prefrontal Cortex | *Robo3, Robo4* | (Anitha et al. 2008) |
| Dyslexia | Dorsolateral Prefrontal Cortex, periventricular nodular heterotopia (Chang et al. 2007), Thalamocortical, Left Occipito-temporal (Fan et al. 2014) | *Robo1* | (Hannula-Jouppi et al. 2005; Bates et al. 2011) |
| Horizontal Gaze Palsy and Progressive Scoliosis | Hypoplasia medullary pyramids,defective Decussation in Pons of CST (Sicotte et al. 2006; Jen 2008) | *Robo3* | (Jen et al. 2004; Abu-Amero et al. 2009; Amouri et al. 2009) |
| Adolescent Idiopathic Scoliosis | Spinal Cord | CNTNAP 2/NrxIV | (Sharma et al. 2011) |
| Neofunctionalization /Evolutionary duplication | - | *srGAP2* | (Dennis et al. 2012) |

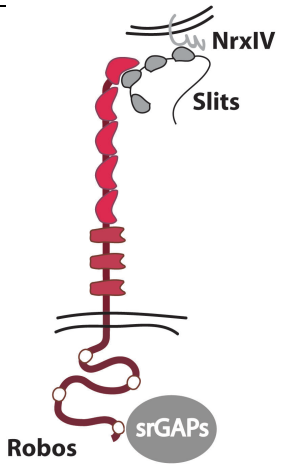

**Table 4.1: Slit/Robo pathway genes associated with variations in Human cortical wiring**

Genes in the Slit/Robo pathway implicated by Genome-wide association studies in diseases or variations of human cortical wiring are displayed along with any current knowledge about the anatomical structures affected by the disease. In the case of Horizontal Gaze Palsy and Progressive Scoliosis (HGPPS) the relationship between gene, the anatomical defects of oculomotor nuclei in the medullary pyramids and lack of decussation of the descending cortico-spinal tract, and the functional deficit (lack of crossed motor output control, and defective vergence eye movements leading to diplopia (double vision)) have been well-elucidated. The recent innovation of diffusion tensor imaging allowing tract-tracing in the human cortex has begun to allow the discovery of the specific defects in the aforementioned HGPPS disorder (Jen 2008, Sicotte et al 2006) as well as another rare disorder of periventricular nodular heterotopia, which shares the functional deficit with dyslexia of impaired language fluency (Chang et al 2007). Hopefully future work will uncover other subtle defects in wiring that may occur due to dysregulated axon guidance genes; it looks like the dorso-lateral prefrontal cortex is a prime candidate for future study given the current data listed above.

## Table 4.2: Genes required for Robo's commissural exclusion

**Genes important for Robo's commissural exclusion**

| *gene* | Mutants have Robo mislocalization to commissural segments | Mutants have ectopic crossing | citation | Genetic interaction with slit-robo | Physical interaction | Protein expression pattern |
|---|---|---|---|---|---|---|
| *sos* | Y | ~1.5/embryo | [Yang et al 2006, Fritz & van Berkum 2002] | Rac, crGAP | Dock, robo | Starts out broadly, becomes enriched in axons by stage 16 |
| *dock* | Y. Robomyc TG in Ap RKC. | 70% (MZ) | [Fan et al 2003] | ena | Robo (CC2 + 3) | neuropil |
| *kuz* | Y published | 50 – 76.7% FasII | Schimmelpfeng et al 2001 (UAS-DN-Kuz), Greg (*kuz* mutants) | slit, robo | ND | New Ab no-go, RKC june 2011 |
| *slit* | Y: TG in Eg's and Ap's, 13C9 in hypomorphs | Hypomorphs, yes. Ap in mutants: yes | RKC | Robo, kuz, etc. etc. | Robo IG1 | Midline glia |
| RacN17 | Yes in sos hets with elav, RKC | TG enhances slit | [Fan et al 2003] | Slit | | |
| *vav*? | [not detected RKC, but note low crossing percentage] | 2% FasII | Malartre et al J Neurosci 2010 | Sos (up to 40%) | | Midline glia, select neurons, larval eye-brain complex |
| *sdc* | Y published | 40% segments FasII. 4 crosses/embryo | Smart et al Van Vactor 2011 Fig3: stage17 | Slit,robo (Johnson 2004) | | Longitudinals and connectives |
| *nrx IV* | Y published | ~3/embryo | Banerjee J et al, Neurosci 2010 | Slit, robo, | Slit, robo, | Neuropil+ glia (stronger) |

## Table 4.2: Genes required for Robo's commissural exclusion

A summary of published and unpublished genes that, like (and including) *kuzbanian*, contribute to the commissurally excluded expression pattern of Robo, also noting the physical and genetic interactors in order to survey the network of molecules involved in this localization pattern. The genes encode the proteins as follows: Son of Sevenless (Yang and Bashaw 2006), (Fritz and VanBerkum 2002); Dreadlocks (Fan et al. 2003); Kuzbanian (Coleman et al. 2010), (Schimmelpfeng et al. 2001); Slit; (Rac DN transgene (Fan et al. 2003)); Vav, not a validated member of this group, but a candidate for future study if combined with other genes listed in this table (Malartre et al. 2010); Syndecan (Johnson et al. 2004), (Smart et al. 2011); and Neurexin-IV (Banerjee et al. 2010).

## BIBLIOGRAPHY


Abu-Amero, K.K., al Dhalaan, H., al Zayed, Z., Hellani, A., and Bosley, T.M. 2009. Five new consanguineous families with horizontal gaze palsy and progressive scoliosis and novel ROBO3 mutations. *J Neurol Sci* **276**(1-2): 22-26.

Amouri, R., Nehdi, H., Bouhlal, Y., Kefi, M., Larnaout, A., and Hentati, F. 2009. Allelic ROBO3 heterogeneity in Tunisian patients with horizontal gaze palsy with progressive scoliosis. *J Mol Neurosci* **39**(3): 337-341.

Anitha, A., Nakamura, K., Yamada, K., Suda, S., Thanseem, I., Tsujii, M., Iwayama, Y., Hattori, E., Toyota, T., Miyachi, T. et al. 2008. Genetic analyses of roundabout (ROBO) axon guidance receptors in autism. *Am J Med Genet B Neuropsychiatr Genet* **147B**(7): 1019-1027.

Atapattu, L., Saha, N., Llerena, C., Vail, M.E., Scott, A.M., Nikolov, D.B., Lackmann, M., and Janes, P.W. 2012. Antibodies binding the ADAM10 substrate recognition domain inhibit Eph function. *J Cell Sci* **125**(Pt 24): 6084-6093.

Bai, G., Chivatakarn, O., Bonanomi, D., Lettieri, K., Franco, L., Xia, C., Stein, E., Ma, L., Lewcock, J.W., and Pfaff, S.L. 2011. Presenilin-dependent receptor processing is required for axon guidance. *Cell* **144**(1): 106-118.

Banerjee, S., Blauth, K., Peters, K., Rogers, S.L., Fanning, A.S., and Bhat, M.A. 2010. Drosophila neurexin IV interacts with Roundabout and is required for repulsive midline axon guidance. *J Neurosci* **30**(16): 5653-5667.

Barak, R., Lahmi, R., Gevorkyan-Airapetov, L., Levy, E., Tzur, A., and Opatowsky, Y. 2014. Crystal structure of the extracellular juxtamembrane region of Robo1. *J Struct Biol* **186**(2): 283-291.

Bartoe, J.L., McKenna, W.L., Quan, T.K., Stafford, B.K., Moore, J.A., Xia, J., Takamiya, K., Huganir, R.L., and Hinck, L. 2006. Protein interacting with C-kinase 1/protein kinase Calpha-mediated endocytosis converts netrin-1-mediated repulsion to attraction. *J Neurosci* **26**(12): 3192-3205.

Bashaw, G.J. and Goodman, C.S. 1999. Chimeric axon guidance receptors: the cytoplasmic domains of slit and netrin receptors specify attraction versus repulsion. *Cell* **97**(7): 917-926.

Bashaw, G.J., Kidd, T., Murray, D., Pawson, T., and Goodman, C.S. 2000. Repulsive axon guidance: Abelson and Enabled play opposing roles downstream of the roundabout receptor. *Cell* **101**(7): 703-715.

Bates, T.C., Luciano, M., Medland, S.E., Montgomery, G.W., Wright, M.J., and Martin, N.G. 2011. Genetic variance in a component of the language acquisition device: ROBO1 polymorphisms associated with phonological buffer deficits. *Behav Genet* **41**(1): 50-57.

Beel, A.J. and Sanders, C.R. 2008. Substrate specificity of gamma-secretase and other intramembrane proteases. *Cell Mol Life Sci* **65**(9): 1311-1334.

Bhat, K.M., Gaziova, I., and Krishnan, S. 2007. Regulation of axon guidance by slit and netrin signaling in the Drosophila ventral nerve cord. *Genetics* **176**(4): 2235-2246.

Brennand, K.J. and Gage, F.H. 2011. Modeling psychiatric disorders through reprogramming. *Dis Model Mech* **5**(1): 26-32.

Brose, K., Bland, K.S., Wang, K.H., Arnott, D., Henzel, W., Goodman, C.S., Tessier-Lavigne, M., and Kidd, T. 1999a. Slit proteins bind Robo receptors and have an evolutionarily conserved role in repulsive axon guidance. *Cell* **96**(6): 795-806.

Butler, S.J. and Dodd, J. 2003. A role for BMP heterodimers in roof plate-mediated repulsion of commissural axons. *Neuron* **38**(3): 389-401.
Campbell, D.S. and Holt, C.E. 2001. Chemotropic responses of retinal growth cones mediated by rapid local protein synthesis and degradation. *Neuron* **32**(6): 1013-1026.
Castellani, V., Falk, J., and Rougon, G. 2004. Semaphorin3A-induced receptor endocytosis during axon guidance responses is mediated by L1 CAM. *Mol Cell Neurosci* **26**(1): 89-100.
Chang, B.S., Katzir, T., Liu, T., Corriveau, K., Barzillai, M., Apse, K.A., Bodell, A., Hackney, D., Alsop, D., Wong, S.T. et al. 2007. A structural basis for reading fluency: white matter defects in a genetic brain malformation. *Neurology* **69**(23): 2146-2154.
Charron, F., Stein, E., Jeong, J., McMahon, A.P., and Tessier-Lavigne, M. 2003. The morphogen sonic hedgehog is an axonal chemoattractant that collaborates with netrin-1 in midline axon guidance. *Cell* **113**(1): 11-23.
Chen, J.H., Wen, L., Dupuis, S., Wu, J.Y., and Rao, Y. 2001. The N-terminal leucine-rich regions in Slit are sufficient to repel olfactory bulb axons and subventricular zone neurons. *J Neurosci* **21**(5): 1548-1556.
Chen, K., Featherstone, D.E., and Broadie, K. 2009. Electrophysiological recording in the Drosophila embryo. *J Vis Exp*(27).
Christoforidis, S., Miaczynska, M., Ashman, K., Wilm, M., Zhao, L., Yip, S.C., Waterfield, M.D., Backer, J.M., and Zerial, M. 1999. Phosphatidylinositol-3-OH kinases are Rab5 effectors. *Nature cell biology* **1**(4): 249-252.
Coleman, H.A., Labrador, J.P., Chance, R.K., and Bashaw, G.J. 2010. The Adam family metalloprotease Kuzbanian regulates the cleavage of the roundabout receptor to control axon repulsion at the midline. *Development* **137**(14): 2417-2426.
Cowan, C.W., Shao, Y.R., Sahin, M., Shamah, S.M., Lin, M.Z., Greer, P.L., Gao, S., Griffith, E.C., Brugge, J.S., and Greenberg, M.E. 2005. Vav family GEFs link activated Ephs to endocytosis and axon guidance. *Neuron* **46**(2): 205-217.
Das, B., Shu, X., Day, G.J., Han, J., Krishna, U.M., Falck, J.R., and Broek, D. 2000. Control of intramolecular interactions between the pleckstrin homology and Dbl homology domains of Vav and Sos1 regulates Rac binding. *J Biol Chem* **275**(20): 15074-15081.
Dennis, M.Y., Nuttle, X., Sudmant, P.H., Antonacci, F., Graves, T.A., Nefedov, M., Rosenfeld, J.A., Sajjadian, S., Malig, M., Kotkiewicz, H. et al. 2012. Evolution of human-specific neural SRGAP2 genes by incomplete segmental duplication. *Cell* **149**(4): 912-922.
Dickson, B.J. 2002. Molecular mechanisms of axon guidance. *Science* **298**(5600): 1959-1964.
Diefenbach, T.J., Guthrie, P.B., Stier, H., Billups, B., and Kater, S.B. 1999. Membrane recycling in the neuronal growth cone revealed by FM1-43 labeling. *J Neurosci* **19**(21): 9436-9444.
Egea, J. and Klein, R. 2007. Bidirectional Eph-ephrin signaling during axon guidance. *Trends Cell Biol* **17**(5): 230-238.
Falk, J., Konopacki, F.A., Zivraj, K.H., and Holt, C.E. 2014. Rab5 and Rab4 regulate axon elongation in the Xenopus visual system. *J Neurosci* **34**(2): 373-391.
Fan, J. and Raper, J.A. 1995. Localized collapsing cues can steer growth cones without inducing their full collapse. *Neuron* **14**(2): 263-274.
Fan, Q., Anderson, A.W., Davis, N., and Cutting, L.E. 2014. Structural connectivity patterns associated with the putative visual word form area and children's reading ability. *Brain Res* **1586**: 118-129.

Fan, X., Labrador, J.P., Hing, H., and Bashaw, G.J. 2003. Slit stimulation recruits Dock and Pak to the roundabout receptor and increases Rac activity to regulate axon repulsion at the CNS midline. *Neuron* **40**(1): 113-127.

Featherstone, D.E., Chen, K., and Broadie, K. 2009. Harvesting and preparing Drosophila embryos for electrophysiological recording and other procedures. *J Vis Exp*(27).

Figard, L. and Sokac, A.M. 2011. Imaging cell shape change in living Drosophila embryos. *J Vis Exp*(49).

Fritz, J.L. and VanBerkum, M.F. 2002. Regulation of rho family GTPases is required to prevent axons from crossing the midline. *Dev Biol* **252**(1): 46-58.

Fukuhara, N., Howitt, J.A., Hussain, S.A., and Hohenester, E. 2008. Structural and functional analysis of slit and heparin binding to immunoglobulin-like domains 1 and 2 of Drosophila Robo. *J Biol Chem* **283**(23): 16226-16234.

Galko, M.J. and Tessier-Lavigne, M. 2000. Function of an axonal chemoattractant modulated by metalloprotease activity. *Science* **289**(5483): 1365-1367.

Galperin, E. and Sorkin, A. 2003. Visualization of Rab5 activity in living cells by FRET microscopy and influence of plasma-membrane-targeted Rab5 on clathrin-dependent endocytosis. *Journal of cell science* **116**(Pt 23): 4799-4810.

Garbe, D.S. and Bashaw, G.J. 2004. Axon guidance at the midline: from mutants to mechanisms. *Crit Rev Biochem Mol Biol* **39**(5-6): 319-341.

Gatto, G., Morales, D., Kania, A., and Klein, R. 2014. EphA4 receptor shedding regulates spinal motor axon guidance. *Curr Biol* **24**(20): 2355-2365.

Georgakopoulos, A., Litterst, C., Ghersi, E., Baki, L., Xu, C., Serban, G., and Robakis, N.K. 2006. Metalloproteinase/Presenilin1 processing of ephrinB regulates EphB-induced Src phosphorylation and signaling. *EMBO J* **25**(6): 1242-1252.

Gilestro, G.F. 2008. Redundant mechanisms for regulation of midline crossing in Drosophila. *PLoS One* **3**(11): e3798.

Gonzalez-Gaitan, M. and Jackle, H. 1997. Role of Drosophila alpha-adaptin in presynaptic vesicle recycling. *Cell* **88**(6): 767-776.

Guichet, A., Wucherpfennig, T., Dudu, V., Etter, S., Wilsch-Brauniger, M., Hellwig, A., Gonzalez-Gaitan, M., Huttner, W.B., and Schmidt, A.A. 2002. Essential role of endophilin A in synaptic vesicle budding at the Drosophila neuromuscular junction. *The EMBO journal* **21**(7): 1661-1672.

Gulsuner, S., Walsh, T., Watts, A.C., Lee, M.K., Thornton, A.M., Casadei, S., Rippey, C., Shahin, H., Nimgaonkar, V.L., Go, R.C. et al. 2013. Spatial and temporal mapping of de novo mutations in schizophrenia to a fetal prefrontal cortical network. *Cell* **154**(3): 518-529.

Gupta, G.D., Swetha, M.G., Kumari, S., Lakshminarayan, R., Dey, G., and Mayor, S. 2009. Analysis of endocytic pathways in Drosophila cells reveals a conserved role for GBF1 in internalization via GEECs. *PLoS One* **4**(8): e6768.

Hannula-Jouppi, K., Kaminen-Ahola, N., Taipale, M., Eklund, R., Nopola-Hemmi, J., Kaariainen, H., and Kere, J. 2005. The axon guidance receptor gene ROBO1 is a candidate gene for developmental dyslexia. *PLoS Genet* **1**(4): e50.

Hattori, M., Osterfield, M., and Flanagan, J.G. 2000. Regulated cleavage of a contact-mediated axon repellent. *Science* **289**(5483): 1360-1365.

Hines, J.H., Abu-Rub, M., and Henley, J.R. 2010. Asymmetric endocytosis and remodeling of beta1-integrin adhesions during growth cone chemorepulsion by MAG. *Nat Neurosci* **13**(7): 829-837.

Hohenester, E. 2008. Structural insight into Slit-Robo signalling. *Biochem Soc Trans* **36**(Pt 2): 251-256.
Howitt, J.A., Clout, N.J., and Hohenester, E. 2004. Binding site for Robo receptors revealed by dissection of the leucine-rich repeat region of Slit. *The EMBO journal* **23**(22): 4406-4412.
Hsouna, A., Kim, Y.S., and VanBerkum, M.F. 2003. Abelson tyrosine kinase is required to transduce midline repulsive cues. *J Neurobiol* **57**(1): 15-30.
Hu, H., Li, M., Labrador, J.P., McEwen, J., Lai, E.C., Goodman, C.S., and Bashaw, G.J. 2005. Cross GTPase-activating protein (CrossGAP)/Vilse links the Roundabout receptor to Rac to regulate midline repulsion. *Proc Natl Acad Sci U S A* **102**(12): 4613-4618.
Huber, A.B., Kolodkin, A.L., Ginty, D.D., and Cloutier, J.F. 2003. Signaling at the growth cone: ligand-receptor complexes and the control of axon growth and guidance. *Annu Rev Neurosci* **26**: 509-563.
Hutson, L.D. and Chien, C.B. 2002. Pathfinding and error correction by retinal axons: the role of astray/robo2. *Neuron* **33**(2): 205-217.
Itofusa, R. and Kamiguchi, H. 2011. Polarizing membrane dynamics and adhesion for growth cone navigation. *Molecular and cellular neurosciences* **48**(4): 332-338.
Janes, P.W., Saha, N., Barton, W.A., Kolev, M.V., Wimmer-Kleikamp, S.H., Nievergall, E., Blobel, C.P., Himanen, J.P., Lackmann, M., and Nikolov, D.B. 2005. Adam meets Eph: an ADAM substrate recognition module acts as a molecular switch for ephrin cleavage in trans. *Cell* **123**(2): 291-304.
Jekely, G., Sung, H.H., Luque, C.M., and Rorth, P. 2005. Regulators of endocytosis maintain localized receptor tyrosine kinase signaling in guided migration. *Dev Cell* **9**(2): 197-207.
Jen, J.C. 2008. Effects of failure of development of crossing brainstem pathways on ocular motor control. *Prog Brain Res* **171**: 137-141.
Jen, J.C., Chan, W.M., Bosley, T.M., Wan, J., Carr, J.R., Rub, U., Shattuck, D., Salamon, G., Kudo, L.C., Ou, J. et al. 2004. Mutations in a human ROBO gene disrupt hindbrain axon pathway crossing and morphogenesis. *Science* **304**(5676): 1509-1513.
Johnson, K.G., Ghose, A., Epstein, E., Lincecum, J., O'Connor, M.B., and Van Vactor, D. 2004. Axonal heparan sulfate proteoglycans regulate the distribution and efficiency of the repellent slit during midline axon guidance. *Curr Biol* **14**(6): 499-504.
Jurney, W.M., Gallo, G., Letourneau, P.C., and McLoon, S.C. 2002. Rac1-mediated endocytosis during ephrin-A2- and semaphorin 3A-induced growth cone collapse. *J Neurosci* **22**(14): 6019-6028.
Kamiguchi, H. and Lemmon, V. 2000. Recycling of the cell adhesion molecule L1 in axonal growth cones. *J Neurosci* **20**(10): 3676-3686.
Kapfhammer, J.P. and Raper, J.A. 1987a. Collapse of growth cone structure on contact with specific neurites in culture. *J Neurosci* **7**(1): 201-212.
Katsuki, T., Ailani, D., Hiramoto, M., and Hiromi, Y. 2009. Intra-axonal patterning: intrinsic compartmentalization of the axonal membrane in Drosophila neurons. *Neuron* **64**(2): 188-199.
Keleman, K., Rajagopalan, S., Cleppien, D., Teis, D., Paiha, K., Huber, L.A., Technau, G.M., and Dickson, B.J. 2002. Comm sorts robo to control axon guidance at the Drosophila midline. *Cell* **110**(4): 415-427.
Keleman, K., Ribeiro, C., and Dickson, B.J. 2005. Comm function in commissural axon guidance: cell-autonomous sorting of Robo in vivo. *Nat Neurosci* **8**(2): 156-163.

Kennedy, T.E. 2000. Cellular mechanisms of netrin function: long-range and short-range actions. *Biochem Cell Biol* **78**(5): 569-575.
Kidd, T., Bland, K.S., and Goodman, C.S. 1999a. Slit is the midline repellent for the robo receptor in Drosophila. *Cell* **96**(6): 785-794.
Kidd, T., Brose, K., Mitchell, K.J., Fetter, R.D., Tessier-Lavigne, M., Goodman, C.S., and Tear, G. 1998a. Roundabout controls axon crossing of the CNS midline and defines a novel subfamily of evolutionarily conserved guidance receptors. *Cell* **92**(2): 205-215.
Kidd, T., Russell, C., Goodman, C.S., and Tear, G. 1998b. Dosage-sensitive and complementary functions of roundabout and commissureless control axon crossing of the CNS midline. *Neuron* **20**(1): 25-33.
Kopan, R. and Ilagan, M.X. 2009. The canonical Notch signaling pathway: unfolding the activation mechanism. *Cell* **137**(2): 216-233.
Kullander, K. and Klein, R. 2002. Mechanisms and functions of Eph and ephrin signalling. *Nat Rev Mol Cell Biol* **3**(7): 475-486.
Lanahan, A.A., Hermans, K., Claes, F., Kerley-Hamilton, J.S., Zhuang, Z.W., Giordano, F.J., Carmeliet, P., and Simons, M. 2010. VEGF receptor 2 endocytic trafficking regulates arterial morphogenesis. *Dev Cell* **18**(5): 713-724.
Lanier, L.M., Gates, M.A., Witke, W., Menzies, A.S., Wehman, A.M., Macklis, J.D., Kwiatkowski, D., Soriano, P., and Gertler, F.B. 1999. Mena is required for neurulation and commissure formation. *Neuron* **22**(2): 313-325.
Le Borgne, R. 2006. Regulation of Notch signalling by endocytosis and endosomal sorting. *Curr Opin Cell Biol* **18**(2): 213-222.
Li, G., D'Souza-Schorey, C., Barbieri, M.A., Roberts, R.L., Klippel, A., Williams, L.T., and Stahl, P.D. 1995. Evidence for phosphatidylinositol 3-kinase as a regulator of endocytosis via activation of Rab5. *Proc Natl Acad Sci U S A* **92**(22): 10207-10211.
Lin, K.T., Sloniowski, S., Ethell, D.W., and Ethell, I.M. 2008a. Ephrin-B2 induced cleavage of EphB2 receptor is mediated by matrix metalloproteinases to trigger cell repulsion. *J Biol Chem*.
Litterst, C., Georgakopoulos, A., Shioi, J., Ghersi, E., Wisniewski, T., Wang, R., Ludwig, A., and Robakis, N.K. 2007. Ligand binding and calcium influx induce distinct ectodomain/gamma-secretase-processing pathways of EphB2 receptor. *J Biol Chem* **282**(22): 16155-16163.
Liu, Z., Patel, K., Schmidt, H., Andrews, W., Pini, A., and Sundaresan, V. 2004. Extracellular Ig domains 1 and 2 of Robo are important for ligand (Slit) binding. *Molecular and cellular neurosciences* **26**(2): 232-240.
Lopez-Bendito, G., Flames, N., Ma, L., Fouquet, C., Di Meglio, T., Chedotal, A., Tessier-Lavigne, M., and Marin, O. 2007. Robo1 and Robo2 cooperate to control the guidance of major axonal tracts in the mammalian forebrain. *J Neurosci* **27**(13): 3395-3407.
Lovell, P. and Moroz, L.L. 2006. The largest growth cones in the animal kingdom: an illustrated guide to the dynamics of Aplysia neuronal growth in cell culture. *Integr Comp Biol* **46**(6): 847-870.
Lowery, L.A., Faris, A.E., Stout, A., and Van Vactor, D. 2012. Neural Explant Cultures from Xenopus laevis. *J Vis Exp*(68): e4232.
Lyuksyutova, A.I., Lu, C.C., Milanesio, N., King, L.A., Guo, N., Wang, Y., Nathans, J., Tessier-Lavigne, M., and Zou, Y. 2003. Anterior-posterior guidance of commissural axons by Wnt-frizzled signaling. *Science* **302**(5652): 1984-1988.

Ma, L. and Tessier-Lavigne, M. 2007. Dual branch-promoting and branch-repelling actions of Slit/Robo signaling on peripheral and central branches of developing sensory axons. *J Neurosci* **27**(25): 6843-6851.

Macia, E., Ehrlich, M., Massol, R., Boucrot, E., Brunner, C., and Kirchhausen, T. 2006. Dynasore, a cell-permeable inhibitor of dynamin. *Dev Cell* **10**(6): 839-850.

Malartre, M., Ayaz, D., Amador, F.F., and Martin-Bermudo, M.D. 2010. The guanine exchange factor vav controls axon growth and guidance during Drosophila development. *J Neurosci* **30**(6): 2257-2267.

Marston, D.J., Dickinson, S., and Nobes, C.D. 2003. Rac-dependent trans-endocytosis of ephrinBs regulates Eph-ephrin contact repulsion. *Nature cell biology* **5**(10): 879-888.

Matusek, T., Gombos, R., Szecsenyi, A., Sanchez-Soriano, N., Czibula, A., Pataki, C., Gedai, A., Prokop, A., Rasko, I., and Mihaly, J. 2008. Formin proteins of the DAAM subfamily play a role during axon growth. *J Neurosci* **28**(49): 13310-13319.

Moline, M.M., Southern, C., and Bejsovec, A. 1999. Directionality of wingless protein transport influences epidermal patterning in the Drosophila embryo. *Development* **126**(19): 4375-4384.

Mumm, J.S., Schroeter, E.H., Saxena, M.T., Griesemer, A., Tian, X., Pan, D.J., Ray, W.J., and Kopan, R. 2000. A ligand-induced extracellular cleavage regulates gamma-secretase-like proteolytic activation of Notch1. *Mol Cell* **5**(2): 197-206.

Murray, M.J. and Whitington, P.M. 1999. Effects of roundabout on growth cone dynamics, filopodial length, and growth cone morphology at the midline and throughout the neuropile. *J Neurosci* **19**(18): 7901-7912.

Myers, J.P. and Gomez, T.M. 2012. Focal adhesion kinase promotes integrin adhesion dynamics necessary for chemotropic turning of nerve growth cones. *J Neurosci* **31**(38): 13585-13595.

Myers, P.Z. and Bastiani, M.J. 1993. Growth cone dynamics during the migration of an identified commissural growth cone. *J Neurosci* **13**(1): 127-143.

Nguyen Ba-Charvet, K.T., Brose, K., Marillat, V., Kidd, T., Goodman, C.S., Tessier-Lavigne, M., Sotelo, C., and Chedotal, A. 1999. Slit2-Mediated chemorepulsion and collapse of developing forebrain axons. *Neuron* **22**(3): 463-473.

Nichols, J.T., Miyamoto, A., and Weinmaster, G. 2007. Notch signaling--constantly on the move. *Traffic* **8**(8): 959-969.

Niclou, S.P., Jia, L., and Raper, J.A. 2000. Slit2 is a repellent for retinal ganglion cell axons. *J Neurosci* **20**(13): 4962-4974.

O'Connor, T.P., Duerr, J.S., and Bentley, D. 1990. Pioneer growth cone steering decisions mediated by single filopodial contacts in situ. *J Neurosci* **10**(12): 3935-3946.

O'Donnell, M., Chance, R.K., and Bashaw, G.J. 2009. Axon growth and guidance: receptor regulation and signal transduction. *Annu Rev Neurosci* **32**: 383-412.

Ohno, H., Stewart, J., Fournier, M.C., Bosshart, H., Rhee, I., Miyatake, S., Saito, T., Gallusser, A., Kirchhausen, T., and Bonifacino, J.S. 1995. Interaction of tyrosine-based sorting signals with clathrin-associated proteins. *Science* **269**(5232): 1872-1875.

Onishi, K., Shafer, B., Lo, C., Tissir, F., Goffinet, A.M., and Zou, Y. 2013. Antagonistic functions of Dishevelleds regulate Frizzled3 endocytosis via filopodia tips in Wnt-mediated growth cone guidance. *J Neurosci* **33**(49): 19071-19085.

Ozdinler, P.H. and Erzurumlu, R.S. 2002. Slit2, a branching-arborization factor for sensory axons in the Mammalian CNS. *J Neurosci* **22**(11): 4540-4549.

Palamidessi, A., Frittoli, E., Garré, M., Faretta, M., Mione, M., Testa, I., Diaspro, A., Lanzetti, L., Scita, G., and Di Fiore, P.P. 2008. Endocytic trafficking of Rac is required for the spatial restriction of signaling in cell migration. *Cell* **134**(1): 135-147.

Pan, D. and Rubin, G.M. 1997a. Kuzbanian controls proteolytic processing of Notch and mediates lateral inhibition during Drosophila and vertebrate neurogenesis. *Cell* **90**(2): 271-280.

Parent, A.T., Barnes, N.Y., Taniguchi, Y., Thinakaran, G., and Sisodia, S.S. 2005. Presenilin attenuates receptor-mediated signaling and synaptic function. *J Neurosci* **25**(6): 1540-1549.

Pasterkamp, R.J. and Kolodkin, A.L. 2003. Semaphorin junction: making tracks toward neural connectivity. *Curr Opin Neurobiol* **13**(1): 79-89.

Pasternak, S.H., Bagshaw, R.D., Guiral, M., Zhang, S., Ackerley, C.A., Pak, B.J., Callahan, J.W., and Mahuran, D.J. 2003. Presenilin-1, nicastrin, amyloid precursor protein, and gamma-secretase activity are co-localized in the lysosomal membrane. *J Biol Chem* **278**(29): 26687-26694.

Piper, M., Anderson, R., Dwivedy, A., Weinl, C., van Horck, F., Leung, K.M., Cogill, E., and Holt, C. 2006. Signaling mechanisms underlying Slit2-induced collapse of Xenopus retinal growth cones. *Neuron* **49**(2): 215-228.

Piper, M., Salih, S., Weinl, C., Holt, C.E., and Harris, W.A. 2005. Endocytosis-dependent desensitization and protein synthesis-dependent resensitization in retinal growth cone adaptation. *Nat Neurosci* **8**(2): 179-186.

Plump, A.S., Erskine, L., Sabatier, C., Brose, K., Epstein, C.J., Goodman, C.S., Mason, C.A., and Tessier-Lavigne, M. 2002. Slit1 and Slit2 cooperate to prevent premature midline crossing of retinal axons in the mouse visual system. *Neuron* **33**(2): 219-232.

Potkin, S.G., Turner, J.A., Fallon, J.A., Lakatos, A., Keator, D.B., Guffanti, G., and Macciardi, F. 2009a. Gene discovery through imaging genetics: identification of two novel genes associated with schizophrenia. *Mol Psychiatry* **14**(4): 416-428.

Potkin, S.G., Turner, J.A., Guffanti, G., Lakatos, A., Fallon, J.H., Nguyen, D.D., Mathalon, D., Ford, J., Lauriello, J., and Macciardi, F. 2009b. A genome-wide association study of schizophrenia using brain activation as a quantitative phenotype. *Schizophr Bull* **35**(1): 96-108.

Potkin, S.G., Turner, J.A., Guffanti, G., Lakatos, A., Fallon, J.H., Nguyen, D.D., Mathalon, D., Ford, J., Lauriello, J., Macciardi, F. et al. 2009c. A genome-wide association study of schizophrenia using brain activation as a quantitative phenotype. *Schizophrenia bulletin* **35**(1): 96-108.

Rajagopalan, S., Nicolas, E., Vivancos, V., Berger, J., and Dickson, B.J. 2000. Crossing the midline: roles and regulation of Robo receptors. *Neuron* **28**(3): 767-777.

Rooke, J., Pan, D., Xu, T., and Rubin, G.M. 1996. KUZ, a conserved metalloprotease-disintegrin protein with two roles in Drosophila neurogenesis. *Science* **273**(5279): 1227-1231.

Sann, S.B., Xu, L., Nishimune, H., Sanes, J.R., and Spitzer, N.C. 2008. Neurite outgrowth and in vivo sensory innervation mediated by a Ca(V)2.2-laminin beta 2 stop signal. *J Neurosci* **28**(10): 2366-2374.

Schimmelpfeng, K., Gogel, S., and Klambt, C. 2001. The function of leak and kuzbanian during growth cone and cell migration. *Mech Dev* **106**(1-2): 25-36.

Schulz, J.G., Ceulemans, H., Caussinus, E., Baietti, M.F., Affolter, M., Hassan, B.A., and David, G. 2011. Drosophila syndecan regulates tracheal cell migration by stabilizing Robo levels. *EMBO Rep* **12**(10): 1039-1046.

Seeger, M., Tear, G., Ferres-Marco, D., and Goodman, C.S. 1993. Mutations affecting growth cone guidance in Drosophila: genes necessary for guidance toward or away from the midline. *Neuron* **10**(3): 409-426.

Seiradake, E., von Philipsborn, A.C., Henry, M., Fritz, M., Lortat-Jacob, H., Jamin, M., Hemrika, W., Bastmeyer, M., Cusack, S., and McCarthy, A.A. 2009. Structure and functional relevance of the Slit2 homodimerization domain. *EMBO Rep* **10**(7): 736-741.

Seki, M., Watanabe, A., Enomoto, S., Kawamura, T., Ito, H., Kodama, T., Hamakubo, T., and Aburatani, H. 2010. Human ROBO1 is cleaved by metalloproteinases and gamma-secretase and migrates to the nucleus in cancer cells. *FEBS Lett* **584**(13): 2909-2915.

Selkoe, D.J. and Wolfe, M.S. 2007. Presenilin: running with scissors in the membrane. *Cell* **131**(2): 215-221.

Seto, E.S. and Bellen, H.J. 2006. Internalization is required for proper Wingless signaling in Drosophila melanogaster. *J Cell Biol* **173**(1): 95-106.

Sharma, S., Gao, X., Londono, D., Devroy, S.E., Mauldin, K.N., Frankel, J.T., Brandon, J.M., Zhang, D., Li, Q.Z., Dobbs, M.B. et al. 2011. Genome-wide association studies of adolescent idiopathic scoliosis suggest candidate susceptibility genes. *Hum Mol Genet* **20**(7): 1456-1466.

Shu, T. and Richards, L.J. 2001. Cortical axon guidance by the glial wedge during the development of the corpus callosum. *J Neurosci* **21**(8): 2749-2758.

Sicotte, N.L., Salamon, G., Shattuck, D.W., Hageman, N., Rub, U., Salamon, N., Drain, A.E., Demer, J.L., Engle, E.C., Alger, J.R. et al. 2006. Diffusion tensor MRI shows abnormal brainstem crossing fibers associated with ROBO3 mutations. *Neurology* **67**(3): 519-521.

Slessareva, J.E., Routt, S.M., Temple, B., Bankaitis, V.A., and Dohlman, H.G. 2006. Activation of the phosphatidylinositol 3-kinase Vps34 by a G protein alpha subunit at the endosome. *Cell* **126**(1): 191-203.

Slovakova, J., Speicher, S., Sanchez-Soriano, N., Prokop, A., and Carmena, A. 2012. The actin-binding protein Canoe/AF-6 forms a complex with Robo and is required for Slit-Robo signaling during axon pathfinding at the CNS midline. *J Neurosci* **32**(29): 10035-10044.

Smart, A.D., Course, M.M., Rawson, J., Selleck, S., Van Vactor, D., and Johnson, K.G. 2011. Heparan sulfate proteoglycan specificity during axon pathway formation in the Drosophila embryo. *Dev Neurobiol* **71**(7): 608-618.

Sorkin, A., Mazzotti, M., Sorkina, T., Scotto, L., and Beguinot, L. 1996. Epidermal growth factor receptor interaction with clathrin adaptors is mediated by the Tyr974-containing internalization motif. *J Biol Chem* **271**(23): 13377-13384.

Sorkin, A. and von Zastrow, M. 2009. Endocytosis and signalling: intertwining molecular networks. *Nature reviews Molecular cell biology* **10**(9): 609-622.

Suter, D.M. 2011. Live cell imaging of neuronal growth cone motility and guidance in vitro. *Methods Mol Biol* **769**: 65-86.

Suter, D.M. and Forscher, P. 1998. An emerging link between cytoskeletal dynamics and cell adhesion molecules in growth cone guidance. *Curr Opin Neurobiol* **8**(1): 106-116.

Taniguchi, Y., Kim, S.H., and Sisodia, S.S. 2003. Presenilin-dependent "gamma-secretase" processing of deleted in colorectal cancer (DCC). *J Biol Chem* **278**(33): 30425-30428.

Teis, D., Taub, N., Kurzbauer, R., Hilber, D., de Araujo, M.E., Erlacher, M., Offterdinger, M., Villunger, A., Geley, S., Bohn, G. et al. 2006. p14-MP1-MEK1 signaling regulates

endosomal traffic and cellular proliferation during tissue homeostasis. *J Cell Biol* **175**(6): 861-868.
Tojima, T., Itofusa, R., and Kamiguchi, H. 2010. Asymmetric clathrin-mediated endocytosis drives repulsive growth cone guidance. *Neuron* **66**(3): 370-377.
Tomita, T., Tanaka, S., Morohashi, Y., and Iwatsubo, T. 2006. Presenilin-dependent intramembrane cleavage of ephrin-B1. *Mol Neurodegener* **1**: 2.
Torreano, P.J., Waterman-Storer, C.M., and Cohan, C.S. 2005. The effects of collapsing factors on F-actin content and microtubule distribution of Helisoma growth cones. *Cell Motil Cytoskeleton* **60**(3): 166-179.
Urra, S., Escudero, C.A., Ramos, P., Lisbona, F., Allende, E., Covarrubias, P., Parraguez, J.I., Zampieri, N., Chao, M.V., Annaert, W. et al. 2007. TrkA receptor activation by nerve growth factor induces shedding of the p75 neurotrophin receptor followed by endosomal gamma-secretase-mediated release of the p75 intracellular domain. *J Biol Chem* **282**(10): 7606-7615.
Vaccari, T., Lu, H., Kanwar, R., Fortini, M.E., and Bilder, D. 2008. Endosomal entry regulates Notch receptor activation in Drosophila melanogaster. *J Cell Biol* **180**(4): 755-762.
van Bergeijk, P., Adrian, M., Hoogenraad, C.C., and Kapitein, L.C. 2015. Optogenetic control of organelle transport and positioning. *Nature* **518**(7537): 111-114.
van der Bliek, A.M., Redelmeier, T.E., Damke, H., Tisdale, E.J., Meyerowitz, E.M., and Schmid, S.L. 1993. Mutations in human dynamin block an intermediate stage in coated vesicle formation. *J Cell Biol* **122**(3): 553-563.
van Tetering, G., van Diest, P., Verlaan, I., van der Wall, E., Kopan, R., and Vooijs, M. 2009. Metalloprotease ADAM10 is required for Notch1 site 2 cleavage. *J Biol Chem* **284**(45): 31018-31027.
Wang, K.H., Brose, K., Arnott, D., Kidd, T., Goodman, C.S., Henzel, W., and Tessier-Lavigne, M. 1999a. Biochemical purification of a mammalian slit protein as a positive regulator of sensory axon elongation and branching. *Cell* **96**(6): 771-784.
Whitford, K.L., Marillat, V., Stein, E., Goodman, C.S., Tessier-Lavigne, M., Chedotal, A., and Ghosh, A. 2002. Regulation of cortical dendrite development by Slit-Robo interactions. *Neuron* **33**(1): 47-61.
Williams, M.E., Wu, S.C., McKenna, W.L., and Hinck, L. 2003. Surface expression of the netrin receptor UNC5H1 is regulated through a protein kinase C-interacting protein/protein kinase-dependent mechanism. *J Neurosci* **23**(36): 11279-11288.
Wilson, N.K., Lee, Y., Long, R., Hermetz, K., Rudd, M.K., Miller, R., Rapoport, J.L., and Addington, A.M. 2011. A Novel Microduplication in the Neurodevelopmental Gene SRGAP3 That Segregates with Psychotic Illness in the Family of a COS Proband. *Case Rep Genet* **2011**: 585893.
Wisco, D., Anderson, E.D., Chang, M.C., Norden, C., Boiko, T., Folsch, H., and Winckler, B. 2003. Uncovering multiple axonal targeting pathways in hippocampal neurons. *J Cell Biol* **162**(7): 1317-1328.
Wolfe, M.S., Citron, M., Diehl, T.S., Xia, W., Donkor, I.O., and Selkoe, D.J. 1998. A substrate-based difluoro ketone selectively inhibits Alzheimer's gamma-secretase activity. *J Med Chem* **41**(1): 6-9.
Wu, W., Wong, K., Chen, J., Jiang, Z., Dupuis, S., Wu, J.Y., and Rao, Y. 1999. Directional guidance of neuronal migration in the olfactory system by the protein Slit. *Nature* **400**(6742): 331-336.
Yang, L. and Bashaw, G.J. 2006. Son of sevenless directly links the Robo receptor to rac activation to control axon repulsion at the midline. *Neuron* **52**(4): 595-607.

Yoo, S., Kim, Y., Noh, H., Lee, H., Park, E., and Park, S. 2011. Endocytosis of EphA receptors is essential for the proper development of the retinocollicular topographic map. *The EMBO journal* **30**(8): 1593-1607.

Yoshikawa, S., McKinnon, R.D., Kokel, M., and Thomas, J.B. 2003. Wnt-mediated axon guidance via the Drosophila Derailed receptor. *Nature* **422**(6932): 583-588.

Yu, T.W. and Bargmann, C.I. 2001. Dynamic regulation of axon guidance. *Nat Neurosci* **4 Suppl**: 1169-1176.

Zampieri, N., Xu, C.F., Neubert, T.A., and Chao, M.V. 2005. Cleavage of p75 neurotrophin receptor by alpha-secretase and gamma-secretase requires specific receptor domains. *J Biol Chem* **280**(15): 14563-14571.

Zimmer, M., Palmer, A., Kohler, J., and Klein, R. 2003. EphB-ephrinB bi-directional endocytosis terminates adhesion allowing contact mediated repulsion. *Nature cell biology* **5**(10): 869-878.

Zlatic, M., Li, F., Strigini, M., Grueber, W., and Bate, M. 2009. Positional cues in the Drosophila nerve cord: semaphorins pattern the dorso-ventral axis. *PLoS Biol* **7**(6): e1000135.